Physics – Uspekhi **48** (1) 37 – 76 (2005)

REVIEWS OF TOPICAL PROBLEMS PACS numbers: **33.80. – b**, 42.62.Fi, 82.40.Fp, 82.50.Bc

Selective processes of IR excitation and dissociation of molecules in gasdynamically cooled jets and flows

G N Makarov

DOI: 10.1070/PU2005v048n01ABEH001901

Contents

Abstract. Research into the selective excitation and dissociation of molecules by intense IR laser radiation in gasdynamically cooled jets and flows is reviewed. Methods for and results of studying the spectral and energy characteristics of molecular excitation and dissociation are described. It is shown that vibrational and rotational temperatures, together with collision processes, have a pronounced effect on the formation of spectral structures and on the selectivity of dissociation. Diode laser spectroscopic data on the dynamics of the molecular excitation from individual rotational sublevels of the ground vibrational state are presented. Molecular excitation models for lower vibrational transitions are discussed and related problems are considered. Experimental and theoretical findings are compared and their discrepancies are analyzed. The isotopically selective dissociation of molecules under low-temperature and low gas concentration conditions is discussed, the related problems are identified, and methods for their solution are considered. Results on how the main dissociation characteristics — selectivity and dissociation yield — vary with the laser radiation and gas flow parameters are presented. Methods for improving dissociation efficiency are described, and optimal conditions for high selectivity and dissociation yield are pointed out.

G N Makarov Institute of Spectroscopy, Russian Academy of Sciences
142190 Troitsk, Moscow Region, Russian Federation
Tel. (7-095) 334 02 32. Fax (7-095) 3340818 86
E-mail: gmakarov@isan.troitsk.ru

Received 25 May 2004, revised 27 August 2004
Uspekhi Fizicheskikh Nauk **175** (1) 41 – 84 (2005)
Translated by Yu V Morozov; edited by A Radzig

1. Introduction

Among all the varieties of directed photophysical and photochemical processes induced by intense infrared (IR) laser radiation, one of the most extensively studied is isotopically selective infrared multiple photon dissociation (MPD) of molecules [1 – 17]. Selective dissociation of CF_2HCl (freon-22) molecules provided a basis for the fabrication of carbon isotopes by laser separation in Russia [17 – 21]. The prospects of applying this technique to the separation of heavier elements (e.g., Si, U, W, Os) justify investigations into

infrared multiple photon excitation (MPE) and dissociation of molecules in gasdynamically cooled jets and flows [22, 23]. Isotope shifts in the IR absorption spectra of molecules containing these elements ($\Delta\nu_{is} \leqslant 5-10$ cm^{-1} for silicon-containing molecules, and $\Delta\nu_{is} \leqslant 1$ cm^{-1} for UF_6, WF_6, and OsO_4) are relatively small. Due to this, linear and multiple photon absorption (MPA) spectra of molecules having different isotopic compositions highly or almost completely overlap. In this situation, selectivity of dissociation can be further improved only by cooling molecules in gasdynamic jets and flows. Gas cooling results in an appreciable narrowing of linear [24, 25] and multiple photon [26–28] IR absorption bands and leads to the formation of readily apparent MPA spectral structure [29–34] and finally to the enhanced selectivity of molecular dissociation.

The use of gasdynamically cooled molecular beams and jets [22, 23, 35, 36] also facilitates measurements under nearly collisionless conditions when perturbation effects are virtually absent [35–38]. Moreover, a much smaller number of occupied quantum states distinctly simplifies investigations into excitation and dissociation processes, as well as interpretation of their results [27, 30, 32]. Taken together, these observations give rational grounds for a deeper insight into the physical mechanisms of interactions between molecules and intense IR radiation, including molecular transition schemes as well as processes and phenomena underlying the selective excitation and dissociation of molecules. Results of studies on selective IR excitation and dissociation of molecules in gasdynamically cooled molecular beams, jets, and flows are the focus of this review. It is largely based on the information gleaned by the author and his colleagues, although results of many other studies will be considered too. Also, it is worth noting that an important incentive for undertaking this review was the author's intent to collect, analyze, and present in one report data from a large number of studies pertinent to the problem of interest that are closely interrelated but widely scattered among numerous publications.

The very first experiments on excitation and dissociation of molecules by intense IR laser radiation in gasdynamically cooled molecular beams (see, for instance, Refs [39–41]) were designed to study molecular fragmentation processes. Later, experiments were focused on the mechanisms of molecular excitation in the region of lower vibrational levels [26–34, 42–49] because molecular beams provide a unique opportunity to simplify molecular spectra and carry out excitation studies under collisionless conditions. Indeed, experiments with molecular beams and jets have greatly promoted the understanding of mechanisms of molecular excitation by intense IR laser radiation (see, for instance, Refs [10, 50–52] and Sections 4 and 5). In the present review, we consider and briefly analyze the results available thus far not only in the context of excitation mechanisms but also from the standpoint of their importance and applicability to isotopically selective molecular dissociation in gasdynamically cooled jets and flows. It should be emphasized that although some of these results on IRMPE of molecules were obtained rather long ago (e.g., in MPA studies), they still remain of interest, first and foremost as a basis for the study of isotopically selective molecular dissociation under gasdynamic cooling. Moreover, they promote the understanding of the so far obscure mechanism of collisionless excitation of molecules by intense IR laser radiation in the region of lower vibrational levels [37, 51] (see also Sections 4.3 and 5). However, the majority of the data considered in the present review (see Sections 6 and 7) have been obtained in recent experiments.

The paper is organized in the following way. Section 2 presents a brief review of molecular states and processes inherent in IRMPD. The adopted IRMPD model of molecules is discussed. Materials included in this section help in better understanding the problems considered in the review. Section 3 deals with methodology. Techniques for the production of gasdynamically cooled molecular jets and streams effluxing through a nozzle are briefly discussed with special reference to those used in our works to obtain intense pulsed molecular beams and jets. The experimental apparatus and procedures for the study of IR multiple photon excitation and dissociation of molecules in gasdynamically cooled jets and flows are described, including the pyroelectric method for the measurement of absorbed energy, methods for the detection of visible luminescence resulting from inverse electronic relaxation and of IR luminescence of HF^* molecules, as well as some other methods.

Section 4 presents the main results of IRMPE studies in molecular beams and jets. Spectral and energy characteristics of IRMPA of molecules are considered, along with effects of vibrational and rotational temperatures of molecules on the formation of multiple photon absorption spectra and the role of exciting pulse intensity in IRMPA and dissociation yields. Section 4 also discusses results of experimental studies on MPA spectra of vibrationally excited molecules and on the resonant multifrequency excitation of upper vibrational states. It is shown that the multifrequency excitation technique makes it possible to effectively populate selected high-lying vibrational levels of the molecules. The results of experiments on the MPA of SF_6 in a large-scale (50-cm-wide) molecular flow of SF_6/Ar are analyzed. The experimental apparatus used in these experiments was a prototype of the industrial unit for laser isotope separation.

The main results of experiments on diode laser spectroscopy of molecular (SF_6 and NH_3) excitation dynamics at individual rotational sublevels of the ground vibration state are presented in Section 5. It reports on rather complicated and high-precision measurements, the results of which can be quantitatively compared with estimates derived from theoretical models. Such a comparison greatly promotes the understanding of the interaction mechanisms between intense IR laser radiation and polyatomic molecules. It is demonstrated that the dependences of the relative number of exited molecules on the energy density of exciting radiation and frequency detuning are very similar even for such spectroscopically different molecules as SF_6 and NH_3 (which can be regarded as mutilevel and two-level systems, respectively). In fact, these dependences are determined by the mode structure of the exciting radiation of a CO_2 laser. Also, it is found that the fraction of molecules excited from individual rotational sublevels strongly depends on the spectral width and the mode composition of the exciting pulse. Models explaining the excitation of molecules in the region of lower vibrational–rotational transitions and related phenomena are considered. Experimental and theoretical findings are compared to account for their discrepancies and to analyze their possible underlying causes.

Section 6 describes experiments on the isotopically selective dissociation of molecules (SF_6 and CF_3I) in gasdynamically cooled jets and flows. Results of investigations into selective dissociation of UF_6 molecules are expounded in brief. CF_3I molecules are utilized to examine

peculiarities of isotopically selective molecular dissociation at low temperatures and small gas concentrations; associated problems and approaches for solving them are also discussed. The behavior of the principal characteristics of molecular dissociation, i.e., selectivity and dissociation yield, is considered with reference to laser radiation and gas flow parameters. Optimal conditions are revealed to give the high magnitudes of selectivity and dissociation yield. Methods for improving the efficiency of isotopically selective molecular dissociation are discussed.

Section 7 gives an account of experimental results in which a new approach to the realization of the isotopically selective dissociation of molecules was employed. The method calls for the production of the residual gas highly enriched in a given isotope in a single cycle of molecular flow irradiation. This technique is based on the use of small-extent flows. The results of experiments on selective dissociation of molecules (exemplified by CF_3I) in small-extent pulsed gasdynamic flows indicate that large enrichment factors for the residual gas can be obtained during one irradiation cycle if the entire flow is subject to high-intensity IR radiation. The possibility of achieving high efficiency of enrichment of the residual CF_3I gas with the ^{13}C isotope is illustrated by the irradiation of a natural isotopic mixture of molecules by a single laser pulse. Finally, Section 8 summarizes the most important results of the studies considered in the review and the ensuing conclusions.

2. Molecular states and processes intrinsic in IRMPD

Before turning to the review of the data of interest, it seems appropriate to consider briefly the molecular states and processes intrinsic in IRMPD [12, 52, 53]. We believe that it may help to better understand the essence of the problem under discussion. A basic feature of IRMPD is the ability of a molecule to absorb a large number (dozens) of IR photons from a laser pulse in an intense IR laser field under collisionless excitation conditions despite the anharmonism of molecular vibrations. The molecule breaks down into fragments (radicals) as it reaches a dissociation threshold. The resulting fragments interact between themselves and with a radical acceptor to yield products that differ from the parent molecules and are readily separated from the starting mixture by traditional physico-chemical methods (e.g., condensation, evaporation, chemical reactions, etc.). In other words, it is possible to obtain products enriched in a chosen (desired) isotope from a natural mixture of isotopomers by means of selective excitation and dissociation of molecules of a given isotopic composition. The residual gas remaining after the irradiation is completed happens to be enriched in nontarget isotopes.

In order to understand why a molecule is able to absorb such a large number of IR photons, it is opportune to consider a qualitative molecular IRMPD model universally accepted as a basic one [6–9, 12, 52–54]. According to this model, a molecule passes in the process three consecutive qualitatively different regions of vibrational energy E_v (Fig. 1): (1) the region of low-lying vibrational levels ($E_v \leqslant E_{qu}$, where E_{qu} is the lower boundary of the vibrational quasi-continuum); (2) the vibrational quasi-continuum region ($E_{qu} \leqslant E_v \leqslant D$, where D is the energy of molecular dissociation by rupture of the weakest bond), and (3) the real continuum region lying above the dissociation threshold ($E_v > D$).

In the region of lower vibrational levels, where the density of vibrational states is relatively small, molecules are excited either as a result of the consecutive absorption of quanta (when different mechanisms of compensation for anharmonicity of molecular vibrations are realized) or in the course of direct multiple photon transitions. Absorption spectra in this region have a characteristically sharp resonance structure. The absorbed energy remains localized largely in the pumped resonant mode.

In the quasi-continuum region with a relatively high density of molecular vibrational states, interactions between different levels result in the formation of broadband spectra of molecular transitions. Despite a smaller absorption cross section, the molecule can be excited up to the dissociation

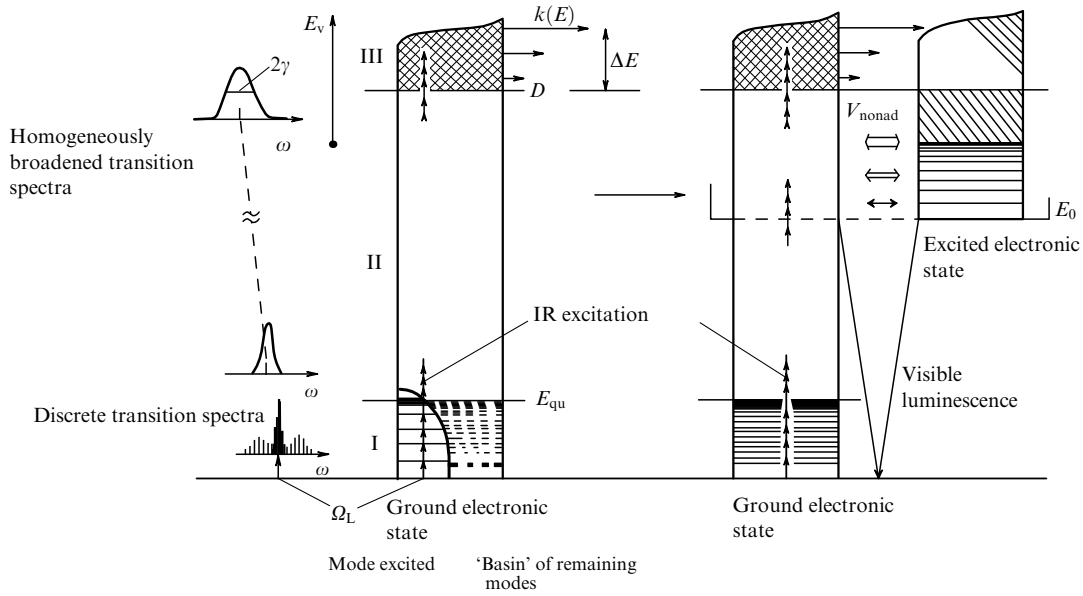

Figure 1. Molecular states and processes inherent in the IRMPE of molecules; $k(E)$ — molecular dissociation rate, γ — homogeneous broadening of the transition spectrum, and Ω_L — laser radiation frequency.

threshold or above it, given the high energy density of the laser pulse. The interaction between levels in this region leads to stochastization of vibrational energy E_v — that is, to the rapid intramolecular redistribution of E_v over all vibrational modes and to the loss of mode selectivity. It is worth noting, however, that recent studies on molecular excitation by ultrashort femtosecond laser pulses (see, for instance, Refs [55 – 57]) have demonstrated mode selectivity of the excitation of upper vibrational levels. These interesting findings deserve special discussion and are beyond the scope of the present review.

In the region above the dissociation threshold, the process of monomolecular dissociation begins to compete with the excitation process. The possible level of overexcitation (i.e., excitation to states above the dissociation threshold) is determined by the relationship between the radiation excitation and molecular dissociation rates [10, 12]. As shown in a large number of experiments, the latter process is fairly well described by statistical theories of monomolecular reactions [58, 59].

If polyatomic fragments are formed in the course of molecular dissociation, they may also be involved in MPA and further dissociate into smaller residues.

The subdivision of an MPE process into the above-listed stages facilitates the qualitative description of the main features of a rather complicated process of nonlinear interactions between IR radiation and a quantum system (polyatomic molecule) having a large number of degrees of freedom. Such a simple model was gradually formulated based on a few key ideas put forward at an early stage of research. The concept of gentle compensation for the anharmonism on lower vibrational transitions (in particular, due to a change in rotational energy) was proposed by Ambartsumyan et al. [60]. The role of multiphoton processes in the region of lower vibrational levels was considered in works [61, 62]. The idea of nonresonant excitation of molecules during transitions between high-lying vibrational states arranged in a quasi-continuum was advanced in Ref. [63] and thereafter discussed in Refs [64 – 67]. Direct experiments on molecular dissociation by double-frequency IR radiation (resonant IR field plus nonresonant IR radiation for lower transitions) confirmed the validity of this qualitative model [68 – 70]. The importance of mixing (or stochastization) of different vibrational modes during the excitation of only one vibrational degree of freedom by IR radiation was discussed by Shuryak [71]. The extent of molecular vibrational overexcitation was examined in Refs [39 – 41, 72]. These experiments with molecular beams demonstrated that dissociation occurs by the rupture of the weakest bond, and subsequent photodissociation of primary fragments is responsible for the appearance of even smaller residues [73].

Numerous later studies of the MPE and MPD of a large number of different molecules confirmed the above qualitative picture (see, for instance, reviews [7, 8, 11, 54, 74]). In addition, they provided a deeper insight into the mechanism of the molecular MPE process. Further development of the simple model described above yielded a more detailed model (see Fig. 1). The most important modification involved taking into account the evolution of the IR absorption spectrum of a vibrational mode (resonant with the IR radiation) that parallels the increase in vibrational energy of the entire molecule [38, 75 – 78].

In the foregoing, we have considered the MPE and MPD of molecules, induced by intense IR laser radiation and involving processes supported by the whole set of vibrational levels of the ground electronic state. Also possible are situations where an excited electronic state bound up with the ground-state term by a nonadiabatic or spin-orbital interaction is below the dissociation threshold for the latter term (see Fig. 1). Then, vibrational levels of the ground electronic state, lying above the energy E_0 of the 0 – 0 ($E_v > E_0$) transition, mix with the levels of the excited electronic state bound up with the ground state by a dipole-allowed transition. As a result, IRMPE of molecules leads to the appearance of luminescence in the visible or ultraviolet (UV) regions of the spectrum. This process, the theory of which was developed in Refs [79, 80], is referred to as 'inverse electronic relaxation' (IER). Its first experimental examination was reported in Refs [81 – 83].

Thus, a full scheme of molecular levels and processes inherent in the MPE of molecules in an intense IR laser field can be represented as in Fig. 1. The region of lower vibrational levels ($0 \leqslant E_v \leqslant E_{qu}$) is characterized by structured (discrete) transition spectra. In this region, with the vibrational energy largely localized in the excitable mode, isotopic selectivity of the dissociation process is formed. It is especially difficult to describe the MPE of molecules in this region because there is no quantitative theory explaining molecular excitation here. The cause is the lack of comprehensive spectroscopic information on the totality of lower vibrational – rotational levels of a given molecule and the difficulty of describing its excitation by real multimode radiation of pulsed IR lasers (see Sections 5.3 and 6). Conversely, the excitation in the vibrational quasi-continuum region ($E_{qu} \leqslant E_v \leqslant D$) is fairly well investigated (see, for instance, Refs [84 – 92]). This region is characterized by homogeneously broadened transition spectra, which ensures the resonant character of interactions between molecules and laser radiation. Here, rapid intramolecular relaxation of the vibrational energy occurs starting from a certain threshold value [93]. The uniform energy distribution over all modes accompanies the loss of mode selectivity. When an excited electronic state lies below the dissociation energy of the ground-state term, the IER — that is, luminescence in the visible or UV region of the spectrum — is likely to develop (see Section 3.3). Finally, molecular dissociation takes place in the region $E_v > D$, being well described by the theories of monomolecular reactions [58, 59].

3. Methods of investigation

3.1 Production of gasdynamically cooled jets and flows

Gasdynamically cooled molecular jets are produced in effluxing a gas through a nozzle into a vacuum chamber where its temperature drops substantially due to adiabatic expansion [22, 23]. In the approximation of an ideal gas in a continuous gasdynamic jet, the flux is proportional to $p_{noz}\, d^2 T_0^{-1/2}$ [94], where d is the diameter of the nozzle opening, while p_{noz} and T_0 are the pressure and the temperature of the gas above the nozzle, respectively. Molecular jets are normally produced using nozzle openings from approximately 5 to 100 μm in diameter. The upstream gas pressure can be changed from hundreds to a few thousand torrs and the gas normally has an ambient temperature. For example, at $d = 50$ μm, $p_{noz} = 2$ atm, and $T_0 = 300$ K, the gas flux is ≈ 4 atm cm^3 s^{-1} (≈ 0.16 mmol s^{-1}). It should be recalled that rather large diffusion pumps are needed to exhaust such a gas flux at a pumping rate of about

10,000 l s^{-1} for helium (and about 4000 l s^{-1} for nitrogen) and a blank-off working pressure of roughly 3×10^{-4} Torr. Using a skimmer, it is possible to separate a molecular beam from a gasdynamically cooled jet. A molecular jet bounded on two or four sides may be regarded as a molecular flow. Such a jet is possible to transform into a molecular beam having the intensity $I \geqslant 2 \times 10^{19}$ molecules (sr s)$^{-1}$. The concentration of molecules in this jet (or beam) some 10 cm from the nozzle is $N \approx 2 \times 10^{12}$ cm^{-3}. Molecular jets and beams with an intensity 2 or 3 orders of magnitude higher are produced using pulsed nozzles [95–97], as a rule with the diameter of the opening from 0.1 to 2 mm.

There are a variety of nozzle types designed to produce pulsed molecular jets [97]. The most common ones include (1) solenoid-controlled nozzles (automobile fuel injectors belong to this type); (2) nozzles with a piezoelectric control mechanism, and (3) nozzles of the 'current loop' type [95–97]. Type 1 nozzles produce pulses from hundreds of microseconds to several milliseconds in duration. Type 2 nozzles are used to produce pulses from approximately 100 μs to 10 ms. 'Current loop' type nozzles generate pulses as long as 30–40 to 150 μs. This last type was employed to obtain molecular beams, jets, and flows in all our studies reported in this review.

The use of molecular beams and jets in experiment implies knowledge of their characteristics [95, 97]. Hence, it is paramount to develop methods for the detection of molecular beams and exploration of their properties. Major characteristics of pulsed molecular beams include intensity, duration, velocity, and the spread of molecular velocities within the beam (the extent to which the gas is cooled). A very important parameter of molecular beams is the energy distribution over the internal degrees of freedom of the molecules (the distribution of molecules over quantum states). We do not consider here methods for detecting and examining molecular beams, since they are described at length in Refs [35, 36, 98, 99]. The most popular of them have been discussed in the recent review [100] (see also Ref. [101]). In what follows, the emphasis will be placed on the methods for the study of molecular excitation and dissociation in beams and jets (see Sections 3.2–3.5), which were used in the studies reviewed in this work.

3.2 Pyroelectric method for the detection of absorbed energy

Most studies on the IRMPE of molecules, included in this review, employed a noncooled pyroelectric detector (PED) to measure the absorbed energy and diagnose molecular beams and jets. A method for the detection of kinetic and internal molecular energies in beams and jets with the help of a PED and a pulsed CO_2 laser was proposed in Ref. [102]. Such a detector had previously been utilized successively to measure the IRMPA of molecules in a cell under static conditions [103, 104], and in a molecular beam [26, 47].

A PED depends for its operation on the changes in the spontaneous dipole moment or spontaneous polarization of a pyroactive element in response to temperature variation. The construction of the detector was described in detail in Ref. [103] (see also Ref. [100]). Its rather good time resolution ($\tau_T \approx 3-5$ μs) is advantageous in that it permits us to obtain time-of-flight (TOF) spectra of molecules in a pulsed beam or jet and thereby measure both the kinetic and internal molecular energies.

The method for the detection of molecular beams and jets using a PED was described at length in Refs [27, 102] (Fig. 2)

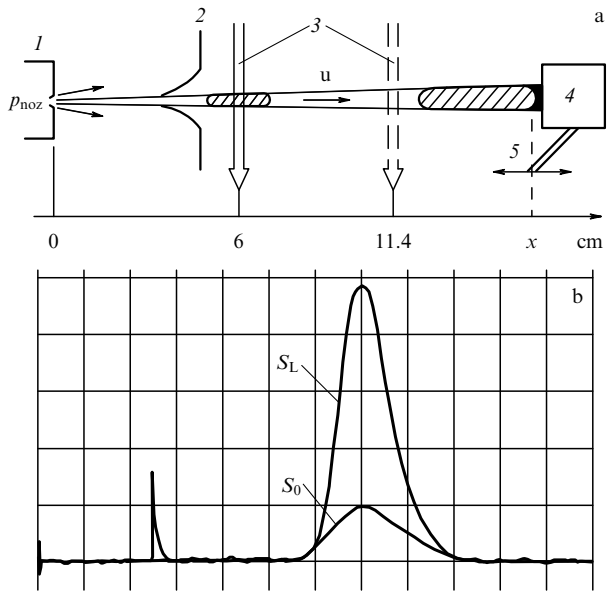

Figure 2. (a) Schematic of the experimental facility: *1* — pulsed nozzle, *2* — skimmer, *3* — laser beams, *4* — pyroelectric detector, *5* — mechanical device to move the detector. Hatched areas depict a 'bunch' of pulsed beam molecules separated from the jet by the skimmer. (b) Oscillograms of the TOF spectra of beam molecules without (S_0) and with (S_L) excitation by a laser pulse. The peak to the left of the TOF spectra is a signal induced by the laser pulse.

and is based on the measurement of the energy of molecules that reach the surface of the active element of the device where the energy is transformed into heat. A signal thus induced by beam molecules is preamplified (×100) and fed to an oscillograph. Experiments were carried out both with a molecular beam formed by a skimmer and without forming a beam. In both cases, the detector measured the energy of the molecules propagating within a solid angle which depended on the dimensions of the active element (4×4 mm^2) and the distance between the nozzle and the PED. This distance could be changed by mechanically moving the PED along the beam axis, which made it possible to measure TOF spectra of molecules in the beam at different distances from the nozzle. These spectra were employed to evaluate the kinetic energy distribution of the beam molecules. In addition, the internal energy of the molecules was measured after they were excited by laser radiation.

In the absence of an exciting laser pulse, a signal from the detector is proportional to the quantity

$$S_0 \sim nv\left(E_a + E + \frac{mv^2}{2}\right) \sim nvE_0\,, \tag{3.1}$$

where n is the number density of the molecules at the surface of the detector, v and m are the velocity and the mass of the molecule, respectively, E is the molecular energy (the sum of vibrational, rotational, and 'local' translational energies), E_a is the absorption heat per molecule, and E_0 is the total energy of a molecule (the expression in parentheses). The signal resulting from the vibrational excitation of molecules by a laser pulse is proportional to the quantity

$$S_L \sim nv(E_0 + E_{ab})\,, \tag{3.2}$$

where E_{ab} is the energy absorbed by a molecule from the laser pulse. Thus, an additional signal induced on the detector

(lacking in the absence of molecular excitation) is a measure of the laser-pulse energy absorbed by the beam molecules upon their vibrational excitation [27, 102].

The translational, rotational, and vibrational temperatures of the beam molecules were determined by analyzing the experimentally found TOF distributions of 'cold' and vibrationally excited molecules [27, 102]. The analysis of the TOF spectra was performed using the standard (two-parametric) expression for the number density distribution of the molecules over velocities in a supersonic molecular beam [22 105]:

$$n(v) \sim \left(\frac{v}{u}\right)^2 \exp\left[-\frac{(v-u)^2}{\alpha^2}\right], \tag{3.3}$$

where u is the mean velocity of the molecules in the beam, $\alpha = (2kT/m)^{1/2}$ is the most probable velocity of the molecules in the beam frame of reference, and k is the Boltzmann constant. We also allowed for the balance of energies of the molecules before and after their emergence from the nozzle. Thus, the method in question made it possible to measure both the kinetic energy of molecules in a beam and their internal energy [27, 102].

3.3 Inverse electronic relaxation as a tool for studying the IRMPE and IRMPD of OsO_4 molecules

IR multiple photon excitation and dissociation of OsO_4 molecules in the studies being reviewed were examined by detecting visible luminescence resulting from IER [81]. As related in Section 2, IER is the process of conversion of the vibrational energy of a molecule to the electron excitation energy [81, 106]. Such transformation leads either to the dissociation of molecules in the excited electronic state or to emission in the UV or visible regions of the spectrum. Inverse electronic relaxation was observed in about 10 molecules (see, for instance, Refs [106, 107] and references cited therein). We discovered it for the first time in the experiments described in Ref. [81] where visible luminescence was observed and identified during IRMPE of OsO_4 molecules. It was shown in work [108] that luminescence intensity is proportional to the dissociation yield of the molecules due to the small difference between the dissociation energy and the energy of the excited electronic state, $\Delta E = D - E_0$, compared with the width of OsO_4 vibrational distribution during the IRMPE of these molecules.

The discovery of IER and the establishment of a direct relationship between luminescence intensity and dissociation yield of OsO_4 molecules proved very helpful for the study of IRMPE and IRMPD of OsO_4 [52, 53, 109, 110], including those in molecular beams and jets [53, 111, 112]. The value of the method for the study of IRMPE based on the observation of IER is in its high sensitivity and the possibility of gathering information during a single pulse because the luminescence intensity is a measure of the dissociation yield per pulse.

3.4 Method for the detection of HF^* luminescence

In the studies of excitation and dissociation of SF_6 molecules, HF^* luminescence (in the 2.5-μm region) that accompanies SF_6 dissociation in the presence of H_2 or CH_4 molecules was detected [113]. Vibrationally excited HF^* molecules were produced in the reaction between fluorine atoms (the primary products of SF_6 dissociation) and hydrogen or methane. The HF^* luminescence intensity correlated well with the dissociation yield of SF_6 [114, 115]. Therefore, in similar manner to the detection of visible luminescence, information about molecular dissociation can be obtained during a single pulse. Notice that this method is rather frequently applied when studying IR dissociation of UF_6 molecules (see, for instance, Ref. [116]).

3.5 Miscellaneous methods for measuring absorbed energy and dissociation yield of molecules

A number of other experimental procedures were used in the works reviewed here. In a study on the IRMPA of SF_6 molecules in a gasdynamic flow with Ar, the absorbed energy was measured by a colorimetric method [33, 34]. It is worthwhile to note that this classical method is infrequently employed in experiments with molecular beams, jets, and flows because of weak energy absorption in a rarefied gas. It was possible to apply this method to the study under consideration by virtue of the large size of the outflow from a 50-cm-long slotted nozzle. The length of the absorbing layer was 1 m owing to the realization of a two-pass scheme. For this reason, the optical density of the absorbing layer even in the presence of a rarefied-gas flow was around 0.03 – 0.25 [33]. This allowed the energy absorbed during the IRMPE of molecules to be directly measured by the colorimetric method. With this technique, the energy absorbed by the molecules was estimated from the measured energy of laser radiation incident on the flow and passing through it (see Section 4.7).

Direct detection of molecular dissociation products and residual post-irradiation gas was also employed in experiments on CF_3I dissociation and in a few studies with SF_6 molecules. These methods are based on the analysis of IR absorption spectra and mass spectra of gases prior to and after irradiation. They are characterized in more detail in Section 6.1.3 and in other sections where concrete experiments are described.

Experiments on the dynamics of the excitation of molecules (SF_6 and NH_3) from individual rotational sublevels were based on the double IR – IR resonance technique with the application of tunable narrow-band pulsed diode lasers to probe the excited molecules. A detailed description of this method is presented in Sections 5.2 and 5.3.

4. Spectral and energy characteristics of IRMPE of molecules

4.1 Energy characteristics of IRMPA

Because multiple photon absorption underlies isotopically selective dissociation of molecules by intense IR laser radiation, studies of MPA in a strong IR field are of primary importance for understanding this phenomenon. For this reason, investigations into MPA [3, 117, 118] were initiated very soon after the first successful experiments on selective molecular dissociation [1, 2].

Studies of IR multiple photon absorption by SF_6 [26 – 28] and CF_3I [42] molecules in gasdynamically cooled molecular beams (for $T_{vib} \leqslant 160$ K and $T_{rot} \leqslant 40$ K) demonstrated that the character of MPA was substantially different from that in a cell at room [3, 117, 118] or low [119 – 121) temperature. The dependences of the absorbed energy E_{ab} on the energy density Φ of the exciting radiation have the form $E_{ab} \sim \Phi^n$, where $n > 1$. Hence, they reflect the multiple photon character of interactions between molecules and IR radiation. When molecules are excited in a cell at $T \approx 300$ K, the index $n < 1$

[122, 123]. The dependences of the form $E_{ab} \sim \Phi^n$ with exponent of a power n in the range $1 \leqslant n \leqslant 1.8$ were earlier observed in Ref. [124] upon excitation of SF_6 molecules cooled to $T \approx 137$ K in a cell at the frequencies of the 10P(20) and 10P(24) CO_2-laser lines near which peaks of two- and three-photon resonances of SF_6 are located [125, 126]. In the case of SF_6 excitation in a pulsed jet, the dependences of the form $E_{ab} \sim \Phi^n$ with $n > 1$ were observed at practically all pumping frequencies (see also Ref. [28]) including the $\nu_2 + \nu_6$ vibrational band [48]. Similar dependences with $n > 1$ were recorded upon the excitation of gasdynamically cooled CF_3I molecules in a beam [42]. In the case of both SF_6 and CF_3I molecules, n values grew (to 2–3) upon a shift in the excitation frequency to the violet side from the linear absorption spectrum (LAS) of the molecule. Here, multiple photon transitions in the system of lower vibrational–rotational levels appeared to be more prominent.

Figure 3 depicts the dependences of the absorbed energy E_{ab} on the energy density Φ of the exciting pulse for the P(18), P(16), and P(14) lines from the 10.6 -μm CO_2-laser generation band [27], the frequencies of which coincide with those of the P-, Q-, and R-branches of the SF_6 LAS for $T_{rot} \leqslant 40$ K [24]. The absorbed energy is fairly well described by the $E_{ab} \sim \Phi^n$ dependence, where n varies roughly from 0.5–0.6 in a range of $\Phi \leqslant 0.1-0.2$ J cm^{-2} [for the P(14) and P(16) lines] to 1.4–1.7 in a range of $0.2 \leqslant \Phi \leqslant 2$ J cm^{-2} (for all three lines). The slope of the dependences decreases again with a further rise in the energy density. As a general rule, the slope of the $E_{ab}(\Phi)$ dependences increases upon a shift in the excitation frequency toward the short-wave region of the LAS. Specifically, $n \approx 1.2-1.4$ when SF_6 is excited on the 10P(20)–10P(26) lines, $n \approx 2$ on the 10P(12) line, and $n \approx 2.5-3$ on the 10P(10) line [45, 46]. These results suggest the importance of multiple photon transitions in the system of lower vibrational levels for the excitation of SF_6 molecules cooled in a pulsed jet under collisionless conditions.

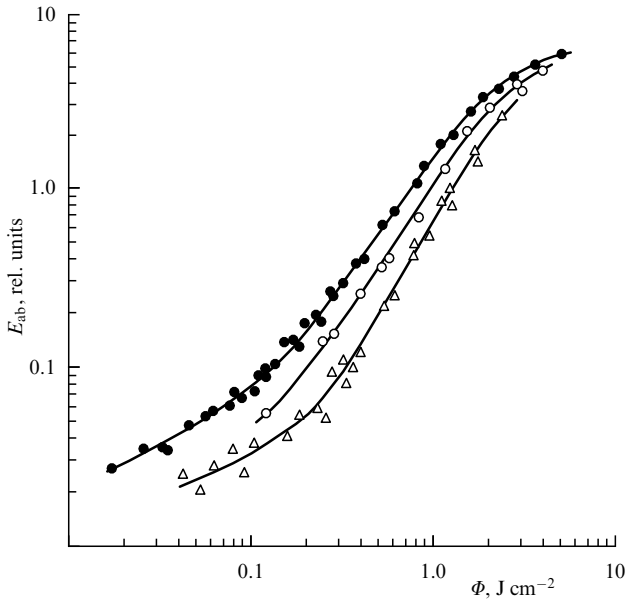

Figure 3. Energy absorbed by SF_6 molecules versus the energy density of exciting radiation for the P(14) (Δ), P(16) (•), and P(18) (○) lines from the 10.6-μm band of a CO_2 laser. Molecules in the jet were excited at 11.4 cm from the nozzle. The pressure of SF_6 above the nozzle was 5 atm. The nozzle was placed at 16.8 cm from the detector. Jet parameters were as follows: $T_{vib} \leqslant 160$ K, $T_{rot} \leqslant 40$ K. (Taken from Ref. [27]).

A decreased slope of the $E_{ab}(\Phi)$ dependences for $\Phi \geqslant 2.5$ J cm^{-2} can be accounted for by the saturation of transitions in the quasi-continuum region, as well as by the dissociation of molecules and their 'escape' from the beam [27, 42]. The maximum absorption upon excitation on the P(16) line is due to the fact that the frequency of this line is minimally detuned from that of the Q-branch for the $\nu_3 = 1 \leftarrow \nu_3 = 0$ transition of the excitable ν_3 vibration and to the rather low rotational and vibrational temperatures of SF_6 ($T_{rot} \leqslant 40$, $T_{vib} \leqslant 160$ K) [27] at which the ground level population is relatively large ($\approx 85\%$ [127]). Under these conditions, the laser radiation on the 10P(16) line interacts with a maximum number of molecules [26, 27].

It follows from Fig. 3 that the molecular absorption cross section σ in a range of $0.2 \leqslant \Phi \leqslant 2$ J cm^{-2} increases with increasing excitation energy density [26, 27]. Indeed, it can be shown that

$$\sigma = -\frac{\ln(T)}{Nl}\,, \tag{4.1}$$

where $T = E_{out}/E_{in}$ is the gas transmission (E_{in}, E_{out} are the incident and transmitted energies, respectively), N is the gas concentration, and l is the length of the absorbing layer. Because only a small fraction of the incident energy was absorbed in the experiments under consideration [26, 27] due to the small optical density of the beam, so $\ln(T)$ can be expressed to sufficient accuracy as

$$-\ln(T) = \ln\left(1 + \frac{E_{ab}}{E_{in} - E_{ab}}\right) \sim \frac{E_{ab}}{E_{in}} \sim \frac{E_{ab}}{\Phi}\,. \tag{4.2}$$

Thus, the absorption cross section is proportional to the slope of the $E_{ab}(\Phi)$ dependence. A larger absorption cross section for $0.2 \leqslant \Phi \leqslant 2$ J cm^{-2} can be accounted for by the multiphoton nature of interactions in the region of lower vibrational levels [26, 27]. It is worth noting that many experiments conducted with molecules at room temperature failed to show a rise in the MPA cross section [122, 123]. It was documented only in the case of collisionless molecular excitation in gasdynamically cooled beams where a very small fraction of molecules interacted with radiation [26–28].

Finally, let us briefly review the results of experiments concerned with investigating IRMPA of a 'large' polyatomic $(CF_3)_3CBr$ molecule in a beam [128, 129]. It has been shown [128] that the excitation of $(CF_3)_3CBr$ in a molecular beam (as opposed to gas excitation in a cell at room temperature [130]) results in a considerable reduction in the MPA cross section (saturation of absorption) for the excitation energy density $\Phi \geqslant 0.8$ J cm^{-2}. The reduced MPA cross section is largely attributable to two causes: (1) dissociation of molecules during the exciting laser pulse action [130, 131], and (2) redshift of the MPA spectrum for vibrationally excited molecules due to anharmonism. Probing excited molecules with a second laser pulse [128] has demonstrated that the decrease in the absorption cross section is related to the displacement of the spectrum of vibrationally excited molecules to longer wavelengths rather than to molecular dissociation under effect of the pumping pulse. As a result, the molecules are out of resonance with the laser pulse. This evidence is confirmed by the measurement of the lifetime of vibrationally overexcited (i.e., excited beyond the dissociation threshold) molecules in crossed laser and molecular beams [129].

Also, it was shown in Refs [128, 129] that double-frequency IR excitation is a more efficient mode of generat-

ing strongly overexcited $(CF_3)_3CBr$ molecules under collisionless conditions (as is the case with 'medium-sized' molecules). Experiments reported in Refs [128, 129] demonstrated that the IRMPE of molecules under saturation of $E_{ab}(\Phi)$ makes it possible to produce large concentrations of vibrationally overexcited long-lived $(CF_3)_3CBr$ molecules (with lifetimes of $10^{-3}-10^{-4}$ s prior to the dissociation). An opportunity appears for utilizing such molecules in experiments, in particular, for measuring IR absorption spectra of overexcited molecules (see, for instance, Refs [75, 132]) and their lifetimes on a real time scale [129, 133].

4.1.1 Estimation of the number of interacting molecules. The data presented in Fig. 3 can be used to estimate a fraction of the molecules excited in a beam that interacts with laser radiation [109]. It was shown in works [26, 27] that the fraction of interacting molecules at a moderate radiant energy density (about $0.1-0.2$ J cm^{-2}) is essentially smaller (in $2-5$ times) than in the case of SF_6 excitation in a cell at room temperature [104, 134, 135]. Such a situation is due to a sharp fall in the number of resonant transitions as a result of gas cooling, as well as of the lack of molecular collisions at which this fraction would be bigger by virtue of rotational relaxation [26, 27].

4.1.2 Effect of vibrational temperature on MPA. The above results were obtained with SF_6 molecules at the vibrational temperature $T_{vib} \approx 160$ K, when 85% of the molecules resided in the ground vibrational state [127]. Under these conditions, the absorption is largely due to radiation transitions from the ground state. Also of interest is the case of rather narrow rotational distribution of molecules possessing at one time the vibrational distribution which is not substantially different from the distribution at room temperature. Notice that such conditions are normally realized in continuous gasdynamic jets and flows (see Section 4.7). Under these conditions, at excitation frequencies detuned toward the red side from the frequency of the Q-branch of the SF_6 LAS (≈ 948 cm^{-1} [136]), the absorption occurs from upper vibrational levels that are densely populated at a high vibrational temperature. Some 30% of the SF_6 molecules reside at the ground level at room temperature [127].

The influence of vibrational temperature on MPA was comprehensively investigated in work [47] (see also Ref. [27]). In Ref. [47], measurements were taken in molecular beams and jets with roughly equal rotational but different vibrational temperatures of molecules. Such beams were produced in the following way. It is well known that in the course of free gas expansion from a nozzle into a vacuum, vibrational temperature becomes 'frozen' much earlier than the rotational one [22]. This means that the ratio between temperatures T_{rot} and T_{vib} strongly depends on the distance between the nozzle and the observation area. Therefore, by placing the skimmer at different distances from the nozzle, it is possible to separate molecular beams with different T_{rot}/T_{vib} ratios from a free jet. For example, with the skimmer positioned 2.5 cm from the nozzle, we managed to obtain a beam in which rotational and vibrational temperatures of the molecules at 6 cm from the nozzle were $T_{rot} \leqslant 50$ K and $T_{vib} \approx 230$ K, respectively [47]. At such a vibrational temperature, only 55% of the molecules remained in the ground state, while the remaining ones were distributed over higher vibrational states [127]. Rotational and vibrational temperatures of the molecules at the same distance from the nozzle in the absence of the skimmer were $T_{rot} \leqslant 40$ K and $T_{vib} \leqslant 160$ K, respectively [47].

Analysis of the $E_{ab}(\Phi)$ dependences in the range $\Phi \approx 0.2-4$ J cm^{-2}, obtained at the same excitation frequencies, demonstrated [27, 47] that at $T_{vib} \approx 230$ K, the maximum absorption occurs at the frequency of the 10P(18) laser line (945.98 cm^{-1}) — that is, at a lower frequency than at $T_{vib} \approx 160$ K. The $E_{ab}(\Phi)$ dependence at this frequency is less steep ($n \approx 1.1$) than at $T_{vib} \approx 160$ K ($n \approx 1.4$). Conversely, in the case of excitation at the frequency of the 10P(14) line, the slope of the $E_{ab}(\Phi)$ dependence is even steeper ($n \approx 3$) than that shown in Fig. 3 ($n \approx 1.8-2$). The absorption upon irradiation at the frequency of this line at $T_{vib} \approx 230$ K is significantly smaller than at the frequencies of lines 10P(16) and 10P(18).

Such behavior of the dependences can be accounted for in the following way. Laser radiation at the frequency of the 10P(18) line at $T_{vib} \approx 230$ K effectively interacts with molecules in both ground and higher vibrational states. The fraction of interacting molecules is significantly larger than at $T_{vib} \approx 160$ K. In contrast, in the case of excitation at the frequency of the 10P(14) line, the fraction of interacting molecules at $T_{vib} = 230$ K is smaller than at $T_{vib} \approx 160$ K, because only those molecules that occupy the ground level and whose population at $T_{vib} \approx 230$ K is approximately 1.5 times smaller than at $T_{vib} \approx 160$ K interact with the laser radiation [127]. Thus, the findings reported in Refs [27, 47] have demonstrated that both the absolute value of absorbed energy and the shape of the $E_{ab}(\Phi)$ curves strongly depend on the initial fraction of interacting molecules. This fraction is in turn dependent on pulse intensity and gas temperature — that is, on the molecular distribution over rotational and vibrational states (see Sections 4.2 and 5).

4.2 The role of exciting pulse intensity (duration) in the MPA and MPD of molecules

Results of the studies on SF_6 [45, 46] and CF_3I [42] excitation in a molecular beam allowed the role of exciting pulse intensity (duration) to be elucidated in the MPA and MPD of molecules. Experimental variation of pulse intensity was achieved by using pulses of equal energy but different duration. The latter was varied either by a change in the composition of the laser mixture or by the laser pulse shortening (e.g., by arranging the optical breakdown of the air in the focus of a telescope placed in the path of the laser beam). In works [45, 46], the pulse duration varied from some 40 ns to 1 μs, and the averaged pulse intensity increased by a factor of 25.

These studies demonstrated that, the excitation energy density being rather small ($\Phi \leqslant 0.1-0.2$ J cm^{-2}), the energy absorbed by the molecules strongly depends on pulse intensity. With increasing energy density, the distinction between MPAs at long and short pulses decreases. For example, at $\Phi \approx 0.2$ J cm^{-2}, an increase in the averaged pulse intensity by a factor of 25 leads to an approximately $9-10$-fold rise in radiation absorption by SF_6 molecules. At $\Phi \approx 3-4$ J cm^{-2}, there is practically no difference between MPAs at long and short pulses [45, 46]. This is due to the fact that the fraction of interacting molecules at a high energy density is close to unity; in other words, almost all molecules are already excited to high-lying states. Moreover, it was shown in works [45, 46] that the SF_6 dissociation yield under collisionless excitation conditions in a cell at room temperature also depends on pulse intensity. The dissociation yield is

much higher (by a factor of 1.5 – 5 depending on the excitation frequency) when the pulses are short. We observed similar dependences of the absorbed energy and dissociation yield on pulse intensity during excitation of CF_3I molecules in a pulsed molecular beam [42]. This also suggests a multiphoton character of molecular excitation in the region of lower vibrational levels.

To summarize, the results of the above studies with gasdynamically cooled SF_6 and CF_3I molecular beams indicate that:

(1) the fraction of molecules interacting with laser radiation at a moderate radiant energy density is significantly smaller than in the case of molecular excitation in a cell at room temperature;

(2) both the absorbed energy and the dissociation yield strongly depend on pulse intensity;

(3) the role of pulse intensity is in turn essentially dependent on the excitation frequency (fraction of interacting molecules);

(4) a strong pulse intensity dependence of the absorbed energy and the dissociation yield is apparent only under collisionless excitation conditions when the fraction of molecules involved in the interaction with laser radiation is determined by the radiation mechanism alone. Collisions between molecules are responsible for the lessening of the difference between the values of the absorbed energy and the dissociation yield for pulses of varying durations. Under certain conditions, they can result in a greater radiation absorption at long pulses [137 – 139]. Experiments in works [45, 46] provided radiation intensity values ($\approx$ 100 MW cm^{-2}) above which the intensity dependence of the dissociation yield is not evidenced if SF_6 molecules are excited by a CO_2 laser pulse of the 'conventional' shape (i.e., comprising a spike with a half-height duration of about 100 ns, and a 0.6-μs tail).

A different situation takes place when 'large' molecules are excited. As demonstrated in Ref. [128], the MPA of $(CF_3)_3CBr$ molecules is independent of pulse intensity but shows close-to-linear dependences $E_{ab}(\Phi)$ in a wide range of radiant energy density (up to $\Phi \approx 0.8$ J cm^{-2}). This may be due to the high spectral density of the molecular transitions (low quasi-continuum spectrum edge) accounting for a minor role of multiphoton processes.

4.3 Spectral characteristics of MPA of molecules

4.3.1 MPA spectra of SF_6 and CF_3I in a pulsed molecular beam. This section is devoted to studies of spectral characteristics of MPA of molecules (exemplified by SF_6 and CF_3I). The importance of such investigations is first and foremost due to the fact that spectral characteristics of the MPA determine selectivity of excitation and dissociation processes. Peculiarities of the spectral structure provide information about mechanisms of molecular excitation in the lower transition region. Moreover, the spectral structure reflects manifestation of the effects of vibrational and rotational temperatures on the formation of selectivity. MPA spectra of SF_6 molecules cooled in a pulsed jet were investigated in Refs [26 – 28, 30, 32, 33, 47 – 49]. It has been shown that the half-height width of these spectra is $\Delta\nu \leqslant 5$ cm^{-1} at the energy density $\Phi \approx 0.05$ – 2.0 J cm^{-2} (Fig. 4), i.e., much smaller than that of SF_6 in a cell at room and low ($T \approx 137 - 172$ K) gas temperatures: $\Delta\nu \approx 14 - 16$ cm^{-1} [117, 118, 124] and $\Delta\nu \approx 8$ cm^{-1} [119, 121, 124, 140], respectively.

MPA spectra of CF_3I molecules cooled in a pulsed jet were examined in Refs [42, 44]. These spectra were found to

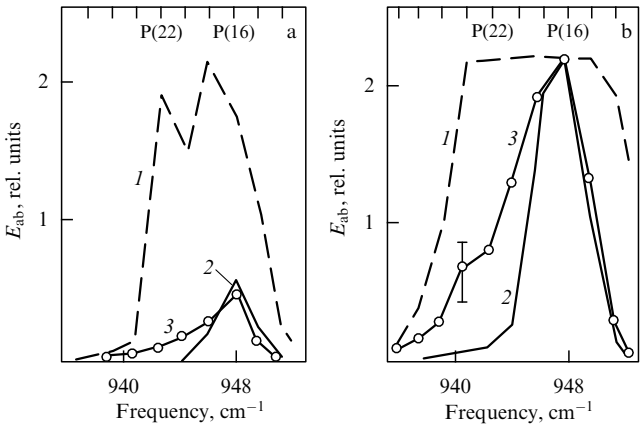

Figure 4. Spectral dependences of the energy absorbed by SF_6 molecules at an excitation energy density of 0.5 J cm^{-2} (a) and 2.5 J cm^{-2} (b). Dependences *1* (first model) and *2* (second model) result from the computed spectra at $T = 40$ K, $\tau_p = 100$ ns and on the assumption of isolated molecules [143] (see the text). Dependences *3* are the experimentally found MPA spectra of SF_6 in a molecular beam ($T_{vib} \leqslant 160$ K, $T_{rot} \leqslant 20$ K, $\tau_p \approx 80$ ns) [26, 27].

have the half-height width $\Delta\nu \leqslant 8$ cm^{-1} [42]; in other words, they were much narrower than MPA spectra of molecules in a cell at room and low ($T \approx 168$ K) gas temperatures: $\Delta\nu \approx 24$ cm^{-1} and $\Delta\nu \approx 16$ cm^{-1}, respectively [141]. Even at the energy density $\Phi \leqslant 0.05$ J cm^{-2}, the MPA spectra of CF_3I molecules showed maxima [42] that might reflect multiple photon transitions in the system of lower vibrational – rotational levels. It should be noted that the structure of MPA and MPD spectra of CF_3I molecules, attributable to transitions in the region of lower vibrational levels, was also observed in works [44, 142] when molecules were excited by a tunable CO_2 laser. Moreover, experiments with CF_3I revealed dependences $E_{ab}(\Phi) \sim \Phi^n$ with $n > 1$ [44].

The small width of the MPA spectra of gasdynamically cooled SF_6 and CF_3I molecules is supposed to be due to low rotational and vibrational temperatures of the molecules in a beam, and to the collisionless nature of excitation. In the case of gasdynamically cooled SF_6 molecules ($T_{vib} \approx 160$ K and $T_{rot} \leqslant 40$ K), the spectral maximum of MPA coincides with the Q-branch of $\nu_3 = 1 \leftarrow \nu_3 = 0$ transition of the excitable ν_3 vibration in $^{32}SF_6$ molecules (≈ 948 cm^{-1}) [136]. It should be emphasized that neither the whole SF_6 MPA spectrum nor its maximum undergoes a redshift as the energy density of laser radiation increases. This observation is at variance with the results of earlier experiments on SF_6 molecules at room temperature [117, 118]. An analysis of this discrepancy will be given in Section 4.4.

4.3.2 Comparison of SF_6 MPA spectra and the results of model computation. Results of our studies on MPA spectra of SF_6 in pulsed molecular beams under conditions of collisionless excitation [26, 27] gave the incentive to model calculations of these spectra. The authors of Ref. [143] proposed two models. In one of them, the widths of lower vibrational levels are assumed to be homogeneous (of order $1/t_2$, where t_2 is the transverse relaxation time), probably due to coupling with other vibrations in the molecule. For this reason, additional terms responsible for this broadening must be included in the Shrödinger equation describing excitation of lower vibrational levels. In the other model, the level width homogeneity is disregarded. Positions of the vibrational – rotational levels

are found taking into consideration their anharmonic splitting and the Coriolis interaction. Calculations were done taking into account all possible stepwise and multiple photon transitions between vibrational levels of the excitable mode ν_3 up to $\nu_3 = 3$ inclusive (the four-level model), the transitions allowed by the conventional selection rules. The IR field was considered to be monochromatic with a rectangular shape of the pulse.

Comparison of the spectra (see Fig. 4) [52] indicates that those obtained in the former model are even qualitatively inconsistent with the experimental MPA spectra of SF_6. Similarly, there is a distinct discrepancy between the observed spectra and those calculated in the framework of the second model (despite certain common features). For example, the experimental spectra are 1.5 – 2 times wider than the theoretical ones. The discrepancy may be due to the fact that experimental and model laser pulses had different shapes and spectral compositions. Specifically, a smooth monochromatic pulse having a half-height duration of 100 ns and no tail was used in the calculations, while the vibrational temperature of molecules was $T_{\rm vib} = 40$ K. The experiments were performed with a multimode pulse comprising a 80-ns spike and a ≈ 0.6-μs tail, while vibrational and rotational temperatures were $T_{\rm vib} \approx 160$ K and $T_{\rm rot} \approx 18$ K, respectively. The theoretical radiation intensity proved to be 2 – 3 times smaller than the experimental one. It was assumed for the purpose of computation that practically all molecules were in the ground vibrational state ($T_{\rm vib} = 40$ K), whereas almost 10% of the molecules in the experiment resided in other low-lying vibrational states where they were more readily excited at frequencies shifted to the long-wave side from the absorption maximum. It is in this region that the observed and calculated spectra were markedly dissimilar.

Paper [143] also reports on calculated frequency dependences of the ratio of energies absorbed by molecules from long and short pulses [45, 46] (see Section 4.2). Results of experiments and the second-model calculations turned out to be in better agreement. However, the models involved fail to explain the high intensity of experimental spectra (large average number of absorbed photons per molecule), even though the spectral dependences of the SF_6 MPA are fairly well described by some other models (see also Ref. [144]). This issue will be considered at greater length in Section 5.

4.4 Factors influencing formation of MPA spectra

Key factors responsible for the formation of MPA spectra of molecules were elucidated in Ref. [47]. For this purpose, we examined the MPA spectra of SF_6 in a molecular beam at different vibrational and rotational temperatures, as well as in a cell at room temperature under relatively low pressure (8.5 mTorr). The effect of collisions on the SF_6 MPA was practically ruled out [104].

As mentioned in Section 4.1.2, we formed a beam of SF_6 molecules with $T_{\rm rot} \approx T_{\rm tr} = (50 \pm 10)$ K and $T_{\rm vib} = (230 \pm 15)$ K using a skimmer placed 2.5 cm from the nozzle [47]. When the skimmer was not in use, rotational and vibrational temperatures in the excitation zone were $T_{\rm rot} \leqslant 40$ K and $T_{\rm vib} \approx 160$ K, respectively. In neither case did the concentration of molecules in the interaction area exceed $N \approx 2 \times 10^{14}$ cm^{-3}. In this way, we were able to study the SF_6 MPA spectra at different rotational and vibrational temperatures under conditions of collisionless excitation. The spectra were measured at the radiant energy density $\Phi \approx 1$ J cm^{-2}. They were compared with each other and with the SF_6 MPA spectrum obtained in work [119] for the excitation of SF_6 molecules in a cell at $T = 147$ K.

These studies showed that the SF_6 MPA spectrum at $T_{\rm vib} = (230 \pm 15)$ K is wider ($\Delta\nu \approx 6.5$ cm^{-1}) than at $T_{\rm vib} = (160 \pm 10)$ K ($\Delta\nu \approx 4.5$ cm^{-1}) and redshifted relative to the spectrum obtained at $T_{\rm vib} = (160 \pm 10)$ K. The spectrum broadens with the increasing rotational temperature of molecules up to 147 K, but the position of the frequency maximum remains unaltered at a given vibrational temperature. The displacement of the MPA spectrum to the long-wave region is due to the fact that only some 55% of the molecules are in the ground state at $T_{\rm vib} = (230 \pm 15)$ K [127], whereas about 45% of them are in higher vibrational states. The absorption spectra of molecules in high-lying states are displaced to the red side as compared with the absorption spectra of molecules residing at the ground level. As a result, the integral spectrum is also shifted towards the long-wave region.

To summarize, experiments with SF_6 molecules [47] (see also Ref. [52]) have demonstrated that the position of the band and the width of the MPA spectrum are largely determined by vibrational gas temperature, i.e., by the initial distribution of molecules over vibrational states. For example, the maxima of the SF_6 MPA spectra at $T_{\rm vib} \approx 160$ K, $T_{\rm vib} \approx 230$ K, and $T_{\rm vib} \approx 300$ K (a case of molecular excitation in a cell at room temperature) occur at frequencies 947.74 cm^{-1} [P(16) laser line], 945.98 cm^{-1} [P(18) laser line], and 942.4 [P(22) laser line], respectively. The experimentally found fact [47, 52] that the MPA spectrum fails to be redshifted with increasing excitation energy density (in the region with $\Phi \geqslant 0.1$ J cm^{-2}) suggests that it is largely formed during lower vibrational – rotational transitions (for $\Phi \leqslant 0.1$ J cm^{-2}).

Analysis of the data obtained in works [47, 52] indicates that the displacement of the MPA spectrum to a longer-wave region with increasing radiant energy density (at least for $\Phi \geqslant 0.1$ J cm^{-2}), observed in earlier studies [117, 118, 124, 140], was due to the effect of molecular collisions because those experiments utilized relatively high gas concentrations ($N \geqslant 10^{16}$ cm^{-3}). Indeed, in the case of a large number of collisions during the course of the exciting laser pulse, rotational relaxation is responsible for the population of many rotational sublevels involved in the radiation absorption of vibrational states (including intermediate ones). This results in a greater contribution from multiphoton and resonant one-photon transitions (e.g., of the $P \to Q \to R$ type [60]) to absorption. The same is true of the contribution from sequential one-photon transitions from all rotational sublevels resonant with the laser field and populated due to rotational relaxation. The absorption cross section for such transitions increases owing to the anharmonicity of vibrations upon a frequency shift towards the long-wave region. Because the average degree of excitation increases with increasing energy density, the MPA spectrum undergoes a corresponding redshift.

In contrast, under collisionless excitation conditions, the contribution of such one-photon transitions to the radiation absorption is negligibly small for the lack of rotational relaxation. Only rotational sublevels populated by the pumping radiation participate in sequential transitions. The absorption cross section in the quasi-continuum region showing weak frequency dependence, the MPA spectrum formed on lower transitions undergoes no substantial change with increasing excitation energy density. Exactly such

behavior of MPA spectra has been observed in experiments with molecular beams [26, 27, 52].

4.5 Structure of the MPA spectra of vibrationally excited SF_6 molecules in a beam

With the use of a single-frequency excitation scheme and a strong IR field, it is not always possible to observe a readily apparent structure of the MPA spectra and unambiguously relate it to certain lower transitions in the molecule. Double-frequency excitation provides more significant opportunities [30, 68–70, 145, 146]. Using a weak IR field of frequency ω_1, an opportunity appears to populate the desired lower vibrational states of the mode being excited and thereafter accomplish probing for the presence of excited molecules at this or that vibrational level by radiation of frequency ω_2. This approach is instrumental in studying IR absorption in the lower transition region of vibrationally excited molecules (VEMs) characterized by different initial energy distributions. The results of one such study on MPA spectra of SF_6 in a pulsed molecular beam [32] are presented below.

4.5.1 Experiment and procedure. Two pulsed CO_2 lasers were used in the study reported in Ref. [32]. Collinear laser beams crossed a molecular beam at a right angle to its axis. The laser beam cross section in the intersection region was 10×8 mm^2. The molecules were excited at a distance of 6 cm from the nozzle. The exciting (ω_1) and probing (ω_2) pulses were separated by 1 ± 0.05 μs. The SF_6 molecular beam in the excitation region had the following parameters [27, 102]: the concentration of molecules $N \leqslant 7 \times 10^{13}$ cm^{-3}, $T_{\rm rot} \approx 20$ K, and $T_{\rm vib} \leqslant 160$ K.

Measurements were made of the total energy E_Σ absorbed by SF_6 molecules from both laser pulses and of the energies absorbed from either of the two pulses, $E_1^0(\omega_1)$ and $E_2^0(\omega_2)$ respectively. In general, the following relationship is valid:

$$E_\Sigma(\omega_1, \omega_2) = E_1^0(\omega_1) + E_2(\omega_1, \omega_2)\,. \tag{4.3}$$

Here, $E_2(\omega_1, \omega_2)$ is the energy absorbed by the molecules from a field of frequency ω_2 after their preliminary excitation by a field with frequency ω_1. Energy E_2 can be represented as

$$E_2(\omega_1, \omega_2) = E_2^{\rm exc}(\omega_1, \omega_2) + E_2^{00}(\omega_2)\,, \tag{4.4}$$

where $E_2^{\rm exc}$ is the energy absorbed by the molecules excited by the first field, and E_2^{00} is the energy absorbed by the unexcited molecules. The $E_2^{\rm exc}$ and E_2^{00} ratio depends on frequency ω_2, but it is important that in all cases

$$E_2^{00}(\omega_2) < E_2^0(\omega_2)\,, \tag{4.5}$$

because $E_2^{00}/E_2^0 = 1 - f_1$, where f_1 is the fraction of molecules excited by radiation of frequency ω_1. In the experiment, the radiant energy density of the first field was $\Phi_1 \leqslant 0.2$ J cm^{-2}; hence, $f_1 \leqslant 0.25$ [26, 27]. Therefore, with a high degree of accuracy ($\geqslant 75$ %), $E_2^{00}(\omega_2) \approx E_2^0(\omega_2)$.

The dependence of the absorbed energy $E_2^{\rm exc}$ on frequency ω_2 of the second field constitutes actually the absorption spectrum of the VEM. It can be found from the measured values of E_Σ, E_1^0 and E_2^0. It follows from relation (4.4) that $E_2^{\rm exc} = E_2 - E_2^{00}$; hence, taking into account Eqns (4.3) and (4.5), we arrive at

$$E_2^{\rm exc}(\omega_2) \geqslant E_\Sigma(\omega_1, \omega_2) - E_1^0(\omega_1) - E_2^0(\omega_2)\,,$$

or, with an accuracy of $(1 - f_1) \geqslant 0.75$, we have

$$E_2^{\rm exc}(\omega_2) \approx E_\Sigma(\omega_1, \omega_2) - E_1^0(\omega_1) - E_2^0(\omega_2)\,. \tag{4.6}$$

This line of reasoning has led to the dependences $E_2^{\rm exc}(\omega_2)$ — that is, the absorption spectra of vibrationally excited SF_6 molecules in a beam [32], although the structure of the VEM absorption spectra is also manifested in the combined spectrum $E_\Sigma(\omega_1, \omega_2)$. It is worth noting that at frequencies detuned from the absorption spectra of unexcited SF_6 molecules, the precision of $E_2^{\rm exc}(\omega_2)$ measurement is significantly higher than indicated in the preceding paragraphs because, in this case, the second radiation field does not practically interact with the unexcited molecules and, hence, E_2^0, $E_2^{00} \ll E_2^{\rm exc}$. A similar method was employed earlier in Ref. [145].

4.5.2 Structural analysis of the absorption spectra of vibrationally excited molecules. When SF_6 molecules are excited in a pulsed molecular beam, almost 85% of the molecules reside in the ground vibrational state, and the width of the linear IR absorption spectrum for the ν_3 vibration does not exceed ≈ 2 cm^{-1} (because only states with $J \leqslant 22$ are populated [51]). This gives reason to think that at moderate energy densities of the first radiation field, $\Phi_1 \leqslant 0.2$ J cm^{-2} (when the power broadening of spectral lines is small), those vibrational sublevels are excited most efficiently for which frequency detunings are ≈ 2 cm^{-1} or smaller.

Let us consider the excitation of SF_6 molecules by the first field at such detunings and frequencies $\omega_1 = 945.98$, 947.74, and 949.48 cm^{-1} that coincide with the LAS frequencies of SF_6 molecules in a beam at $T_{\rm rot} \approx 20$ K and correspond to the P(18), P(16), and P(14) CO_2-laser lines. Figure 5a schematically shows the anharmonically splitted vibrational levels of SF_6 molecules, including $4\nu_3$ and the most resonant vibrational transitions for these frequencies [147–149]. It follows from the figure that frequencies 947.74 and 949.48 cm^{-1} are most resonant with the same vibrational transitions, differing only in the degree of detuning of the IR radiation from these transitions that is approximately twice as much for a frequency of 949.48 cm^{-1}. For this reason, it can be expected that the spectral dependences $E_2^{\rm exc}(\omega_2)$ upon molecular excitation by the first field at the frequencies of the P(16) and P(14) CO_2-laser lines will be similar in shape but quite different in terms of intensity.

It also follows from Figure 5a that, for the P(16) and P(14) lines, detunings for one-photon transitions are approximately two times less than for two-photon ones. Conversely, for the line P(18), detunings for one-photon transitions are 3–4 times those for two-photon transitions. For example, such detunings for a sequence of the first four levels during the excitation of SF_6 molecules at the frequency of the P(18) CO_2-laser line are 2.1, 2.5, and 1.4 cm^{-1} for one-photon transitions, and 0.4, 1.0, and 0.3 cm^{-1} for two-photon ones. For this frequency, there occurs an almost resonant four-photon $0 \to 4E$ transition with a detuning equal to only 0.1 cm^{-1} [148, 149]. This means that, SF_6 being excited at the frequencies of the P(16) and P(14) lines and for relatively small values of the radiant energy density ($\Phi_1 \leqslant 0.2$ J cm^{-2}), the molecules undergo excitation up to the first vibrational $1F_1$ level but less likely to the $2F_2$ and $3A_2$ levels (Fig. 5a). The key role is played here by one-photon transitions, while two-photon transitions are of minor importance. At the frequency of the P(18) line and for $\Phi_1 \leqslant 0.2$ J cm^{-2}, however, the

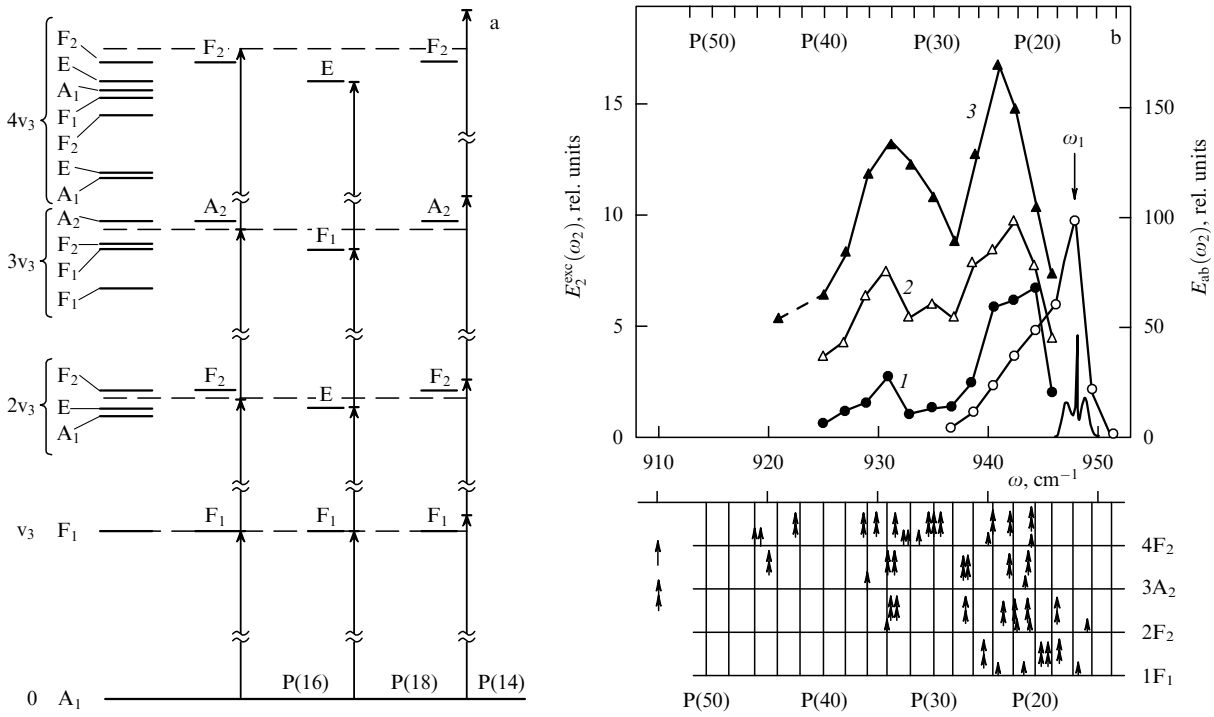

Figure 5. (a) Schematic representation of anharmonic vibrational levels of the $^{32}SF_6$ ν_3 mode [147, 148] and the most resonant vibrational transitions between them during the excitation of molecules at the frequencies of the P(18), P(16), and P(14) lines of the CO_2-laser 10.6-μm band. Straight dashed lines show harmonic positions of the levels for the ν_3 mode. (b) Frequency dependences of the energy absorbed by SF_6 molecules vibrationally excited by pumping at the frequency 947.74 cm^{-1} [10P(16) line] and energy densities Φ_1: *1* — 0.023 J cm^{-2}, *2* — 0.06 J cm^{-2}, and *3* — 0.2 J cm^{-2}. Energy density of the probing field, $\Phi_2 = 0.22$ J cm^{-2}, is constant. For comparison, the MPA spectrum of unexcited molecules ($\Phi_1 = 0$, $\Phi_2 = 0.56$ J cm^{-2}, right scale) and the qualitative LAS pattern of SF_6 molecules in a beam are presented. (Taken from Ref. [32].)

molecules are instantaneously excited up to the 2E level but less likely to the $1F_1$, $3F_1$, and 4E levels. In this case, the two-photon transitions acquire importance. As Φ_1 grows, the probabilities of the population of higher vibrational levels ($2F_2$ and $3A_2$ in the first case, $3F_1$ and 4E in the second case) and of the $1F_1$ state have to increase.

Thus, it follows from the consideration of the structure of transitions in the region of lower vibrational levels [147–149] that excitation of SF_6 in a molecular beam must result in different VEM distributions depending on the exciting field frequency [32]. This, in turn, must be manifested in the VEM absorption spectra as differences in their structure and intensity. In order to predict the expected structure of VEM absorption spectra in a field with the ω_2 frequency, it is necessary (by analogy with the earlier described procedure) to analyze (in accordance with Refs [148, 149]) detunings of the ω_2 frequencies relative to single- and multiphoton transitions from the states excited by the first radiation field. This procedure is easier to depict graphically, as shown for the ω_2 frequencies by one and two arrows, respectively, in Fig. 5b.

The study reported in Ref. [32] was designed to examine VEM absorption spectra taken upon excitation of SF_6 molecules at the frequencies of the P(18), P(16), and P(14) lines of a CO_2 laser. Figure 5b displays the VEM absorption spectra for the case of SF_6 excitation at the frequency of the P(16) line at different energy densities of the first field. For comparison, an MPA spectrum of unexcited SF_6 molecules ($\Phi_1 = 0$) and the qualitative LAS pattern of cooled SF_6 molecules in a beam are also depicted. It can be seen that the experimental results are in good agreement with the predicted ones. Specifically, the absorption maximum at $\Phi_1 = 0.023$ J cm^{-2} is located at the second-field frequency that corresponds to the P(20) CO_2-laser line. At such laser fluence, the $1F_1$ and $2F_2$ states are populated in general. It follows from the detuning diagram that one- and two-photon transitions from the $2F_2$ level are very close to the frequencies of the second field ω_2 coincident with the frequencies of the P(20), P(22), P(26), and P(34) lines of a CO_2 laser. The respective dependence (curve *1*) indicates that maximum absorption occurs at these frequencies.

As Φ_1 grows (see curve *2* at $\Phi_1 = 0.06$ J cm^{-2}), one- and two-photon transitions from the third level $3A_2$ near the P(34) line become apparent. The absorption on the P(26) line increases, and two peaks at the frequencies of the P(34) and P(22) lines are distinguished in the VEM absorption spectra. In other words, the $2F_2$ and $3A_2$ vibrational states are effectively populated even at $\Phi_1 = 0.06$ J cm^{-2}. The populations of the vibrational levels under consideration at $\Phi_1 = 0.2$ J cm^{-2} become virtually identical, the spectrum structure is smoothed, and two maxima [P(34) and P(24) lines] appear in the VEM absorption spectra that may be attributed to transitions from $2F_2$ and $3A_2$ states to the $4\nu_3$ level (F_2, 3788.9 cm^{-1}) and higher states. It should be noted that the dip in the VEM absorption spectrum at a frequency of $\omega_2 \approx 937$ cm^{-1} [P(28) line] is due to the absence of resonance channels for the further excitation of SF_6 molecules (present in vibrational states populated by the first radiation field) in this frequency range.

When SF_6 molecules are excited at the frequency $\omega_1 = 949.48$ cm^{-1}, the structure of VEM absorption spectra is almost identical, as predicted in Ref. [32]. Also, the spectra show two maxima each at the same frequencies ($\omega_2 = 931$ and 940.5 cm^{-1}). However, the intensities of the spectra are much

smaller at the same Φ_1 and Φ_2 values because of the substantial detunings from resonances for the exciting field.

At a constant energy density of the first field, the initial vibrational distribution of excited molecules is fixed; therefore, changes happening in the structure of VEM absorption spectra with increasing energy density of the second field are largely due to a rise in the number of resonance channels for the further excitation of molecules in the vibrational states populated by the first field. This means that they must reflect the resonance character of this excitation. Indeed, it was shown in Ref. [32] that the spectral structure differs at different Φ_2 as a consequence of resonances of a different order between anharmonic sublevels of the initial and higher vibrational states populated with the first laser field.

To conclude, the structural analysis of VEM absorption spectra, based on the findings reported in Refs [147 – 149], has demonstrated a fairly good correspondence of frequency-related positions of the observed maxima to one-photon and two-photon resonances between anharmonic vibrational sublevels of the ν_3 mode for an $^{32}SF_6$ molecule. It should be emphasized, however, that the present discussion is not concerned with narrow resonances or individual transitions between excited vibrational – rotational levels. Such resonances can be seen only with diode lasers and high-pressure smoothly tunable CO_2 lasers. It was demonstrated in the above experiments that in the conditions of deep cooling the absorption spectra of the molecules were considerably narrowed because of the contracted rotational distributions. Therefore, even discretely tunable lasers could be used to observe the structure of transitions in the region of lower vibrational states, conditioned by single- and multiple photon resonances, and to selectively populate the anharmonically splitted vibrational levels.

4.6 Resonant excitation of upper vibrational states in molecules (SF_6, OsO_4) by simultaneous IR pulses

As shown in Section 4.5, the use of molecular beams permits us to obtain and study the structure of radiation transitions in the region of lower vibrational levels of molecules at moderate intensities of radiation pulses due to the possibility of selectively populating individual vibrational states. Nevertheless, conditions necessary for the resonant excitation of high-lying vibrational levels are rarely realized with the use of single-frequency radiation of discretely tunable IR lasers. On the one hand, this precludes high excitation efficiency (i.e., excitation of a large number of molecules); on the other hand, the excited molecules are distributed among numerous levels. In this context, a method described in Refs [49, 112] is of particular interest because it allows for resonant MPE of molecules in upper vibrational states by simultaneously acting photons on different frequencies, the photons whose total energy satisfies the multiple photon resonance condition [150]:

$$\omega_{\rm res} = \sum_i^n \omega_i\,, \qquad i = 1, 2, \ldots, n\,. \tag{4.7}$$

This method essentially differs from the methods of double-frequency [68, 69] and multifrequency [111, 151] molecular excitation by delayed pulses. Simultaneous and sequential pulses activate quite different excitation channels. With simultaneous pulses, it is easy to achieve resonant excitation of high-lying vibrational states and study multiple photon transitions in the region of lower vibrational levels even with the aid of a discretely tunable IR laser [49, 112].

Let us consider this method in more detail by applying it to the resonant excitation of high-lying vibrational states of SF_6 molecules [49]. The authors of Ref. [49] used two or three CO_2 lasers whose pulses were synchronized in time to within ± 50 ns. SF_6 molecules cooled in a pulsed jet ($T_{\rm rot} \approx 20$ K, $T_{\rm vib} \leqslant 160$ K) were excited at a distance of 6 cm from the nozzle. Laser beams were made to converge in space and intersect the molecular beam transversely to its axis. The experiment was designed to measure the energy absorbed by SF_6 molecules from laser pulses during multiple photon excitation (with all exciting pulses acting simultaneously) and sequential two- or three-frequency excitation (with a 1 ± 0.05-μs delay between two successive pulses). For comparison, the molecular absorption during one-frequency excitation was also measured.

The results are presented in Fig. 6. Figure 6a displays spectral dependences of the energy absorbed by SF_6 mole-

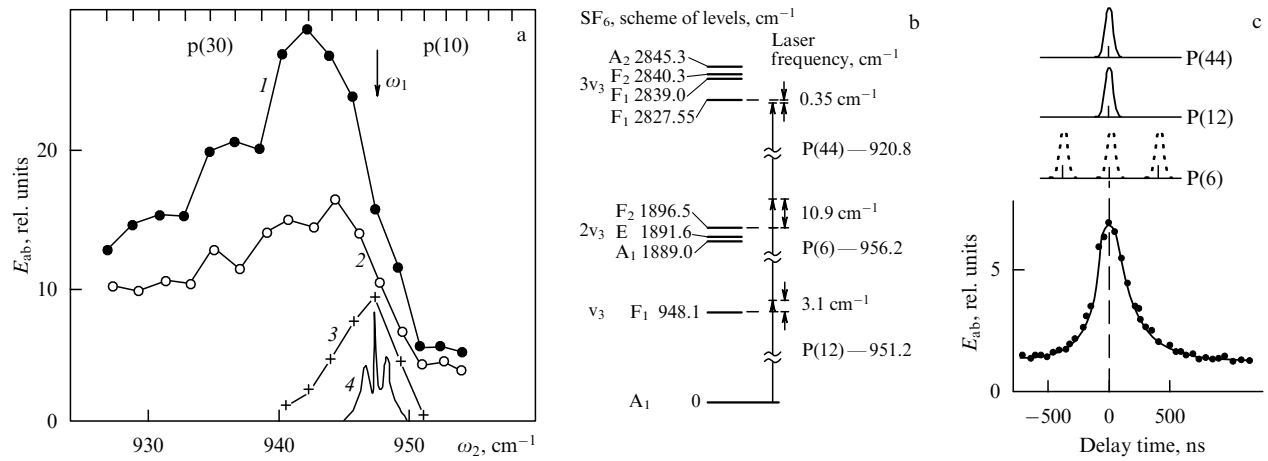

Figure 6. (a) Spectral dependences of the energy absorbed by SF_6 molecules on the field frequency ω_2 during double-frequency excitation by simultaneous ($\tau_{\rm del} \leqslant 50$ ns, curve *1*) and sequential ($\tau_{\rm del} = 1 \pm 0.05$ μs, curve *2*) pulses at the excitation energy densities $\Phi_1 = 0.07$ J cm^{-2}, $\Phi_2 = 0.6$ J cm^{-2} and fixed frequency $\omega_1 = 947.74$ cm^{-1} [10P(16) CO_2-laser line]; curve *3* — MPA spectrum of SF_6 in a single-frequency field [26]; curve *4* — LAS at $T \approx 55$ K [24]. (b) Schematic of the three-frequency excitation of the $F_1 3\nu_3$ state in SF_6. (c) Dependences of the energy absorbed by SF_6 molecules on the delay time between two preliminarily synchronized pulses [P(12) + P(44)] and the third pulse [P(6)] at the laser fluences of 0.6, 0.2, and 0.5 J cm^{-2} for the P(6), P(12), and P(44) lines, respectively (Taken from Ref. [49].)

cules on the frequency ω_2 of the field for the case of acting two simultaneous pulses of frequencies $\omega_1 = 947.74$ cm^{-1} and ω_2 ($\tau_{\rm del} \leqslant 50$ ns, curve *1*) and also for the 'conventional' double-frequency excitation by the same pulses ($\tau_{\rm del} \approx 1$ μs, curve *2*). It can be seen that the energy absorbed under the simultaneous effect of the two pulses with frequencies ω_1 and ω_2 is much higher than in the case of usual double-frequency excitation. The efficiency of simultaneous pulse excitation is especially high as compared with excitation by sequential pulses when the laser radiation frequencies do not coincide with the LAS frequencies of molecules. For example, when frequency ω_1 was detuned from the LAS by 7 – 8 cm^{-1} toward the short-wave side, and frequency ω_2 by 10 – 12 cm^{-1} to the long-wave side, the energy absorbed under the effect of simultaneous pulses was 3 – 8 times that during sequential double-frequency excitation of molecules at the same frequencies.

Figures 6b and 6c illustrate the potential of the method under consideration for resonant MPE of upper vibrational states. Figure 6b shows schematically the three-photon excitation of the F_1 state at the $3\nu_3$ level of SF_6 by pulses of three different frequencies. None of these frequencies, either alone or in pairs, is in resonance with the low-lying transitions of the molecule, but their sum satisfies the multiphoton resonance condition: $\omega_1 + \omega_2 + \omega_3 = \omega\big(3\nu_3(F_1)\big)$. The excitation scheme in Fig. 6b corresponds to minimal detunings of individual frequencies and their sum from intermediate levels of SF_6 molecules. The minimal detunings of the frequencies being used from the intermediate levels amount to 3 and 11 cm^{-1}. The detuning of the combined frequency $\omega_1 + \omega_2 + \omega_3$ from the three-photon resonance frequency is approximately 0.35 cm^{-1} [148]. Figure 6c depicts the dependence of the energy absorbed by SF_6 molecules on the delay time between two preliminarily synchronized pulses on the P(44) and P(12) laser lines and the third pulse for the P(6) line. Evidently, the absorbed energy significantly increases when all three pulses coincide in time. The increase may be due to the three-photon population of the $3\nu_3(F_1)$ state and, possibly, to the further excitation of molecules to higher levels. It was estimated [49] that at least 10 – 12% of the molecules underwent excitation. We observed a similar picture in the case of a delay in any of the three pulses.

Similarly, two pulses at the frequencies of the P(4) + P(34) and P(6) + P(32) lines were used to excite the two-photon $A_{1g}2\nu_3$ (1888.8 cm^{-1}) resonance, with almost 35% of the molecules transferred to this state at an energy density of ≈ 0.5 J cm^{-2}. Notice that a similar method of biharmonic IR excitation of molecules was employed in Ref. [112] using the frequency of a high-pressure smoothly tunable CO_2 laser as one of the two exciting frequencies. The excitation of molecules mixed up with inert carriers in a gasdynamically cooled jet was accompanied by the effective population of the $A_{1g}2\nu_3$ state in SF_6 and the $2\nu_3$ state in OsO_4. Subsequent dissociation of the excited SF_6 and OsO_4 molecules in Ref. [112] was carried out by the third radiation pulse of the CO_2 laser after a 2-μs delay. The population of high-lying vibrational levels was assessed from the dissociation yield by measuring HF^* luminescence intensity during SF_6 excitation, and visible luminescence during excitation of OsO_4 molecules.

The above results indicate that the excitation procedure described is more efficient and selective than the sequential double-frequency excitation when employed to populate high-lying vibrational states of molecules and form narrower vibrational distributions of excited molecules; it also permits us to use more completely the potentialities of discretely tunable IR lasers for the purpose of selective molecular excitation. Also, the results demonstrate that multiple photon transitions in the system of lower vibrational levels play an important role in collisionless conditions of molecular excitation in a gasdynamically cooled molecular beam. It should be noted that the multifrequency method for the resonant excitation of upper vibrational levels can serve as a tool for the simultaneous enhancement of the efficiency and selectivity of IRMPE and IRMPD processes. The method appears to be of special interest bearing in mind that the excitation of molecules by single-frequency radiation even in low-intensity fields ($\leqslant 10^4 - 10^5$ W cm^{-2}) produces relatively wide MPA spectra; this observation is equally true for molecular excitation in gasdynamically cooled jets and flows (see Sections 4.7 and 5).

4.7 Multiple photon absorption of SF_6 molecules in a gasdynamic flow with Ar

In the case of molecules containing heavy elements, such as U, W, or Os, the IR absorption spectra of molecules of different isotopic composition overlap even at low temperatures. A high degree of excitation selectivity can be obtained only when linear and/or multiple photon absorption spectra of a flow-cooled gas acquire a highly apparent structure. For this purpose, the molecules must be excited by radiation fields of moderate energy density in order to lessen dynamic power broadening of transitions. The important characteristics of the molecular excitation processes include absolute value of the absorbed energy and absorption cross section, as well as their dependences on the excitation energy density. It will be shown in Section 4.7.1 that there is a large difference between vibrational and rotational temperatures of molecules in gas flows, with a consequent formation of the MPA spectrum structure other than that formed at room temperature and in pulsed beams. Hence the importance and actuality of investigations into the IRMPA of molecules in gasdynamically cooled flows. Such experiments were carried out in Refs [33, 34] on a large-scale unit using a molecular flow of SF_6/Ar mixture. The SF_6 molecule was chosen because it used to be a classical object of IRMPE studies and serves as a model of UF_6 both structurally and spectroscopically.

4.7.1 Experiment and procedure. Multiple photon absorption of SF_6 molecules in a flow with argon was studied at moderate excitation energy densities (from about 0.1 to 100 mJ cm^{-2}) most interesting for the two-step (IR – IR and IR – UV) isotopically selective dissociation of molecules. Measurements were made with a Gaussian laser beam. This approach yielded, in addition, functional dependences of the absorbed energy $\langle n \rangle$ (in quanta per molecule) and the absorption cross sections σ on the local energy density. The molecules cooled as they outflowed through a slotted nozzle of a Laval type with the slot 50 cm long. The experiments were performed with an SF_6/Ar mixture at a pressure ratio of 1/100. The total gas pressure above the nozzle could be changed and in the present study was equal to 0.1 or 0.15 atm. The excitation of molecules in the flow was carried out at a distance of 3.5 cm from the nozzle outlet. The pressure of the gas and concentration of SF_6 molecules in the excitation region were evaluated to be $p \approx 1.12$ and 2.15 Torr, and $N \approx 1.85 \times 10^{15}$ and 3.8×10^{15} cm^{-3} at the stagnation pressures $p_{\rm noz} = 0.1$ and 0.15 atm, respectively. The estimation of molecular concen-

tration was done using the gas kinetic relation $N = p/kT$, where p is the gas pressure, and T is the translational temperature of the gas in the flow. The vibrational (T_{vib}) and rotational (T_{rot}) temperatures of SF_6 molecules in the flow were calculated from the LAS of the ν_3 vibration in flowing SF_6 taken by a Fourier-transform IR spectrometer [152]. These temperatures were as follows: $T_{vib} \approx 230$ K and $T_{rot} \approx 60$ K at $p_{noz} = 0.1$ atm, and $T_{vib} \approx 220$ K and $T_{rot} \approx 55$ K at $p_{noz} = 0.15$ atm. The mean rate of flow in the excitation zone was roughly 450 m s^{-1}.

A transversely-excited atmospheric-pressure CO_2 laser (TEA-CO_2 laser) was utilized to excite the molecules. An aperture inserted in the laser cavity served as a TEM_{00}-mode selector. The laser pulse energy was as great as 30 mJ. The pulse consisted of a spike with a half-height duration of about 100 ns, and a 1.5-μs tail that contained almost 60% of the total energy. The energy density distribution across the laser beam was obtained by its direct scanning in mutually perpendicular directions with an energy detector in front of which a slit 0.1 mm wide was placed. The distribution turned out to be Gaussian.

The laser radiation was directed into the gas flow to cross it perpendicularly to the flow axis and was reflected back at a small angle ($\approx 3°$) relative to the first pass. Therefore, the total length of the absorbing layer amounted to $l = 100$ cm. The incident (E_{in}) and transmitted (E_{out}) laser beam energies were measured, both with the SF_6/Ar flow and in its absence. The laser radiation came into the flow through a ZnSe antireflecting window. The energy detectors and the recording system had a linear response over a wide range from about 10 μJ to 100 mJ. The signals from the detectors were averaged over 30 pulses. The laser ran at a repetition rate of about 3 Hz. The absorbed energy E_{ab} was determined based on the transmitted energies measured without and with the SF_6/Ar flow. In most cases, the absorbed energy was less than $\approx 25\%$ of the incident energy. Consequently, the variation of the energy density along the laser beam axis was negligible; nevertheless, it was taken into account in the calculations of the absorbed energy and the absorption cross section.

The absorbed energy was expressed in quanta per molecule as

$$\langle n \rangle = \frac{E_{ab}}{\hbar\omega N V}\,, \tag{4.8}$$

where $\hbar\omega$ is the laser photon energy, N is the concentration of SF_6 molecules in the excitation region, and V is the irradiated volume (with $V = Sl$, $S = \pi a^2 = 0.23$ cm^2, where S is the laser beam cross section, a is the Gaussian beam radius on which the intensity decreases by e^2 times, and $l = 100$ cm is the length of the interaction area). The radiant energy density was defined as $\Phi_{av} = (E_{in} + E_{out})/2\pi a^2$, which corresponds to the laser fluence averaged over the length of the interaction area and the Gaussian beam cross section.

Studies [33, 34] provided $\langle n \rangle(\Phi_{av})$ dependences for some CO_2-laser emission lines coincident with the absorption spectrum of the ν_3 vibration in molecules. The dependences $\langle n \rangle(\Phi_{av})$ were utilized to derive dependences of the effective absorption cross section $\sigma(\Phi_{av})$ on the excitation energy density averaged over the interaction region. We used for this purpose the adopted definition (4.1): $\sigma = -\ln(T)/Nl$, where $T = E_{out}^{gas}/E_{out}^{0}$ is the ratio of transmitted energies with the SF_6/Ar flow and without gas. If the absorption is small, it is possible to obtain, as usual [27]:

$$\langle n \rangle = \sigma \Phi_{av}\,, \quad \text{or} \quad \sigma = \frac{\langle n \rangle}{\Phi_{av}}\,. \tag{4.9}$$

Thus, $\langle n \rangle$ and σ represent the values averaged over the volume of the interaction region; they may be significantly different from the $\langle n \rangle$ and σ values characteristic of a laser beam spatially homogeneous in terms of intensity (energy density). Hence, experimental dependences of $\langle n \rangle$ and σ on the local energy density are needed to correctly interpret the findings obtained and compare them with the available results of other studies.

4.7.2 Dependences of the absorbed energy on the excitation energy density. It was shown in Refs [33, 34] that during molecular excitation at the frequencies of the P(14)–P(20) lines the dependences $\langle n \rangle(\Phi_{av})$ are rather similar up to $\Phi_{av} \approx 10$ mJ cm^{-2}: they have a slope of 0.75 on a logarithmic scale, i.e., $\langle n \rangle \sim \Phi_{av}^{0.75}$. In the region with $\Phi_{av} \geqslant 50$ mJ cm^{-2}, these dependences become steeper, especially the $\langle n \rangle$ dependences on the local energy density. The dependences obtained in works [33, 34] are in good agreement with the data on MPA of SF_6 in a cell at room temperature [104] and at $T \approx 150$ K [123] at pressures $p \geqslant 0.1$ Torr, when the MPA is affected by molecular collisions. For the SF_6 molecules at room temperature, $p\tau_{rot} \approx 36$ ns Torr and 32 ns Torr for the ground and the first excited states, respectively [153, 154]. In the case under consideration, rotational relaxation time τ_{rot} appears to be 2–3 times longer due to the low temperature of the molecules ($T_{tr} \approx 60$ K). Nevertheless, some rotational relaxation of SF_6 molecules was apparent during the transmission time of the exciting laser pulse (≈ 1.5 μs), when the gas pressure in the excitation area was ≈ 20 mTorr for SF_6, and ≈ 2 Torr for Ar [104]. It is worth noting that the dependences of interest had similar slopes for $\Phi_{av} \leqslant 0.1$ J cm^{-2}, when SF_6 underwent excitation in a molecular beam [27].

4.7.3 MPA spectra of SF_6 in a flow with Ar. As indicated in the beginning of Section 4.7, the experiments being considered revealed a large difference between rotational and vibrational temperatures of molecules ($T_{vib} \approx 230$ K, and $T_{rot} \approx 60$ K). This finding suggests that the experimental conditions were dissimilar to those typical of the SF_6 excitation both in a cell at $T_{vib} = T_{rot} \approx 140-150$ K [119–121, 124] and in pulsed molecular beams [26, 27]. At $T_{vib} = T_{rot} \approx 150$ K, about 85% of the molecules were in the ground vibrational state [127]. As a result, 'hot bands' were markedly suppressed, even though the rotational distribution of the molecules remained sufficiently wide. In experiments with molecular beams of SF_6 [26, 27], the temperatures obtained were $T_{vib} \leqslant 150$ K and $T_{rot} \leqslant 40$ K. At such temperatures, both vibrational and rotational distributions of molecules are normally rather narrow. In the experiments being reviewed, the rotational distribution was narrow, and the vibrational one relatively wide. Specifically, some 50% of the molecules at $T_{vib} \approx 230$ K were distributed across the low-lying excited vibrational states (ν_6, ν_5, $2\nu_6$, ν_4, ...) [127]. This brought into existence rather intense 'hot bands' in the LAS (Fig. 7) that could not but affect the formation of structure in the MPA spectra.

Figure 7 shows frequency dependences of the absorbed energies (MPA spectra of SF_6) at three different energy

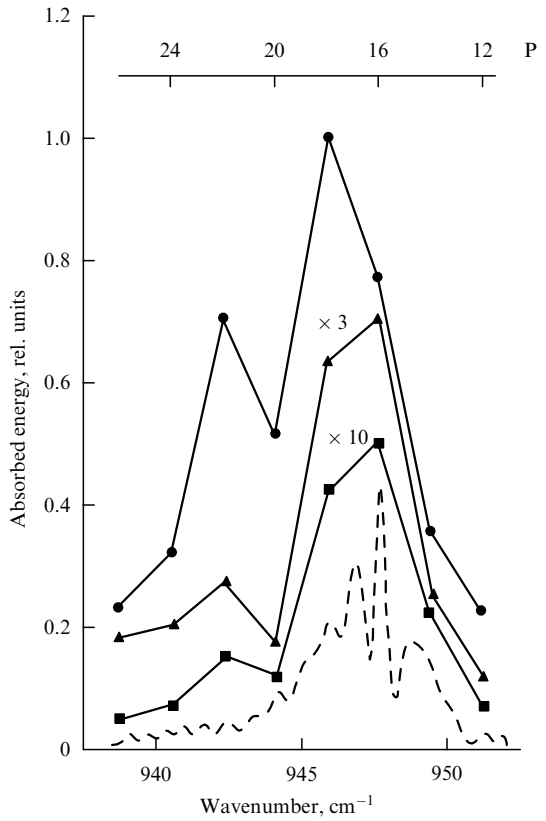

Figure 7. Frequency dependences of the absorbed energy in an SF_6/Ar flow (MPA spectra of SF_6) at different excitation energy densities: 1 mJ cm^{-2} — ■, 10 mJ cm^{-2} — ▲, and 80 mJ cm^{-2} — ●. Dashed curve — LAS of SF_6 in a flow with Ar at $T \approx 230$ K and $T_{rot} \approx 60$ K [152]. Positions of the CO_2-laser lines are shown in the upper part of the figure. (Taken from Refs [33, 34].)

densities of the exciting radiation. In order to better illustrate the evolution of the spectra with growing energy density, they are presented at 1 mJ cm^{-2} and 10 mJ cm^{-2} values as magnified on the axis of ordinates, while the absorption energy is expressed in relative units. The absolute value of the absorbed energy in the maximum of the MPA spectrum at 80 mJ cm^{-2} amounts to approximately 1 quantum per molecule [33]. For comparison, the figure shows a linear absorption spectrum of SF_6 molecules at $T_{vib} \approx 230$ K and $T_{rot} \approx 60$ K in a similar SF_6/Ar flow through a nozzle with a slot 12 cm long; the spectrum was obtained with a Fourier-transform IR spectrometer [152]. Two characteristic features of the MPA spectra deserve attention: (1) a shift in the main maximum from the P(16) laser line to the P(18) line with increasing energy density, and (2) the presence of the second maximum on the P(22) line. Similar temperature conditions were created in Ref. [47] in studying a molecular beam of SF_6 (see Section 4.4), where a single maximum in the MPA spectrum was apparent on the P(18) line, whereas with cooled SF_6 molecules the maximum occurred on the P(16) line [26, 27, 119, 124]. The shift of the MPA peak from P(16) to P(18) was due to the relatively large contribution to the absorption made by the molecules residing in lower vibrational states (ν_6, ν_5, $2\nu_6$, ν_4 and some others) densely populated at $T_{vib} \approx 230$ K [47]. The maximum on the P(22) line was probably associated with the transition from the ground vibrational state to the $(300)F_{1u}$ level, induced by the three-photon resonance at a frequency of 942.5 cm^{-1} [155], and/or with transitions from the low-lying excited vibrational states, caused by the multiple photon resonance. It should be noted that the MPA spectra in Ref. [47] showed no apparent structure because of a relatively high excitation energy density ($\geqslant 0.5$ J cm^{-2}) (see also Section 4.5).

To sum up, Refs [33, 34] reported on the IRMPA of SF_6 molecules cooled down to $T_{vib} \approx 230$ K and $T_{rot} \approx 60$ K in an argon-containing flow at radiant energy densities in a range of $\approx 0.1-100$ mJ cm^{-2}. The studies revealed the dependences of the absorbed energy $\langle n \rangle$ and the cross section σ on both the interaction volume-averaged and the local energy densities of the exciting pulse. It was shown that the nonlinear (multiphoton) character of interactions between the molecules and the IR radiation field manifested itself more evidently in the dependences of $\langle n \rangle$ and σ on the local energy density. The SF_6 MPA spectra were obtained for the case of a large difference between vibrational and rotational temperatures of molecules at small excitation energy densities. The structure of the MPA spectra was due to a relatively high vibrational temperature of the molecules and to the multiphoton character of excitation in the region of lower vibrational levels.

Paper [156] deserves to be cited as reporting a study of multiple photon absorption by UF_6 in a pulsed flow with CH_4 and Ar at a molar gas ratio of 0.5, 2.5, and 97%, respectively. The width and the pulse duration of the molecular flux were 50 cm and around 10 ms, respectively. Molecular absorption was measured in the ν_3 vibration region of $^{238}UF_6$ (≈ 627.7 cm^{-1}) [157]. The molecules were pumped by a Raman laser operated within a 16-μm bandwidth. The laser beam was produced by Raman scattering of a pulsed CO_2-laser light in para-hydrogen [158, 159]. The laser pulse duration at half-height measured 50 ns. The laser beam intersected the molecular flow only in one direction. The partial pressure and temperature of UF_6 molecules in the excitation area were 0.045 Torr and 90 K, respectively. The total gas pressure amounted to 9 Torr. The excitation-energy-density dependence of the absorption cross section was examined in the range between 50 and 500 mJ cm^{-2}. The maximum absorption occurred at a frequency of 627.8 cm^{-1}, and its cross section at this frequency was found to be proportional to the excitation energy density at a power of $-1/3$, i.e., $\sigma \sim \Phi^{-1/3}$. The maximum absorption corresponded to approximately 1.4 quanta per molecule at an energy density of 0.2 J cm^{-2}. It should be noted that such energy-density dependence of the absorption cross section was observed in many studies where other molecules were subjected to collisional excitation (see references cited in work [156] and also Ref. [122]). We obtained a similar dependence of $\sigma(\Phi)$ (in a range of $0.1-50$ mJ cm^{-2}) by exciting SF_6 molecules in an Ar-containing flow [33] (see above). Such dependences are typical of the nonlinear absorption of 'medium-sized' molecules in a strong IR field at moderate excitation energy densities [27, 122, 123].

5. Diode spectroscopy of molecular excitation dynamics

As evidenced by discussion in Section 4.3.2, experimental SF_6 MPA spectra in the case of collisionless excitation in a molecular beam are at variance with the results of model calculations. The quantitative description of the molecular MPE process in the region of lower vibrational levels would be possible based on a theoretical model (including the spectroscopic description of the molecule and its interaction

with the laser field) were its results in reasonable agreement with experimental findings. When theoretical and experimental data are compared, the following characteristics of the excitation process are of primary interest: the population of vibrational states; the distribution of molecules in a given vibrational state over rotational levels; the fraction of molecules that failed to interact and the fraction of those that reached quasi-continuum, and the dependence of these characteristics on the frequency and energy density of the exciting laser radiation.

The SF_6 molecule provides a classical focus of MPE studies. The spectroscopic parameters of its ν_3 mode resonant with the CO_2-laser radiation are fairly well known [136]. Some works on the MPE of SF_6 molecules in the region of lower vibrational levels report experimental findings that can be compared with the results of model computations. By way of example, irradiation by a high-pressure smoothly tunable CO_2 laser produced SF_6 MPE (MPA) spectra taken in a gasdynamic jet at $T \approx 30$ K [30]. The method of coherent anti-Stokes Raman scattering (CARS) was used in Ref. [160] to probe the ν_1 mode and thus to examine the distribution of SF_6 molecules across different vibrational states of the ν_3 mode after the excitation by a CO_2-laser pulse. The irradiation brought about populations of several first ($\nu_3 = 0-3$) vibrational states of the excitable mode, which were integrated over rotational and anharmonically splitted vibrational sublevels. At the same time, of primary importance for elucidating the mechanism of molecule migration across the lower discrete levels during MPE is the experimental assessment of two parameters. One is a fraction of the excited molecules resided on individual rotational sublevels of the ground vibrational state, the other is the molecular distribution throughout the rotational sublevels of exited vibrational states. These studies reported in Refs [37, 51, 161 – 166] will be briefly reviewed in the present section. They were carried out using the double IR – IR resonance method with a pulsed tunable diode laser (TDL) as a source of probing radiation.

Among important advantages of probing molecules by pulsed TDL are high absorption sensitivity allowing measurements to be made at a relatively low concentration of molecules in a gasdynamic jet ($N \leqslant 10^{13}$ cm^{-3}), high spectral resolution ($\approx 10^{-3}$ cm^{-1}), and the possibility of obtaining an absorption spectrum during the transmission time of a single pulse. The main results of these studies will be discussed below. To begin with, it is appropriate to consider briefly some models proposed to explain IRMPE of molecules that provide a deeper insight into the mechanism of molecular excitation in the lower level region and the encountered difficulties.

5.1 Molecular IRMPE models

Soon after the first experiments on the collisionless dissociation of molecules (SiF_4 [63], BCl_3 [1], and SF_6 [2]) in a CO_2-laser pulse field with intensity $10^8 - 10^9$ W cm^{-2}, it was conjectured that the anharmonism of vibrations in the lower level region is overcome by virtue of dynamic 'broadening' of the absorption lines by resonant IR radiation [1, 63]. The extent of the broadening is determined by the field amplitude E and the characteristic dipole transition moment $\mu \approx 3 \times 10^{-19}$ (in CGSE units); at the field intensity $I \approx 10^8 - 10^9$ W cm^{-2}, the broadening amounts to $\Delta\nu_R = \mu E/\hbar c \approx 2-5$ cm^{-1}, sufficient to compensate for anharmonic detunings on several lower transitions at an anharmonicity constant of 3 cm^{-1}. However, subsequent studies [3, 167] with SF_6 and OsO_4 molecules have demonstrated that excitation of high-lying vibrational states also takes place in the fields with intensity $10^6 - 10^7$ W cm^{-2}, where power broadening is insufficient to overcome anharmonism of vibrations even on the $v = 1 \rightarrow v = 2$ transition.

Later theoretical studies [61, 62] considered the feasibility of multiple photon transitions in the system of lower vibrational levels. Calculations were done in the model of a one-dimensional anharmonic oscillator disregarding the real spectral structure of polyatomic molecules. It followed from those works that multiple photon transitions are possible only at rather high IR radiation intensities ($10^7 - 10^8$ W cm^{-2}).

At the same time, experiments on the double-frequency IR dissociation of SF_6 molecules [68, 69] showed that molecular excitation up to a quasi-continuum region did occur in fields of much lower intensity ($10^4 - 10^5$ W cm^{-2} in all). This finding challenged the previously accepted concept of overcoming anharmonism of vibrations by means of dynamic broadening of transitions and thus stimulated the search for and the study of other models accounting for MPE of molecules in moderately intense fields. By way of example, the authors of Ref. [60] proposed a model of rotational compensation for anharmonism of vibrations that fairly well explained the possibility of passing the system of lower vibrational levels by a small fraction alone ($\leqslant 1\%$) of molecules resided on certain rotational sublevels. Further experiments with SF_6 molecules demonstrated [168] that a large fraction of them were excited at $10^5 - 10^6$ W cm^{-2} intensities virtually regardless of the initial rotational state. It followed from works [68, 69, 168] that the models designed to adequately describe the behavior of molecules in the region of lower vibrational levels must not only predict molecular excitation in moderately intense fields but also explain simultaneous involvement of their large portion in this process.

Two models proposed in Ref. [169] and Refs [170, 171] meet this criterion. One of them [169] takes into consideration forbidden transitions during the lower level excitation that occur with a violation of the selection rule $\Delta R = 0$ [172] ($\mathbf{R}$ is the rotational component of the total moment $\mathbf{J} = \mathbf{R} + \mathbf{l}$, where $\mathbf{l}$ is the vibrational moment arising from the excitation of degenerate vibrations). It should be noted, however, that weak transitions are poorly known; therefore, calculations based on them are of questionable value for the interpretation of experimental findings.

The other model [170, 171] accounts for anharmonic splitting of levels. In the case of triply degenerate vibrations of spherical top molecules (SiF_4, SF_6, OsO_4, etc.), the anharmonism of vibrations results not only in the displacement of levels relative to their harmonic position but also in their splitting and the formation of vibrational level bands (Fig. 5a). The anharmonic splitting is enhanced as the principal quantum number increases; this facilitates the compensation for the anharmonic shift and opens numerous possibilities for stepwise and multiple photon resonances in the system of lower vibrational levels. Calculations [173] accounting for the anharmonic splitting of levels indicated that two- and three-photon transitions are saturated even in the fields of $10^5 - 10^6$ W cm^{-2} intensities due to the presence of slightly detuned intermediate levels. As a consequence, a large fraction of molecules can be excited to high-lying vibrational states.

Of primary importance for understanding the mechanism by which a molecule passes the system of lower vibrational

levels are MPA (MPE) spectra recorded at moderate excitation energy densities, when the absorption is largely associated with lower transitions. Experiments using a high-pressure smoothly tunable CO_2 laser demonstrated a sharp resonance structure in the SF_6 MPA spectra — that is, two-photon resonance peaks [125, 126]. In later studies, such a structure in the MPA and MPD spectra was observed during the excitation of CF_3I [42, 44] and some other [142] molecules. Experiments with SF_6 [26 – 28, 46], CF_3I [42, 44], and OsO_4 [111] molecules cooled in a supersonic jet showed (see Section 4.1) that the dependences of the absorbed energy E_{ab} on the excitation energy density in the majority of cases acquire the form $E_{ab} \sim \Phi^n$, where $n > 1$, characteristic of multiple photon transitions. It was concluded, based on this finding, that multiple photon transitions in the system of lower vibrational levels play an important role in molecular excitation, at least in certain conditions. Experimentally found spectral dependences of the absorbed energy and MPA spectra proved to be sometimes well described by theoretical models taking into consideration single- and multiple photon transitions in the system of lower vibrational levels (see, for instance, Refs [143, 174 – 176]).

However, the available theoretical models fail to account for the high intensity of experimentally obtained MPA spectra — that is, for the large average number of absorbed radiation quanta per molecule at a given strength of the IR field. The intensity of predicted MPA spectra is usually several orders of magnitude lower than that of observed ones. The existing models are equally unfit for explaining some other experimental data on molecular absorption in an intense IR field. Some of these data will be presented in Section 5.5.

It follows from the above that further experimental and theoretical studies are needed to completely describe molecular excitation by intense IR laser radiation. The results obtained in works [37, 51, 161 – 166] and considered in Sections 5.2 and 5.3 mark an important step in this direction.

5.2 First results

The first results of investigations into the depletion of individual rotational sublevels of the ground vibrational state during molecular excitation by intense IR laser radiation were obtained in Refs [161, 162] using SF_6 molecules. In these experiments, SF_6 molecules cooled in a gasdynamic jet were excited by a pulse from a CO_2 laser. The laser pulse comprised a spike with a half-height duration of ≈ 100 ns, and a 0.6-μs tail. The peak energy was up to 2 joules. The molecules were probed with a tunable diode laser. The gasdynamic jet was produced using a pulsed nozzle with an opening diameter of 0.75 mm. The pressure of SF_6 above the nozzle could be changed from 1 to 5 atmospheres.

The geometry of the molecular excitation scheme and probing used in the majority of experiments is illustrated in Fig. 8a. The molecules were excited 6 cm from the nozzle, and probed at a distance of 11.5 cm from it. The exciting and probing beams were directed through the jet transversely to its axis. Their apertures were ≈ 12 mm and ≈ 5 mm, respectively. The molecules vibrationally excited by the CO_2-laser pulse were probed with the diode laser as they traversed the probing zone. The time of flight of the molecules from the excitation zone to the probing zone was approximately 120 μs. The concentration of molecules in the jet as they passed the excitation and probing zones was $N \leqslant (1.5-7.5)\times 10^{13}$ cm^{-3} and $N \leqslant (0.3-1.5)\times 10^{13}$ cm^{-3}, respectively. A two-pass probing scheme was employed to enhance the sensitivity of recording the absorption of the diode laser radiation by the molecules. The rotational

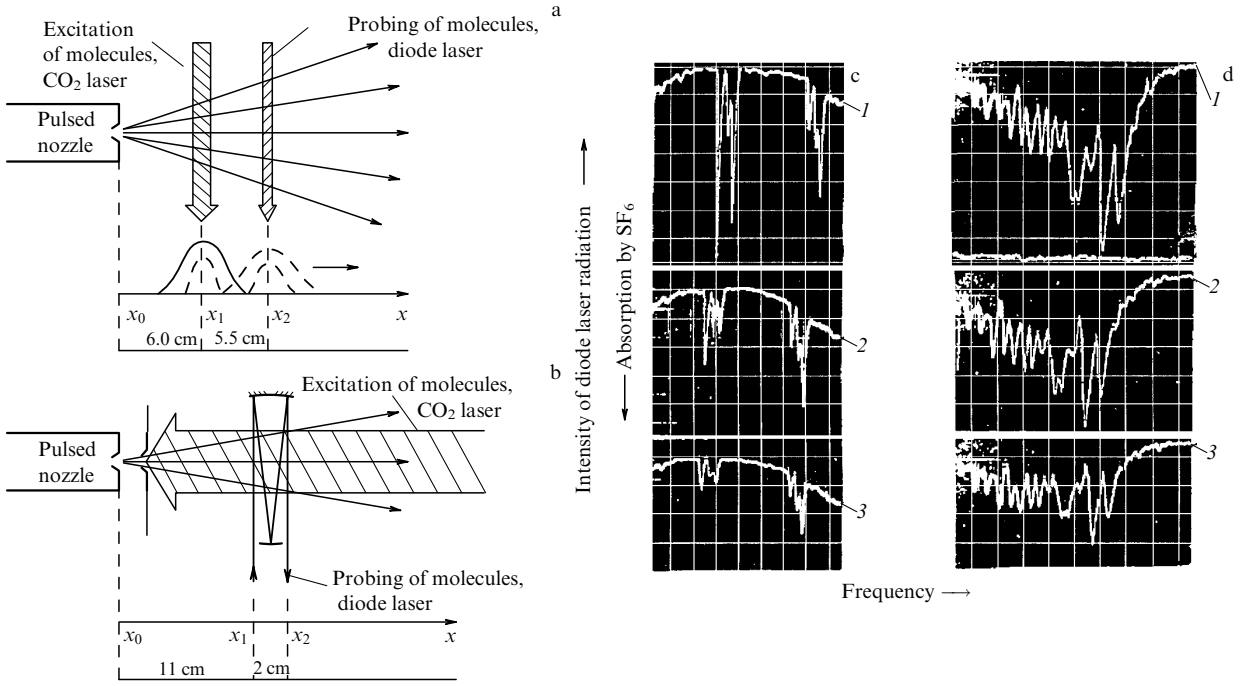

Figure 8. (a, b) Schematic of excitation and probing of molecules in a pulsed jet. The multipass mirror system in Fig. 8b is arrayed in the White cell configuration with 28 passes. The oscillograms show SF_6 absorption lines — the P(10) and P(9) multiplets (c) and the Q-branches (d) without molecular excitation in a pulsed jet (oscillograms *1*) and with an excitation energy density of 0.5 and 1.3 J cm^{-2} (oscillograms *2* and *3*, respectively). Shown at the top of Fig. 8d (under oscillogram *1*) is the zero excitation level corresponding to 100% absorption of diode laser emission. The radiation frequency is 947.74 cm^{-1} [P(16) line of the CO_2 laser]. The scanning rate is 7.5 μs or ≈ 0.015 cm^{-1} per division. The SF_6 pressure above the nozzle is 5 atm. (Taken from Refs [37, 161, 162].)

temperature of SF_6 molecules in the excitation and probing zones was $T_{rot} \approx 18$ K. It was estimated from the population of the rotational sublevels, which was in turn deduced from the magnitude of absorption of the diode laser radiation by the SF_6 molecules on the $v_3 = 0 \rightarrow v_3 = 1$ transitions in the P-branch [177]. Under experimental conditions, the SF_6 molecules in the jet came into roughly one gas-kinetic collision during the delay time between the excitation and probing episodes. This could lead to some distortion of the molecular rotational distribution created by the CO_2-laser pulse.

In some experiments, we used an excitation and probing scheme similar to that in Fig. 8b but with two passes of diode laser radiation. The CO_2-laser beam was directed counter to the gas jet. Such a geometry allowed us to reduce the delay time between the exciting and probing moments to 5–10 μs, and to realize collisional conditions of molecular excitation (at small distances from the nozzle) [162].

A PbSnSe-based pulsed diode laser was utilized in the study. The frequency tuning rate amounted to $(2-3)\times 10^{-3}\,\text{cm}^{-1}\,\mu\text{s}^{-1}$. In most experiments, a range from 946.3 cm^{-1} to 948.2 cm^{-1} was selected for probing. At $T_{rot} \approx 18$ K, this range overlapped almost completely the frequency range of the P- and Q-branches of the $v_3 = 0 \rightarrow v_3 = 1$ transition in the molecule. The spectral resolution was ≈ 0.003 cm^{-1}. This allowed for the resolution of individual rotational components of the multiplets in the P-branch, the components corresponding to the states with $J \leqslant 20$, populated basically at $T_{rot} \approx 18$ K.

Oscillograms showing the variations in radiation absorption (transmission) of SF_6 molecules in the region of the P(10) and P(9) multiplets and the Q-branch of the $v_3 = 1 \leftarrow v_3 = 0$ transition under the action of CO_2-laser pulses are presented in Figs 8c and 8d. It can be seen that the excitation of SF_6 molecules resulted in their enhanced bleaching (reduced absorption) due to the depopulation of the ground vibrational state (depletion of rotational sublevels). The fraction f_J of molecules resided on individual rotational sublevels and excited by a laser pulse was determined by measuring the bleaching of the respective lines.

Experiments reported in papers [161, 162] demonstrated that even with a small exciting-pulse energy density $\Phi \leqslant 0.02$ J cm^{-2}, when the Rabi frequency $\Delta\nu_R = \mu E/\hbar c \leqslant 0.04$ cm^{-1} and the width of the laser line $\Delta\nu_L \leqslant 0.015$ cm^{-1} [178, 179] did not exceed the difference in frequency between the adjacent multiplets in the P-branch, the laser radiation interacted with all rotational states populated at $T_{rot} \approx 18$ K, irrespective of the detuning between the frequency of pumping radiation and the frequencies of P-branch absorption lines of the $v_3 = 1 \leftarrow v_3 = 0$ transition in SF_6. When pumping occurred at the 10P(16) CO_2-laser line (947.74 cm^{-1}), the detunings were $\Delta\nu \approx 0.05$ cm^{-1} for the P(5) multiplet and $\Delta\nu \approx 0.7$ cm^{-1} for the P(16) multiplet of an SF_6 molecule. Similar depletion of many rotational states was observed when a delay time between the exciting and probing pulses lay in the range from 5 to 10 μs (with counterwise excitation geometry, see Fig. 8b). With the radiation energy density $\Phi \leqslant 0.5$ J cm^{-2}, there was preferential depletion of rotational sublevels having smaller detunings from the frequency of the exciting pulse. In contrast, f_J was virtually independent of J for $\Phi \geqslant 1.3$ J cm^{-2}.

At relatively high laser fluences, $\Phi = 0.5-1.3$ J cm^{-2}, the interaction of all rotational states was also observed as SF_6 molecules were pumped at the frequencies of the P(12), P(20), P(24), and P(28) lines of a CO_2 laser [161, 162], which were considerably detuned (by 3–11 cm^{-1}) from the SF_6 LAS having a width of less than 2 cm^{-1} at $T_{rot} \approx 18$ K.

Paper [162] also reports an experimental study on the effect of collisions on the depletion of rotational sublevels. The collisional conditions of molecular excitation were realized with a coaxial geometry (Fig. 8b). The molecules were excited in the zone of collisions at the nozzle outlet. Under collisional excitation conditions, the depletion of the ground vibrational state was much more efficient than in collisionless ones. Suffice it to say that with the pumping of SF_6 at the 10P(16) CO_2-laser line under conditions of collisional excitation, the quantity f_J at $\Phi \approx 0.1$ J cm^{-2} was 7–9 times more than in the absence of collisions. Moreover, all rotational states were depopulated almost identically ($f_J \approx 0.75$ for all J) due to the effect of rotational relaxation and vibration–vibration exchange [162].

In conclusion, studies [161, 162] demonstrated for the first time the depletion of individual rotational states of molecules (exemplified by SF_6) during IRMPE and measured the fraction of molecules excited from each rotational sublevel. They also showed that the efficient depletion of the rotational states at the ground vibrational level occurred even in the case of a large (8–11 cm^{-1}) detuning of the exciting pulse frequency from the SF_6 LAS. The ground vibrational level of SF_6 molecules under collisional excitation conditions was depopulated much more effectively than in collisionless ones.

5.3 Collisionless excitation of SF_6 and NH_3 by a CO_2-laser pulse

The excitation dynamics of molecules residing in individual rotational states of the ground vibrational level upon their pumping by intense IR laser pulses was investigated in more detail in Refs [37, 51, 163–166] using SF_6, $^{14}NH_3$, and $^{15}NH_3$ molecules as an example. The experimental technique was essentially the same as in Section 5.2, but some important differences dictate the necessity to describe them and the experimental procedure at greater length.

5.3.1 Experiment. Unlike earlier experiments [161, 162], the pulsed gasdynamic jet was formed using a nozzle with a 2×0.2 mm^2 slot. The concentration of molecules in the excitation and probing zones was varied in the range of $\approx (0.35-1.75) \times 10^{13}$ cm^{-3} by changing the gas pressure above the nozzle between 0.1 and 0.5 atmospheres. The cooled molecules were excited by a tailless pulse of a CO_2 laser. The energy of the pulse was about 1 J, and its half-height duration measured ≈ 100 ns. The exciting radiation intensity was modulated with the aid of plane-parallel CaF_2 plates that attenuated the radiation. The excitation energy density varied over a broad range from 10^{-6} to 0.4 J cm^{-2}.

A tunable diode laser (TDL) based on $Pb_{1-x}Sn_xSe$ was applied for probing. The TDL emission range was 900–1000 cm^{-1}. The laser operated in a pulse-periodic mode. The spectral resolution was determined by the TDL frequency tuning rate $d\nu/dt = (1-3) \times 10^{-3}$ cm^{-1} μs^{-1} and the operating speed of the recording system; it equalled 1×10^{-3} cm^{-1}. TDL radiation was detected by means of an HgCdTe photoresistor. The time resolution of the IR detector was approximately 500 ns. The signal from the detector output was amplified and fed either to a storage oscilloscope or to a high-speed analog-to-digital converter linked to a microcomputer. The molecular spectrum in the jet was recorded during a single pulse at a signal-to-noise ratio of at least 100. The

results of the measurements were averaged over at least 10 pulses to reduce errors due to jet instability and variations in the CO_2-laser power. Time synchronization of separate blocks was provided by a digital time-delay system with an accuracy better than 10 ns. The delay time τ_{del} between the instants of excitation and probing did not exceed 10 – 15 μs. When SF_6 molecules were utilized, this allowed measurements to be made under collision-free conditions. In experiments with NH_3 molecules, their relaxation was measured during intervals between excitation and probing instants [37, 163].

The excitation and probing geometry used in these experiments is given in Fig. 8b. The molecules were excited by a CO_2-laser beam propagating counter to the molecular stream. The probing beam of the TDL was aligned at a right angle to the jet. Parallel polarization of the exciting and probing radiation was utilized. A three-mirror multipass system arrayed in the White cell configuration on a 185-cm-long base with 28 passes was used to increase the measurement sensitivity. The cross section of the probing region was less than 0.5×2 cm^2. The width of the molecular jet was varied by means of conical apertures and ranged from 3 to 12 cm in the probing zone.

5.3.2 Procedure. In these experiments, the absorption amplitude A in the center of the line being probed and its variations ΔA after molecular excitation by a CO_2-laser pulse were measured with the aid of a TDL. The results thus obtained were used to estimate the relative change $f^* = \Delta A/A$ in absorption (bleaching). The value of A in all experiments did not exceed 20% of the diode-laser signal amplitude. It is well known [180] that the meaning of f^* strongly depends on whether the measurements are carried out under two-level double-resonance (DR) with the coinciding excitable and probing transitions or under three-level DR with a common initial state for the excitable and probing transitions and different final states. In most experiments with SF_6, measurements were performed in a three-level DR mode [37, 51]; therefore, the fraction of molecules leaving the depopulated level of the ground vibrational state was equivalent to the observed bleaching: $f_J = f_J^*$. In the case of NH_3 molecules, the measurements were taken under conditions of two-level DR [37, 163]; hence, the fraction of molecules that escaped from the depleted level of this state made only half the observed bleaching value: $f_J = f_J^*/2$.

5.3.3 Depletion of individual rotational states of SF_6. Figure 9 displays the dependences of the fraction (f_J) of molecules that have interacted with the radiation field on rotational quantum number J'', obtained during SF_6 excitation at the frequency of the 10P(16) CO_2-laser line (947.74 cm^{-1}) and at different energy densities Φ of the exciting radiation. It can be seen that, in a range of energy densities $10^{-6} \leqslant \Phi \leqslant 10^{-2}$ J cm^{-2}, molecules were appreciably excited only from sublevels $J'' = 4$ and $J'' = 5$ characterized by a small detuning $\Delta\nu$ from the exciting radiation frequency (0.009 cm^{-1} and 0.048 cm^{-1}, respectively). An effect of molecular involvement from many rotational levels of the ground vibrational state began to be manifested for $\Phi > 10^{-2}$ J cm^{-2}. At the energy density $\Phi = 0.1$ J cm^{-2}, the dependence $f_J(J'')$ had a highly apparent resonance structure. According to Refs [161, 162], a further increase in Φ to 0.5 – 1.3 J cm^{-2} causes the structure of $f_J(J'')$ to smooth out and the value of f_J to reach 0.5 – 0.7.

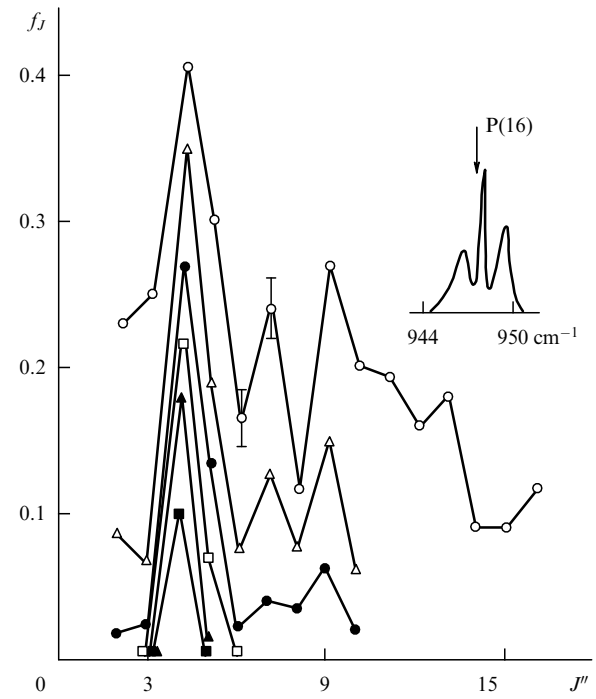

Figure 9. Fraction f_J of SF_6 molecules excited from individual rotational sublevels of the ground vibrational state versus rotational quantum number J'' at a frequency of 947.74 cm^{-1} [line P(16)] and different energy densities of the exciting CO_2-laser pulse: 0.1 J cm^{-2} — ○, 0.03 J cm^{-2} — △, 0.01 J cm^{-2} — ●, 10^{-3} J cm^{-2} — □, 10^{-4} J cm^{-2} — ▲, and 10^{-5} J cm^{-2} — ■. (Taken from Ref. [51].)

In experiments [51, 163], the depletion of many rotational states of the ground vibrational level was also observed when SF_6 molecules were excited by a CO_2-laser pulse at frequencies 945.98 and 949.48 cm^{-1} of the 10P(18) and 10P(14) lines, respectively. Detunings of these lines from the center of the Q-branch of the $0 \to 1\nu_3$ transition were 1.5 cm^{-1} for 10P(18), and 2.0 cm^{-1} for 10P(14). The obtained dependences $f_J(J'')$ had different structures [51, 163], probably due to the presence of individual multiple photon excitation channels on different lines of a CO_2 laser.

5.3.4 Population of the $\nu_3 = 1$ level of SF_6 molecules. We studied the population of the $\nu_3 = 1$ state during the SF_6 excitation by the 10P(16) CO_2-laser line. The population was assessed by two different methods [51, 163]. One of them was based on the comparison of the bleaching of the absorption lines in the P- and R-branches for the rotational levels with J'' in a range of $2 \leqslant J'' \leqslant 10$. The other characterized the population of the $\nu_3 = 1$ state from measurements of the induced absorption at a frequency of ≈ 941.0 cm^{-1} corresponding to the Q-branch of the $2\nu_3 A_{1g} \leftarrow \nu_3$ transition. The measured data obtained by both methods indicate that, even during the excitation near the Q-branch of the ν_3 band at the frequency of the 10P(16) CO_2-laser line, only a small fraction ($\leqslant 5\%$) of the molecules that left the ground state occupies the vibrational level $\nu_3 = 1$; the remaining molecules are excited up to higher states.

5.3.5 Dependences $f_J(\Phi)$ for SF_6 and NH_3. We measured energy-density dependences of the fraction of molecules excited from individual rotational sublevels with J'' of the ground vibrational state for the P(3) – P(6) transitions in the

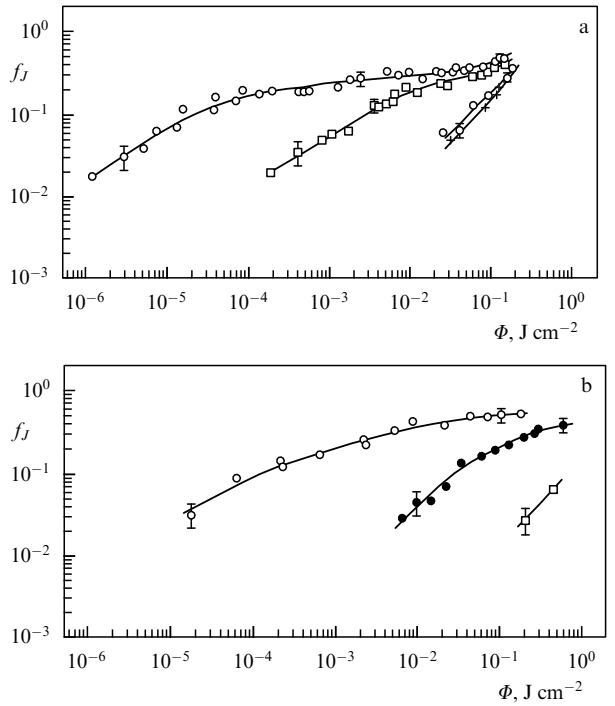

Figure 10. (a) Dependences $f_J(\Phi) \approx f_J^*(\Phi)$ of the fraction of SF_6 molecules excited from individual rotational levels $J'' = 4$ (○), $J'' = 5$ (□), $J'' = 3$ (◇), and $J'' = 6$ (+) of the ground vibrational state by the P(16) CO_2-laser line (947.74 cm^{-1}) on the radiant energy density at the corresponding detunings for the P(J'') transitions from the excitation line frequency: 0.009, 0.048, 0.066, and 0.106 cm^{-1}. (b) Dependences $f_J(\Phi) \approx f_J^*(\Phi)/2$ of the fraction of $^{14}NH_3$ molecules excited from individual rotational levels of the ground vibrational state on the energy density of the CO_2-laser pulse. Transitions sQ(5,4) (○), sQ(2,2) (●), and aR(1,1) (□) in $^{14}NH_3$ molecules were excited on the 10R(6), 10R(8), and 10R(14) CO_2-laser lines at the detunings of the transition frequency from the excitation line frequency: 0.019, 0.031, and 0.049 cm^{-1}, respectively. (Taken from Refs [37, 51].)

ν_3 band of SF_6, closest to the 10P(16) CO_2-laser line in terms of frequency (Fig. 10a). It is a remarkable fact that the excited molecule fraction strongly depends on the detuning $\Delta\nu$ between the exciting radiation frequency and the frequency of the vibrational–rotational transition in the molecules. In addition, the dependences $f_J(\Phi)$ are nonlinear when the detuning is small.

In order to elucidate the mechanism responsible for the observed $f_J(\Phi)$, similar measurements were carried out using $^{14}NH_3$ and $^{14}NH_3$ molecules [37, 51]. It should be borne in mind that the high anharmonicity of the ν_2 mode due to inverse doubling [172] prevents multistep absorption in NH_3. The measured dependences $f_J(\Phi)$ for $^{14}NH_3$ molecules are presented in Fig. 10b. The dependences $f_J(\Phi)$ for $^{15}NH_3$ have a similar character [37, 51]. Comparison of the dependences $f_J(\Phi)$ in Figs 10a and 10b reveals the qualitative similarity of SF_6 and NH_3 curves. In either case, the fraction of molecules excited by the laser field rapidly falls off with increasing detuning $\Delta\nu$; under resonance conditions (for $\Delta\nu \leqslant 0.02$ cm^{-1}), the $f_J(\Phi)$ dependences feature a highly nonlinear character over a wide range of energy densities, $10^{-6} \leqslant \Phi \leqslant 10^{-1}$ J cm^{-2}. It may thus be assumed that the character of $f_J(\Phi)$ dependences both for SF_6 and NH_3 is due to the properties of the exiting laser field rather than to the specific features of the molecular system.

5.4 Effect of the mode composition of CO_2 laser radiation on molecular excitation efficiency

The effect of the mode composition of CO_2 laser radiation on the efficiency of molecular excitation was examined in Refs [51, 163] by measuring $f_J(\Phi)$ in SF_6 for the $J'' = 4$ level. For this level, resonant excitation conditions at the 10P(16) CO_2-laser line were realized on the P(4) transition ($\Delta\nu = 9 \times 10^{-3}$ cm^{-1}) with pulses of different spectral (mode) composition. The depletion was probed on the R(4) transition. For the purpose of measurement, the CO_2 radiation spectrum was varied in the following way. First, the molecules were excited by a 'usual' pulse containing a few longitudinal and transverse modes. An aperture inserted in the laser cavity served to separate one transverse mode. Thereafter the spectrum of longitudinal modes narrowed as the pressure of the working mixture in the CO_2 laser decreased from 1 to 0.5 atmospheres. Finally, one longitudinal mode was separated from the laser emission spectrum with a germanium Fabry–Perot etalon inserted in the cavity. The course of consecutive changes in the measured dependences $f_J(\Phi)$ (see Fig. 11) confirmed the speculation that the mode structure of laser radiation plays an important role in molecular excitation. By way of example, the excitation of 5% of the molecules, $f_J = 0.05$, requires that the energy density Φ of a pulse having the narrowest possible spectrum (in the presence of the Fabry–Perot etalon) must be more than two orders of magnitude (approximately 200 times) that of a broad-spectrum pulse (top and bottom curves in Fig. 11).

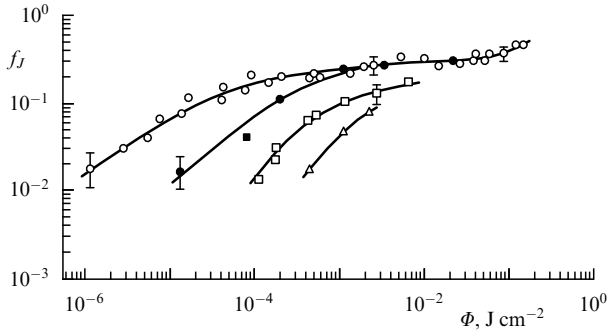

Figure 11. The energy-density dependences $f_J(\Phi)$ for the fraction of SF_6 molecules excited from the $J'' = 4$ level by the 10P(16) line of a CO_2 laser, obtained with pulses of different mode composition: ○ — radiation pulse containing a few transverse modes and some 10 longitudinal modes, ● — radiation pulse with a single transverse mode, □ — narrowed spectrum of longitudinal modes, and △ — spectrum containing one or two longitudinal modes (see the text) (Taken from Ref. [51].)

5.5 Comparison of experimental and theoretical findings

The results of experiments [51, 162, 163] gave the incentive to model calculations of SF_6 excitation [175, 176, 181]. These calculations were based on the known molecular constants of SF_6. Positions of the vibrational–rotational (V–R) levels of the SF_6 ν_3 mode resonant with the CO_2 laser radiation were evaluated up to the states with $\nu_3 = 3$ [149, 182, 183]. The most precise values of these molecular constants were obtained by examining the $1\nu_3 \leftarrow 0$ fundamental band by absorption saturation spectroscopy [182], measuring the spectrum of the $3\nu_3 \leftarrow 0$ overtone transition with a differential spectrometer [149], and evaluating two-photon absorption on the $2\nu_3 \leftarrow 0$ transition [183]. These constants were applied when calculating positions of the V–R levels of the ν_3

resonance mode up to $\nu_3 = 3$ with an accuracy of at least 1×10^{-3} cm^{-1}. However, further experimental and theoretical studies are needed to ensure adequate prediction of the positions of higher levels. Difficulties encountered in such studies are due to the necessity of considering not only the ν_3 mode but also its coupling with other vibrational modes, including accidental resonances between separate V – R levels.

Calculations of excitation dynamics for ground-state SF_6 molecules [175] take into account vibrational levels of the ν_3 resonance mode up to $\nu_3 = 4$ inclusive (five-level model). Positions of the V – R levels were computed with regard for effects of anharmonic splitting, centrifugal distortion, and vibration/rotation coupling. The rotational structure was computed up to $J = 30$. The exciting field was regarded as monochromatic, and its switching on and off instantaneous. The model took into consideration all possible transitions, including four-photon ones.

In Ref. [176], the $f_J(J'')$ dependences were computed taking into account the vibrational $\nu_3 = 0-3$ levels. Two models were considered: a model involving a simple anharmonic oscillator and a rigid top, as well as a model that took into account the spherical anharmonic splitting, centrifugal distortion, and Coriolis interaction, similar to Ref. [175]. In the former model, the exciting radiation was assumed to be monochromatic, and in the latter the laser line was supposed to possess a Lorentzian profile.

Finally, study [181] aimed to elucidate factors responsible for the depletion of the ground state in accordance with model [175] and to compare the role of single- and multiple photon transitions. For this purpose, dependences $f_J(J'')$ were computed for different radiation intensities taking into consideration only two vibrational states of the ν_3 resonance mode, namely, the ground and the first excited ones (two-level model).

Comparison of the results obtained in works [175, 176] and those in an earlier experiment [162] reveals satisfactory agreement between the theoretical dependences $f_J(J'')$ from Ref. [175] and the experimental data from Ref. [162] at $\Phi = 0.5$ J cm^{-2} and 1.3 J cm^{-2} during the excitation of SF_6 molecules at the frequency of the 10P(16) line of a CO_2 laser. However, the observed and computed values differ significantly for $\Phi \leqslant 0.1$ J cm^{-2}, especially in the region $J'' = 4$, where the measured f_J is almost 30% lower than the calculated one. The authors of Ref. [175] explained this difference by the effect of rotational relaxation in a time of molecule's flight between excitation and probing zones. However, the results obtained in Refs [51, 163] indicate that rotational relaxation has practically no effect on f_J under the experimental conditions described in Ref. [162]. The models proposed in Refs [175, 176] also failed to account for the experimental results reported in Ref. [162] at large detunings between the exciting radiation frequency and the SF_6 LAS.

Now, let us compare theoretical predictions with the experimental findings obtained in Refs [51, 163]. Figure 12 shows dependences $f_J(J'')$ for the case of excitation energy density $\Phi = 0.1$ J cm^{-2} ($I \approx 1$ MW cm^{-2}). It follows that the five-level model [175] fairly well describes the structure of the dependence $f_J(J'')$. Indeed, there is a close coincidence between practically all local maxima and minima of the theoretical curve and those observed for $J'' \leqslant 8$. Only at $J'' = 3-6$ are theoretical values more than 1.5 times greater than experimental ones. However, this agreement is only apparently so.

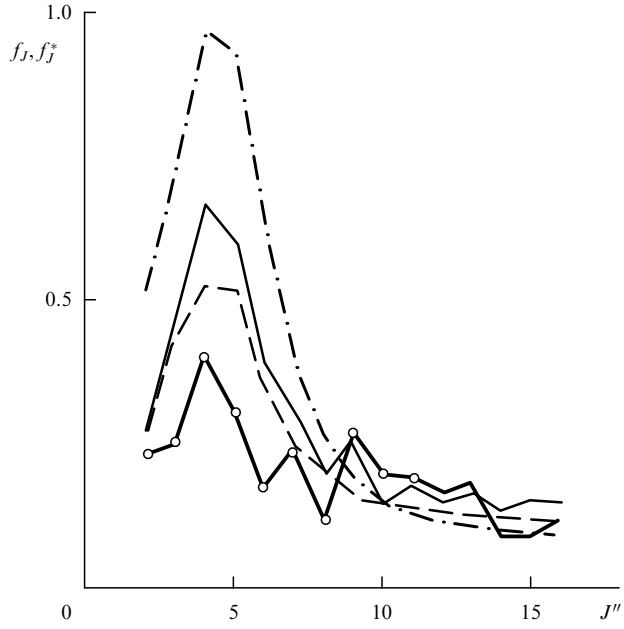

Figure 12. Theoretical depletion $f_J(J'')$ of rotational levels of the SF_6 ground state due to the excitation by the 10P(16) line of a CO_2 laser in the framework of the five-level model ($\nu_3 = 0-4$) [175] (thin solid line), two-level model ($\nu_3 = 0-1$) [181] (dashed line), and the experimental results of study [51] (circles). The dot-and-dash line depicts the theoretical dependence $f_J^*(J'')$ of transition bleaching in probing the P-branch of the ν_3 band in SF_6. (Taken from Refs [51, 163].)

Paper [181] exposed major drawbacks in the assumptions on which the above calculations are based and showed significant discrepancies between theory [175] and experiment. It follows from Fig. 12 that the dependences $f_J(J'')$ predicted by cumbersome calculations taking into account five vibrational states $\nu_3 = 0-4$ and by the straightforward computation in the framework of a two-level model ($\nu_3 = 0, 1$) practically coincide (apart from fine structural details). Thus, the five-level model predicts that one-photon transitions $0 \to \nu_3$ from the ground to the first excited vibrational state $\nu_3 = 1$ play a key role in the depopulation of the ground state, whereas multiple photon transitions are of minor importance for this process. It was concluded that the molecules leaving the ground state basically populate the $\nu_3 = 1$ state. Therefore, probing in the P- and R-branches must reveal a substantially different degree of bleaching (in Fig. 12, the dependence $f_J^*(J'')$ that arises from probing the P-branch in models [175, 176, 181] is shown by the dot-and-dash line). At the same time, experimental studies indicate that the values of f_J^* observed in the P- and R-branches coincide within the limits of experimental error for all J'' from the interval $2 \leqslant J'' \leqslant 10$ with the exception of $J'' = 4$.

The above experimental data indicate that the role of one-photon transitions $0 \to \nu_3$ (leading to the population of the $\nu_3 = 1$ state) in the depletion of rotational levels of the ground state is insignificant. This inference does not agree with theory [175]. First, the theory predicts that the $\nu_3 = 1$ state must be essentially populated. Second, two-, three-, and four-photon transitions theoretically make no important contribution to the depletion of the ground state [181].

As shown in the work [181], the main source of the discrepancy as regards the population of the $\nu_3 = 1$ state lies in the disagreement between the experimental conditions and

the assumption of a field being instantaneously switched on, leading to the overestimation of the role of one-photon transitions when the detuning of the 10P(16) line from the center of the Q-branch of the ν_3 band in SF_6 is rather small. It has been reported in Ref. [51] that the rectangular monochromatic pulse model fails to adequately describe the molecular excitation in a real IR field.

At least one cause of the discrepancy between the predicted [175] and observed results regarding the role of multiple photon transitions is a neglect of the real (nonzero) width and the mode structure of CO_2-laser emission spectra in theoretical models. Our data indicate that vibrational excitation processes in SF_6 and NH_3 molecules under collisionless conditions are qualitatively similar. The efficiency of depletion of rotational sublevels of the lower vibrational state rapidly decreases with increasing detuning between the exciting radiation frequency and the respective transition frequency. Under resonant conditions ($\Delta\nu \leqslant 0.02$ cm^{-1}), the $f_J(\Phi)$ dependence is nonlinear in character over a wide range of energy densities ($10^{-6} \leqslant \Phi \leqslant 10^{-1}$ J cm^{-2}). Consecutive 'simplification' of the emission spectrum of a CO_2 laser (switch-over to the generation on one transverse mode and narrowing the spectrum of longitudinal modes to that of a single mode) leads to a marked decrease in excitation efficiency.

In models [175, 176] used for the description of SF_6 MPE in the region of lower vibrational levels, the laser field is assumed to be monochromatic, and the radiation pulse to be rectangular in time profile. The main reason for this approach is the greater computational difficulties posed by the introduction into analysis of the real (more or less smooth) temporal form of the radiation pulse, to say nothing of the multimode field. To our knowledge, the interaction between pulsed multimode IR radiation and molecules has never addressed in the literature even for the simplest case of a two-level system and double-frequency field. Meanwhile, it follows from experimental findings that the assumption of monochromaticity, i.e., the neglect of the real field structure and its temporal form, cannot be regarded as a physically grounded simplification [51, 52, 164].

5.6 Summary

The above-cited works [37, 51, 161–166] were focused on investigating the depletion of individual rotational levels of the ground vibrational state in SF_6 and NH_3 molecules excited by an intense CO_2 laser radiation. Dependences $f_J(J'')$ for the fraction of excited SF_6 molecules on the rotational quantum number at different excitation frequencies proved to have various structures. When the molecules were excited at the frequency of the 10P(16) CO_2-laser line (in the Q-branch of SF_6), the dependences $f_J(J'')$ were obtained over a wide range of energy densities, $10^{-5} \leqslant \Phi \leqslant 10^{-1}$ J cm^{-2}. It was shown that the dependences of the fraction of excited molecules on the excitation energy density in the range of $10^{-6} \leqslant \Phi \leqslant 10^{-1}$ J cm^{-2} and on the frequency detuning are similar in character for spectroscopically different SF_6 and NH_3 molecules; they are determined by the mode structure of the exciting CO_2 laser radiation.

Comparison of bleaching effect observed in the P- and R-branches of the ν_3 band in SF_6 molecules under the action of an IR pulse showed that only a small fraction of the molecules that escaped from the ground state during the excitation at the frequency of the 10P(16) CO_2-laser line populated the state $\nu_3 = 1$. This observation was also confirmed by the lack of noticeable absorption in the frequency range near 941 cm^{-1} corresponding to the Q-branch of the $2\nu_3 A_{1g} \leftarrow \nu_3$ transition. It was shown that the involvement of molecules in interactions with the laser field at a given frequency detuning sharply decreases as the CO_2-laser emission spectrum narrows.

Diode laser studies on the depletion of individual rotational sublevels of the ground vibrational state of molecules (SF_6, NH_3) under the action of an intense IR laser pulse provided material for the comparison with theoretical estimates. The comparison of experimental and calculated data [175, 176] revealed a striking discrepancy between the observed and predicted populations of the $\nu_3 = 1$ state in SF_6 molecules, and the role of multiple photon transitions. This disagreement was due to the neglect of the real time and mode structures of the exciting CO_2 laser pulse in theoretical models. At the same time, it was shown in experiments that both the width and the mode structure of the pulse generation spectrum play an important role in the molecular excitation.

6. Selective IR dissociation of molecules in a pulsed gasdynamic flow

In this section, we shall fully consider the results of experiments on isotopically selective dissociation of SF_6 and CF_3I molecules in gasdynamically cooled pulsed flows. In addition, we shall briefly discuss certain publications on the UF_6 selective dissociation. It is worthwhile to emphasize that of primary interest in selective dissociation studies using gasdynamically cooled molecular flows are molecules characterized by a small isotope shift ($\Delta\nu_{is} \leqslant 1-5$ cm^{-1}) in the IR absorption spectra. It is most difficult to achieve high selectivity of dissociation for such molecules at room temperature. We have chosen to study the well-known molecules CF_3I and SF_6 for better understanding the-processes taking place during dissociation in gasdynamic flows, examining causes contributing to the output of target products and enrichment factors, and learning how to obtain and effectively collect the products being formed.

6.1 Selective dissociation of CF_3I

Isotopically selective dissociation of CF_3I molecules was examined in Refs [184–186]. The objective of these studies was to evaluate the possibility of obtaining the product enriched in a given isotope during isotopically selective IRMPD of molecules in gasdynamic flows and to measure the dependence of its yield and enrichment factor on laser radiation parameters and molecular flow characteristics. It should be recalled that processes of IR multiple photon excitation and dissociation of CF_3I have been extensively investigated [187–192], including those in a molecular beam [42, 44]. This molecule possesses a relatively small dissociation energy (≈ 2.3 eV [193]) and readily dissociates at moderate energy densities of the laser radiation, $\Phi \leqslant 4$ J cm^{-2} [187–191]. Its dissociation yields stable products (C_2F_6 and I_2). The CF_3I molecule was first regarded as a starting material for the large-scale laser separation of carbon isotopes [194], which required a comprehensive study of the IR absorption spectra of $^{12}CF_3I$ and $^{13}CF_3I$ isotopomers and a measurement of isotopic shifts in these spectra (the isotope shift in the ν_1 vibrational band being excited is $\Delta\nu_{is} = 27.9$ cm^{-1}) [195].

6.1.1 Relationship between parameters of the separation process. Laser irradiation of a spatially restricted pulsed molecular beam of CF_3I with a complete number of particles N_{fl} results in the following molecular concentrations in the flow:

$$N_{12} = N_{12}^0(1 - \beta_{12}\eta)\,, \tag{6.1}$$

$$N_{13} = N_{13}^0(1 - \beta_{13}\eta)\,, \tag{6.2}$$

where N_{12}^0, N_{13}^0 are the concentrations of $^{12}CF_3I$ and $^{13}CF_3I$ isotopomers in the starting mixture, β_{12}, β_{13} are the dissociation yields of these molecules, respectively, and $\eta = N_{irr}/N_{fl}$.

Let the laser radiation be tuned in resonance with molecular vibrations, so that the $^{13}CF_3I$ molecules predominantly dissociate, i.e., $\beta_{13} > \beta_{12}$. The selectivity of dissociation is defined, as usual, in the following way:

$$\alpha_{13} = \frac{\beta_{13}}{\beta_{12}}\,. \tag{6.3}$$

The enrichment factor for the residual gas has the form

$$K_{12}^{res} = \frac{N_{12}/N_{13}}{N_{12}^0/N_{13}^0} = \frac{N_{12}N_{13}^0}{N_{12}^0N_{13}}\,, \tag{6.4}$$

or, taking into account Eqns (6.1)–(6.3), we get

$$K_{12}^{res} = \frac{1 - \beta_{12}\eta}{1 - \beta_{13}\eta} = \frac{1 - \beta_{13}\eta/\alpha_{13}}{1 - \beta_{13}\eta}\,. \tag{6.5}$$

The enrichment factor of the products (without regard for the loss of selectivity in chemical reactions) is given by

$$K_{13}^{prod} = \frac{N_{13}^{prod}/N_{12}^{prod}}{N_{13}^0/N_{12}^0} = \frac{\beta_{13}}{\beta_{12}} = \alpha_{13}\,. \tag{6.6}$$

It follows from formula (6.5) that, for $\eta \ll 1$, the enrichment factor for the residual gas is low even at large values of the parameters α_{13} and β_{13}. This means that a large enrichment factor can be obtained only for the products.

6.1.2 Experiment. The schematic of the experiment is depicted in Fig. 13a. The molecular flow was produced using a pulsed nozzle of the 'current loop' type [95, 97]. The half-height duration of the nozzle-opening pulse was $\tau_{noz} \approx 150$ μs. The diameter of the nozzle slot measured 0.75 mm. The pressure above the nozzle could be varied from ≈ 0.1 to 5 atmospheres. The number N_{fl} of molecules flowing through the nozzle during each pulse depended on the gas stagnation pressure and the amplitude of a current pulse applied to the nozzle. Experimentally, N_{fl} varied from $\approx 10^{16}$ to $\approx 1.5 \times 10^{17}$ molecules per pulse. The nozzle could operate both in a single-pulse mode and in a mode with a pulse repetition rate of up to 1 Hz.

The vacuum chamber (with a volume of $V_{ch} \approx 20$ l) in which the molecular flow formed was pumped down to a residual pressure of $\leqslant 10^{-5}$ Torr by a TMN-500 turbomolecular pump (the pumping rate measured 500 l s^{-1}). The pressure in the chamber was controlled with a PMI-10 ionization transducer. The length τ_{noz} of the nozzle-opening pulse and the mean flow rate v_x were measured with a PED by the TOF technique [27, 102]. The mean rate of CF_3I flow in the excitation zone was $v_x = (400 \pm 20)$ m s^{-1} [196].

The molecular flow was formed using two thin (100 μm) metallic strips attached directly to the nozzle backward cone

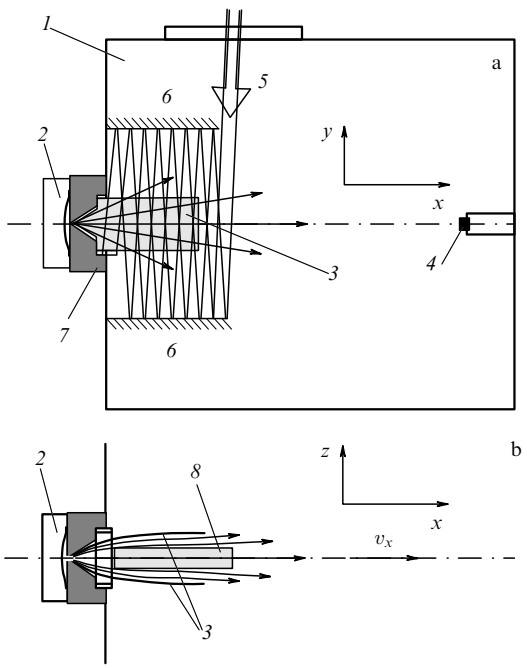

Figure 13. Experimental facility (a) and schematic representation of the formation of a molecular flow (b): *1* — vacuum chamber, *2* — pulsed nozzle, *3* — flow-forming strips, *4* — pyroelectric detector, *5* — laser beam, *6* — reflecting mirrors, *7* — absorber, and *8* — cross section of the irradiated volume in the *xz*-plane. (Taken from Ref. [184].)

(the opening angle about 60°, height 14 mm) in such a way that they formed a dihedral angle (see Fig. 13b). In plane *xz*, these two strips had a varying curvature radius. The maximum opening angle of the strips (inside the nozzle cone) ranged to about 30°. Outside the cone, the strips were 3.0×2.5 cm^2 in size. The distance between them at the outlet of the cone was ≈ 1.0 cm, the maximum distance 1.6 cm. The molecules in the flow were irradiated as they passed between the strips.

The molecules were excited by the radiation of a tunable CO_2 laser that generated pulses with an energy of up to 1.5 J. The laser radiation was focused on the area in the vacuum chamber between the flow-forming strips by a lens with $f_L = 2$ m. The laser beam cross section at the lens focus was $\approx 0.6 \times 0.6$ cm^2. A two-mirror system inside the chamber was used to realize a multipass irradiation scheme with 7–9 passages of the laser beam across the molecular flow. Thereafter, the beam was sent to the absorber (teflon plate). Due to the multipass irradiation scheme utilized in this experiment, the dimensions of the irradiated area parallel to axes *x* and *z* were $\Delta x \approx 3.5$ cm and $\Delta z \approx 0.6$ cm, respectively. The flow was fully irradiated along the *y*-axis. The minimum distance between the nozzle back edge and the front edge of the excitation area was roughly 1.8 cm.

The start times for the nozzle, the CO_2 laser, and the recording system of the molecular flow (comprising a pyrodetector, amplifier (×100), and C9-8 digital oscillograph) were synchronized by a GI-1 delayed pulse generator. Synchronization of the laser pulse and the molecular flow was controlled with the help of a PED by the signal induced in the detector by vibrationally excited CF_3I molecules [42, 196].

6.1.3 Procedure for the collection of products and residual gas and their analysis. The vacuum chamber in which the molecular beam formed had a by-pass pumping channel,

besides the main one. This channel enclosed a cryogenic trap (placed directly at the chamber outlet) cooled by liquid nitrogen, an optical cell with an 'appendix' trap, and a PMT-6 pressure gauge.

Procedures for the irradiation and gas collection were as follows. First, the vacuum chamber and the by-pass channel with the cryogenic trap were pumped out by a turbomolecular pump down to a pressure of about 10^{-5} Torr. Then, the pumping channel of the chamber was closed, the cryogenic trap filled with liquid nitrogen, the nozzle and the CO_2 laser brought into operation, and the gas flow subjected to irradiation. In some experiments, a buffer (H_2, D_2) or acceptor (O_2) gas was fed into the vacuum chamber prior to molecular flow irradiation. The resulting products (C_2F_6, COF_2) and the residual gas (CF_3I) accumulated in the trap. One irradiation cycle consisted of 5 to 200 pulses. Special attention was paid to maintaining the pressure inside the chamber at 10^{-2} Torr or below throughout irradiation.

The irradiation cycle completed, oxygen was fed into the vacuum chamber up to a pressure of about 1 Torr to facilitate collection of all residual gas and reaction products in the trap. Thereafter, the oxygen was slowly evacuated from the chamber through the cryogenic trap till the pressure fell to $\approx 3 \times 10^{-3}$ Torr, leaving CF_3I and C_2F_6 condensed in the trap. The gas from the trap was collected into the optical cell for IR and mass analysis. Because the saturation vapor pressure of CF_3I and C_2F_6 molecules at liquid-nitrogen temperature was rather low ($< 10^{-4}$ Torr), the described procedure allowed practically all CF_3I and C_2F_6 molecules present in the chamber to be collected into the optical cell.

IR analysis of the gas was performed with a Specord 75 IR spectrophotometer. The gas absorption was measured over the frequency range of $680-1400\ \mathrm{cm}^{-1}$, which spans the most intense absorption bands of CF_3I and C_2F_6 molecules [195, 197]. Mass analysis of the gas was made using an MX-7303 mass spectrometer. The isotopic composition of CF_3I was deduced from the CF_3I^+ ion peaks ($m/e = 196$ and 197) and that of C_2F_6 from the $C_2F_5^+$ ion peaks ($m/e = 119$, 120, and 121). The factor of C_2F_6 enrichment in the ^{13}C isotope was determined from the formula

$$K_{13}^{\mathrm{prod}} = \frac{2I_{121} + I_{120}}{(I_{120} + 2I_{119})\xi}\,, \tag{6.7}$$

where I_{121}, I_{120}, and I_{119} are mass-peak intensities of the $C_2F_5^+$ ion, and $\xi \approx [^{13}C]/[^{12}C] \approx 0.011$ is the ratio of the percentage contents of carbon isotopes in the initial CF_3I gas.

6.1.4 Measurement of molecular flow parameters. *Determination of the number of molecules in the flow*. The total number N_{fl} of molecules in the flow was determined by two methods. One of them estimated N_{fl} from the pressure increment Δp in the vacuum chamber during n nozzle pulses produced with the pumping channel closed:

$$N_{\mathrm{fl}} = \frac{\Delta p V_{\mathrm{ch}}}{nkT}\,, \quad T \approx 300\ \mathrm{K}\,. \tag{6.8}$$

With the second method, N_{fl} was determined from the IR absorption spectrum of CF_3I molecules collected in the optical cell from the vacuum chamber after n nozzle pulses. The estimated N_{fl} was closely correlated with the measured value.

Molecular flow extent Δx_{fl}. The extent of a molecular flow in the irradiation zone was also measured in two ways: (1) by the TOF method using a PED [27, 102], and (2) from the dependence of the C_2F_6 yield ($Q_{C_2F_6}$) after irradiation of the CF_3I flow on the delay time t_{del} between a nozzle pulse and the respective exciting laser pulse [184]. The duration of the molecular flow in these measurements was found to be $\Delta\tau_{\mathrm{fl}} \approx 200$ μs. A similar result was obtained by measuring the duration with the help of the TOF method. The mean velocity of molecules being $v_x \approx 400\ \mathrm{m\ s^{-1}}$, the flow extent in the irradiation zone amounted to $\Delta x_{\mathrm{fl}} \approx v_x \Delta\tau_{\mathrm{fl}} \approx 8$ cm.

Estimation of the number of irradiated molecules in the flow. Knowing the extent of the molecular flow and irradiation geometry (see Fig. 13b), it is possible to tentatively estimate the fraction η of the irradiated molecules in the flow, assuming the 'average' concentration of molecules in the irradiated volume to be equal to their 'average' concentration in the entire flow (certainly, it is a very rough approximation):

$$\eta = \frac{N_{\mathrm{irr}}}{N_{\mathrm{fl}}} \approx \frac{V_{\mathrm{irr}}}{V_{\mathrm{fl}}}\,, \tag{6.9}$$

where V_{irr} is the irradiated volume, and V_{fl} is the total volume of the flow. The calculated value came to $\eta \approx 0.2$.

6.1.5 Dependence of the C_2F_6 yield on the energy flux density. The dependence of the C_2F_6 yield on the exciting energy flux density averaged over the laser beam cross section in the region of $\approx 0.6-3\ \mathrm{J\ cm^{-2}}$ was investigated in Ref. [184]. The molecular flow was irradiated at a frequency of 1073.3-cm^{-1} 9R(12) laser line. The CF_3I pressure above the nozzle measured 5 atm. The delay time $t_{\mathrm{del}} = 240$ μs between the nozzle and CO_2-laser pulses fell into the region of optimal delays for the C_2F_6 yield.

The averaged energy density in the irradiation zone was defined as $\Phi_{\mathrm{av}} = E/S$, where E is the pulse energy, and $S = 0.6 \times 0.6 = 0.36\ \mathrm{cm}^2$ is the laser beam cross section. The measured parameters included the dependence of the C_2F_6 yield on the energy flux density (a tendency toward saturation for $\Phi_{\mathrm{av}} \geqslant 2\ \mathrm{J\ cm^{-2}}$ was apparent) and the dissociation yield of CF_3I molecules. It was found that the C_2F_6 yield at $\Phi_{\mathrm{av}} = 3\ \mathrm{J\ cm^{-2}}$ was $Q_{C_2F_6} = 1.75 \times 10^{-9}$ mol per pulse, with the amount of the residual CF_3I gas being $Q_{CF_3I} = 3.2 \times 10^{-8}$ mol per pulse. This means that under these conditions the dissociation yield of $^{12}CF_3I$ molecules must be not less than

$$\frac{2Q_{C_2F_6}}{\eta(Q_{CF_3I} + 2Q_{C_2F_6})} = 0.5\,.$$

In fact, the dissociation yield was higher than that. Part of the CF_3 radicals was lost on the walls and thus failed to contribute to the formation of C_2F_6 molecules (see Sections 6.1.6 and 6.1.7).

6.1.6 Dependence of the C_2F_6 yield on the CF_3I pressure above the nozzle. The study reported in paper [184] was also aimed at elucidating the dependence of the C_2F_6 yield on the gas pressure above the nozzle. The molecular flow was irradiated at a frequency of 1073.3-cm^{-1} 9R(12) laser line. Figure 14 shows the dependences of the yield of the target product and the residual CF_3I gas entering the chamber through the nozzle during one pulse, as well as their ratio

$$R = \frac{Q_{C_2F_6}}{Q_{CF_3I}}$$

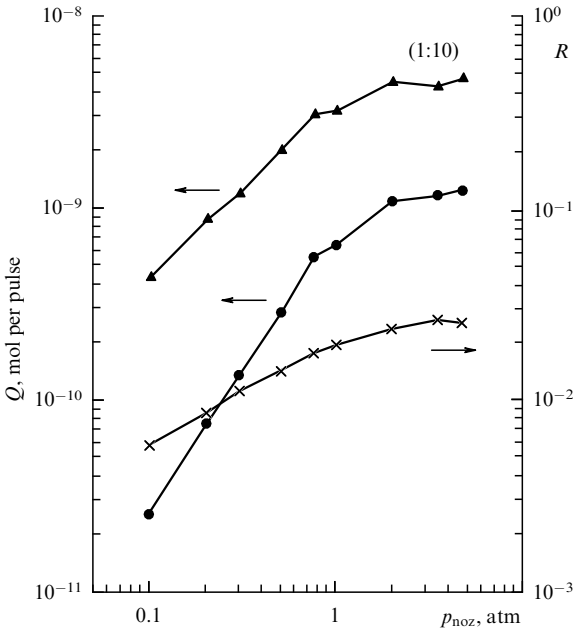

Figure 14. Yields of C_2F_6 (●) and residual CF_3I gas (▲) and their ratio $R = Q(C_2F_6)/Q(CF_3I)$ (×) plotted versus CF_3I pressure above the nozzle. CF_3I molecules were irradiated by the 1073.3-cm^{-1} 9R(12) laser line at the energy density $\Phi = 2.5$ J cm^{-2}. Delay time $t_{del} = 240$ μs. (Taken from Ref. [184].

on the CF_3I pressure above the nozzle. It can be seen that the C_2F_6 yield drops sharply with decreasing CF_3I pressure above the nozzle. Within a range of 0.1 to 1.0 atm, one finds $Q_{C_2F_6} \sim p_{noz}^{1.6}$. Such a dependence suggests an important role of radical concentration in the C_2F_6 production. It is worthwhile recalling that study [190] revealed a roughly quadratic dependence of the C_2F_6 yield on the CF_3I pressure when the $^{12}CF_3I$ dissociation occurred at room temperature in a cell placed in the path of a focused laser beam. Evidently, the lower the concentration of radicals, the more of them that are lost on the walls and thus fail to contribute to the C_2F_6 production. This observation is confirmed by the results of a study on the dependence of the C_2F_6 yield on the number of radiation pulses.

6.1.7 Dependence of the C_2F_6 yield on the number of pulses. In the above studies [184, 185], no buffer or acceptor gas was introduced into the vacuum chamber prior to irradiation. CF_3I molecules accumulated in the chamber themselves served as the buffer gas. The objective of this experiment was to evaluate the effect of buffer gas (CF_3I) pressure on the C_2F_6 yield. It was shown [184, 185] that the C_2F_6 yield substantially decreased with a decreasing number n of radiation pulses. For example, the C_2F_6 production at $n = 100$ was almost twice that at $n = 5$. This difference was due to the fact that buffer gas (CF_3I) pressure in the chamber was still too low ($\leqslant 1$ mTorr) when the number of pulses was small ($n \leqslant 10$), while the mean free path of CF_3 radicals was large enough ($\geqslant 10$ cm). This led to a significant loss of the radicals on the walls of the chamber; as a result, they were exempt from the C_2F_6 production. The optimum yield of C_2F_6 was achieved at $n \approx 100$ [184, 185]. It remained practically independent of n at a further rise in the number of pulses in the range of interest. To conclude, these data and those presented in Fig. 14 indicate that filling the vacuum chamber with a buffer or acceptor gas helps to reduce the loss of CF_3 radicals and thus enhance the yield of target products.

6.1.8 Effect of a buffer (acceptor) gas on the product yield. Indeed, experiments carried out in Refs [184, 185] demonstrated that the C_2F_6 yield in the presence of H_2 or D_2 as a buffer gas in the chamber was 25 – 30% higher than during irradiation of CF_3I molecules in the absence of an admixed gas. When O_2 was used as an acceptor gas, COF_2 molecules were produced along with C_2F_6. The total yield of C_2F_6 and COF_2 molecules was considerably higher than the production of C_2F_6 alone when CF_3I was irradiated in the absence of an acceptor. The effect of a buffer (acceptor) gas on the product yield during isotopically selective dissociation of CF_3I in a gasdynamically cooled flow was thoroughly investigated in Ref. [185].

It should be recalled that the influence of buffer (acceptor) gases on the CF_3I dissociation yield and product yield during molecular excitation in a cell have been studied in many works (see, for instance, references cited in paper [185]). Most of these experiments were carried out at relatively high pressures of CF_3I (0.2 – 1 Torr) and the buffer (acceptor) gas (0.5 – 20 Torr), i.e., when the yields of CF_3I dissociation and the reaction products were greatly influenced by rotational and vibrational – translational relaxations of molecules. At the same time, there was practically no loss of CF_3 radicals on the walls of the chamber under this pressure; therefore, the effect of such losses on the product yield can be disregarded. In experiments with molecular jets and flows, molecule concentrations are rather low, so that rotational and vibrational – translational relaxation of CF_3I molecules is practically absent. Therefore, their effect on the product yield is small, while the loss of CF_3 radicals on the walls is significant. For this reason, the role of buffer and acceptor gases largely consists of reducing the loss of CF_3 radicals on the walls of the vacuum chamber and suppressing the recombination of the primary dissociation products. The loss of CF_3 radicals may be due to the reaction with molecular iodine.

We proposed filling the chamber where a molecular flow is formed with a buffer (acceptor) gas to a pressure of 1 – 3 mTorr in order to reduce the loss of CF_3 radicals produced in molecular dissociation and thus to increase the yield of the target products [184, 185].

The low gas pressure in the chamber does not appreciably affect molecular flow parameters and gas temperature at small distances from the nozzle ($x \leqslant 5$ cm). However, it is associated with a substantial decrease in the mean free path of the radicals, leading to the enhancement of their lifetime in the gaseous phase. Simultaneously, the probability of their contact with the walls decreases. H_2, D_2, and O_2 were used as buffer (acceptor) gases. When no such gas was introduced into the chamber, the CF_3I molecules themselves fulfil the role of a buffer gas as they entered the chamber from the nozzle in the course of flow irradiation.

We conducted experiments of three types when studying the effects of buffer (acceptor) gases on the product yield [185]:

(1) a molecular flow of CF_3I was irradiated in the absence of a buffer or acceptor gas in the chamber. The CF_3I molecules accumulated in the chamber in the course of the experiment themselves played the role of the buffer gas;

(2) a molecular flow of CF_3I was irradiated in the presence of a buffer (acceptor) gas (H_2, D_2, or O_2) in the chamber;

Table 1. Results of experiments with molecular flows of CF_3I and CF_3I/O_2 [185].

Experiment number	Composition of gas mixture	Gas pressure above the nozzle, atm	Buffer (acceptor) gas pressure in the chamber, mTorr	CO_2-laser line, frequency, cm^{-1}	Energy flux density, J cm^{-2}	C_2F_6 yield, nmol per pulse	COF_2 yield, nmol per pulse	$\frac{[COF_2]}{[C_2F_6]}$
1	CF_3I	4.0	—	9R(12) 1073.3	3.0	15.3	—	—
2	CF_3I	4.0	H_2, 3.0	9R(12)	3.0	17.6	—	—
3	CF_3I	4.0	D_2, 3.0	9R(12)	3.0	19.5	—	—
4	CF_3I	4.0	O_2, 3.0	9R(12)	3.0	10.2	16.8	1.65
5	CF_3I	5.0	O_2, 3.0	9R(12)	2.4	8.3	14.3	1.72
6	CF_3I/O_2 (1:5)	2.4	—	9R(12)	2.4	1.0	2.3	2.3
7	CF_3I/O_2 (1:1)	2.7	—	9R(12)	2.4	3.5	9.0	2.57
8	CF_3I/O_2 (1:1)	2.7	—	9P(16) 1050.4	2.4	0.12	0.99	8.25
9	CF_3I/O_2 (1:1.2)	2.75	—	9P(8) 1057.3	1.3	0.026	0.53	20.5

(3) a molecular flow of CF_3I/O_2 was irradiated without prior filling of the vacuum chamber with any gas.

In all these cases, the molecules in the flow were excited in the ν_1 vibrational absorption band of $^{12}CF_3I$ molecules (1075 cm^{-1}) [195]. The conditions and the results of nine experiments are presented in Table 1. Each irradiation session consisted of 100 – 200 pulses. It was found (experiments 1 – 3) that the C_2F_6 yield in the presence of a buffer gas (H_2 or D_2) in the chamber was somewhat higher than in the case of CF_3I irradiation in the absence of any gas (by approximately 15% in the presence of H_2, and 25 – 30% in the presence of D_2). Such a moderate contribution of H_2 and D_2 filling of the chamber to the C_2F_6 yield was accounted for by the presence of CF_3I molecules which, even in the absence of other gases, could by themselves fulfil the part of the buffer gas as they outflowed through the nozzle and accumulated in the chamber in the course of the experiment.

When the chamber contained oxygen as a radical acceptor, the C_2F_6 yield decreased by approximately 1.5 times (experiments 1 and 4), but COF_2 molecules were produced. In this case, the total yield of C_2F_6 and COF_2 molecules was higher than that of C_2F_6 alone when the CF_3I molecular flow was irradiated in the absence of a buffer gas in the chamber. The total number of CF_3 radicals that went into the C_2F_6 and COF_2 production (experiment 4) was approximately 22% higher than in the case of CF_3I irradiation in the absence of a buffer gas in the chamber (experiment 1).

When the molecular flow containing CF_3I/O_2 was irradiated (experiments 6 – 9), the resulting products were dominated by COF_2. The fewer the products formed, i.e., the smaller the CF_3I dissociation yield (low energy density, marked detuning of the exciting radiation frequency from the center of the absorption band of the molecule), the larger the fraction of COF_2 molecules in the products (experiments 8 and 9). Such a behavior of COF_2 and C_2F_6 yields during CF_3I dissociation in the O_2-containing flow can be explained in the following way. In the presence of an excessive amount of oxygen, the COF_2 yield appears to be linearly dependent on the concentration of CF_3 radicals being formed. At the same time, concentration effects are of primary importance in the formation of C_2F_6 molecules because it requires pair collisions of CF_3 radicals to take place. Therefore, as the concentration of CF_3 radicals decreases, the C_2F_6 production drops at a higher rate than the COF_2 yield. It has also been found in Ref. [185] that the use of oxygen as a radical acceptor greatly promotes the absolute yield of C_2F_6 and COF_2 molecules if the chamber is filled with oxygen, while the intense CF_3I flow being used contains no oxygen (experiments 4 and 5).

6.1.9 Frequency dependence of ^{13}C content in the C_2F_6 product. Figure 15 displays the dependence of the carbon ^{13}C content in the C_2F_6 product on the CO_2-laser exciting radiation frequency. For comparison, a linear absorption spectrum of CF_3I molecules over a range from 1020 to 1090 cm^{-1} is also presented (obtained with a Specord 75 IR spectrophotometer having a resolution of about 1 cm^{-1}). Shown at the top of the figure is the position of CO_2 laser lines. It can be seen that the frequency dependence possesses a rather narrow ($\approx$ 10 cm^{-1}) contour. The ^{13}C content in C_2F_6 is especially high when the

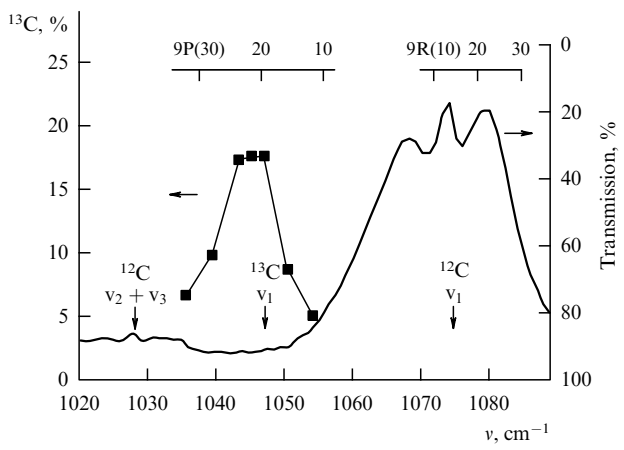

Figure 15. ^{13}C content in C_2F_6 versus exciting radiation frequency during irradiation of CF_3I molecules at the energy density $\Phi = 1.6$ J cm^{-2}. The CF_3I pressure above the nozzle is 5 atm, delay time $t_{del} = 250$ μs. The thin solid line displays a CF_3I LAS (right scale). (Taken from Ref. [184].)

dissociation of CF_3I molecules occurs on the 9P(20) – 9P(24) lines. With a detuning of the exciting radiation frequency to either the violet or the red side with respect to these lines, the ^{13}C content in the C_2F_6 product sharply decreases. The fall is due to a rise in the $^{12}CF_3I$ dissociation yield with the frequency shift to the blue side, resulting from the excitation of the ν_1 vibration (1075 cm^{-1} [195]), and with the frequency redshift, resulting from the excitation of the $\nu_2 + \nu_3$ vibration (1028 cm^{-1} [195]). As a consequence, the optimal conditions in selectivity α_{13} for the CF_3I dissociation are realized within rather a narrow spectral interval, namely, on the 9P(20) – 9P(24) lines.

6.1.10 Dependence of ^{13}C enrichment factor of the C_2F_6 product on the concentration of CF_3I molecules in the flow. Study [186] was designed to evaluate the dependence of the ^{13}C enrichment factor of the C_2F_6 molecules on the concentration of molecules in the flow. For this purpose, we examined the dependence of the ^{13}C enrichment factor K_{13}^{prod} of the C_2F_6 product on the complete number N_{fl} of molecules in the flow and on the delay time t_{del} between the nozzle pulse and the respective exciting laser pulse. Figure 16a demonstrates the dependence $K_{13}^{prod}(N_{fl})$. The molecules were irradiated at a frequency of 1043.16-cm^{-1} 9P(24) laser line resonant with the ν_1 vibration in $^{13}CF_3I$ [195]. It is at this frequency that the highest enrichment factor for C_2F_6 was measured [184]. Also, the figure shows the dependence of the C_2F_6 yield on N_{fl}, $Q_{C_2F_6}(N_{fl})$. Evidently, both the yield and K_{13}^{prod} decrease with decreasing N_{fl}. For example, a decrease in N_{fl} from $\approx 1.4\times10^{17}$ to $\approx 5.2\times10^{16}$ molecules per pulse results in a fall of K_{13}^{prod} from about 25 to 10. Figure 16b displays the dependence $K_{13}^{prod}(t_{del})$. For comparison, the dependence $Q_{C_2F_6}(t_{del})$ is also presented as obtained by the excitation of $^{12}CF_3I$ molecules at a frequency of 1071.9-cm^{-1} 9R(10) laser line [184] that characterizes the time evolution of molecular flow intensity. It can be seen that K_{13}^{prod} substantially decreases as the delay time increases or decreases from the value of $t_{del} \approx 280$ μs at which the most intense part of the molecular flow was irradiated. This finding confirms once again that K_{13}^{prod} significantly decreases with a decreasing concentration of CF_3 radicals produced in the flow.

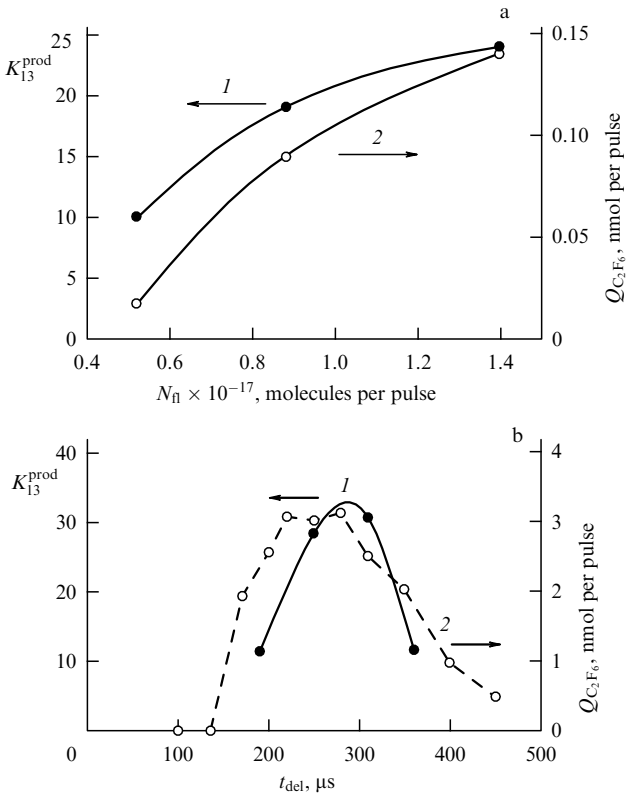

Figure 16. (a) Dependence of the ^{13}C enrichment factor of C_2F_6 (curve *1*) and the C_2F_6 yield (curve *2*) on the complete number N_{fl} of CF_3I molecules in the flow; delay time $t_{del} = 250$ μs. (b) Dependence of the ^{13}C enrichment factor of C_2F_6 on the delay time t_{del} (curve *1*). CF_3I molecules were irradiated by the 1043.16-cm^{-1} 9P(24) laser line at the energy density $\Phi = 1.6$ J cm^{-2} and $p_{noz}(CF_3I) = 5$ atm. Curve *2* in Fig. 16b shows the dependence of the C_2F_6 yield on t_{del}, obtained by molecular irradiation at the frequency 1071.9 cm^{-1} [9R(10) line], $\Phi = 3$ J cm^{-2}, and $p_{noz}(CF_3I) = 4$ atm. (Taken from Ref. [186].)

The main cause leading to the decrease in K_{13}^{prod} with a decreasing concentration of CF_3I molecules in the flow is the loss of CF_3 radicals on the walls of the chamber. As shown in Ref. [184], progressively greater fraction of CF_3 radicals are lost on the walls and fail to be involved in the C_2F_6 production as their concentration in the flow decreases. Because selectivity of the dissociation in the experiments being described was lower than the $^{12}C/^{13}C$ content ratio in the initial CF_3I gas ($\alpha_{13} < [^{12}C]/[^{13}C]$), the quantity of $^{13}CF_3$ radicals produced was invariably smaller than $^{12}CF_3$. For this reason, relatively more $^{13}CF_3$ radicals were lost on the walls, which led to a decrease in K_{13}^{prod} with the decreasing concentration of the molecules irradiated in the flow.

Thus, it was shown in work [186] that the factor K_{13}^{prod} of C_2F_6 enrichment in the ^{13}C isotope strikingly decreases with the decreasing concentration of CF_3I molecules in the flow. The decrease in K_{13}^{prod} is associated with the loss of CF_3 radicals on the walls of the chamber where the molecular flow forms. Therefore, the yield of the ^{13}C-enriched product can be increased by increasing the concentration of $^{13}CF_3$ radicals in the flow ($N \geqslant 10^{13}$ cm^{-3}) and/or by introducing a radical acceptor (e.g., O_2) into the chamber.

In connection with the problems considered in this section, it is appropriate to mention work [198] in which the study of isotopically selective IRMPD of CF_3Br molecules in a supersonic molecular jet revealed relatively poor selectivity in the C_2F_6 product ($K_{13}^{prod} \approx 6.9$) at rather low gas temperature ($T_{rot} \approx 70$ K). We believe that such impaired selectivity was due to the concentration effect in the course of C_2F_6 production underlain by pair collisions of CF_3 radicals and to the possible loss of the radicals on the chamber walls. This inference is confirmed by the results of our experiments with CF_3I molecules.

6.2 Selective dissociation of SF_6

We shall consider in this section the results of investigations into the isotopically selective dissociation of SF_6 molecules [199]. Let us recall that this molecule was the subject of extensive surveys (see, for instance, Refs [10 – 12]), while very few studies were concerned with selectivity in the SF_4 product [67, 140]. Most works devoted to the SF_6 selective dissociation examined spectral (frequency) dependences of the $^{32}SF_6$ dissociation yield. Such dependences were obtained for molecular excitation in a cell at room [67, 200, 201] and low (190 K [68], 175 K [140], 140 K [201]) temperatures, in a molecular beam [43, 73, 202], and in a pulsed gasdynamic jet [115]. Spectral dependences of the $^{32}SF_6$ dissociation yield were also studied during the excitation of molecules by a double-frequency IR field [43, 68, 115]. In Ref. [73], such

dependences were obtained at different gas temperatures above the nozzle in the range between 210 and 450 K. A most comprehensive investigation into the spectral dependences of the dissociation yield of SF_6 molecules in a cell at room and low gas temperatures was reported in work [201]. It is worthwhile to note that the spectral dependence of the dissociation yield may be used to evaluate the selectivity of the process. At the same time, the observed selectivity is, as a rule, lower than the one calculated from spectral dependences of the dissociation yield [67, 140]. The discrepancy is due to the loss of selectivity in chemical reactions. Therefore, the knowledge of product selectivity is needed to apply the IRMPD technique to the practical separation of isotopes.

The primary objective of work [199] was to investigate the spectral dependence of the SF_4 yield during SF_6 dissociation in a pulsed gasdynamic flow and to assess selectivity of this process from the ^{34}S enrichment factor of the product. The work was not aimed at obtaining maximum selectivity values. Therefore, molecular dissociation was effected by single-frequency radiation at relatively high energy densities. Using a gasdynamically cooled pulsed molecular flow, we sought to compare selectivity in a product with the one expected from the spectral dependence of the $^{32}SF_4$ yield.

6.2.1 Experiment and procedure. The experimental facility and measuring techniques employed in work [199] were described earlier in Sections 6.1.2 and 6.1.3. Molecules in a flow were excited by the radiation of a CO_2 laser having a pulse energy of up to 3 J. The laser radiation was focused into the region between the flow-forming strips by a cylindrical lens with a focal length of $f_L = 12$ cm. The minimal laser beam cross section in the lens focal area was approximately 0.6×18 mm^2. The laser beam crossed the molecular flow and fell on the absorber (teflon plate). The minimal distance between the nozzle back edge and the front edge of the excitation area was approximately 4 cm. The SF_4 product resulting from the SF_6 dissociation and those SF_6 molecules that failed to dissociate accumulated in the cryogenic trap. Main attention in the course of molecular flow irradiation was given to maintaining the gas pressure inside the vacuum chamber below 5–6 mTorr at the end of each irradiation cycle. This was needed to avoid strong scattering of the molecular flow from the background gas.

The analysis of SF_4 molecules in the mixture with SF_6 was seriously hampered because the mass spectra of both molecules overlapped. For this reason, we analyzed the isotopic composition of an SF_4 molecule based on its IR absorption spectrum. The absorption band of $^{32}SF_4$ is especially intense in the 728-cm^{-1} region (ν_6 vibration [203]). The isotope shift for $^{32}SF_4$ and $^{34}SF_4$ molecules in this band measures $\Delta\nu_{is} \approx 12.3$ cm^{-1} [204].

The dependences of the SF_4-product yield $Q_{32}^{prod}(\Phi_{av})$ on the excitation energy density averaged over the interaction volume were obtained in work [199] for a variety of CO_2-laser emission lines in a range from 10P(10) to 10P(36). These measurements were employed to construct spectral dependences of the SF_4 yield.

6.2.2 Spectral dependence of the SF_4 yield. Figure 17a presents the dependence of the $^{32}SF_4$ yield on the radiation frequency of a CO_2 laser that excites SF_6 molecules. The dependence was obtained for the averaged energy flux density $\Phi_{av} \approx 12$ J cm^{-2} (at a pulse energy of $E_p = 2.5$ J). A similar dependence for the $^{34}SF_4$ yield is plotted for the purpose of analysis through the

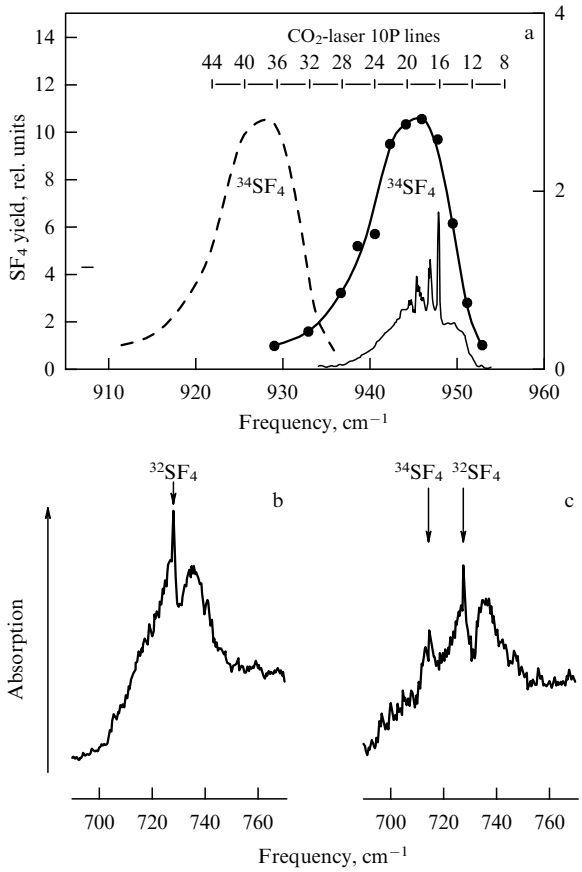

Figure 17. (a) Dependences of the yields of $^{32}SF_4$ (thick solid line) and $^{34}SF_4$ (dashed line) on the radiation frequency of a CO_2 laser exciting SF_6 molecules, $p_{noz}(SF_6) = 1.26$ atm; the thin solid line shows the SF_6 LAS at $T \approx 300$ K [123]; IR absorption spectra of $^{32}SF_4$ molecules (b) and ^{34}S-enriched SF_4 molecules (c). SF_4 molecules in Figs 17b and 17c were obtained by SF_6 irradiation at the frequency of 947.74-cm^{-1} 10P(16) laser line resonant with $^{32}SF_6$, and at the frequency of 929-cm^{-1} 10P(36) laser line resonant with $^{34}SF_6$, respectively. (Taken from Ref. [199].)

displacement of the experimental dependence $Q_{32}^{prod}(\nu)$ by the isotope shift ($\Delta\nu_{is} \approx 17.4$ cm^{-1} [205]). By way of comparison, the bottom part of the figure shows the $^{32}SF_6$ LAS at $T \approx 300$ K, borrowed from Ref. [123].

The dependence $Q_{32}^{prod}(\nu)$ is significantly narrower (half-height width $\Delta\nu \approx 11$ cm^{-1}) than the frequency dependence of the $^{32}SF_6$ dissociation yield observed in work [67] during SF_6 excitation in a cell at room temperature (half-height width $\Delta\nu \approx 18$ cm^{-1}). This difference is undoubtedly due to the low temperature of SF_6 molecules in our experiments. The peak of the dependence $Q_{32}^{prod}(\nu)$ lies close to 946-cm^{-1} 10P(18) laser line. It should be noted that Ref. [73] describes the frequency dependence maximum for the $^{32}SF_6$ dissociation yield in a supersonic molecular jet at SF_6 temperature $T \approx 295$ K in the source and radiant energy density $\Phi = 5$ J cm^{-2} as lying close to 943 cm^{-1}, and the half-height contour width as being $\Delta\nu \approx 14$ cm^{-1}. Our results, which exhibit a rather narrow contour of the frequency dependence of the $^{32}SF_4$ yield and a relatively small displacement of its maximum relative to the Q-branch of the $\nu_3 = 1 \leftarrow \nu_3 = 0$ transition in $^{32}SF_6$, can be accounted for [27] by the fact that in our experiments the vibrational temperature of SF_6 molecules in the jet was much lower than in the continuous molecular beam [73].

Bearing in mind the derived dependence $Q_{32}^{\text{prod}}(\nu)$, it is possible to estimate the expected efficiency of SF_4 enrichment in the ^{34}S isotope (selectivity of the process). The enrichment factor is denoted as $K_{34}^{\text{prod}} = Q_{34}^{\text{prod}}/(Q_{32}^{\text{prod}}\xi)$, where $\xi = [^{34}S]/[^{32}S] \approx 0.044$ is the ratio of percentage contents of ^{34}S and ^{32}S isotopes in the natural SF_6 gas. Assuming similarity of spectral dependences of the $^{34}SF_4$ and $^{32}SF_4$ yields (following from Fig. 17a), the enrichment factor will be equal to the ratio of specific yields of $^{34}SF_4$ and $^{32}SF_4$ molecules at any frequency. In this case, for instance, at a frequency of 929-cm^{-1} 10P(36) laser line, the expected ^{34}S enrichment factor of SF_4 molecules is approximately 12. However, the real enrichment factor of the SF_4 product can be smaller than expected because of the effect of secondary chemical reactions (see, for instance, Refs [67, 140]). It will be shown in Section 6.2.3 that in our experiments the ^{34}S enrichment factor of SF_4 molecules was close to the expected one.

6.2.3 ^{34}S-isotope enrichment factor of SF_4. The SF_4 product was enriched in an ^{34}S isotope by the excitation of SF_6 molecules at a frequency of 929-cm^{-1} 10P(36) laser line redshifted approximately 1.6 cm^{-1} relative to the Q-branch of the $\nu_3 = 1 \leftarrow \nu_3 = 0$ transition of the ν_3 vibration in $^{34}SF_6$ ($\approx$ 930.6 cm^{-1} [205]). It may be supposed that the dissociation yield of $^{34}SF_6$ molecules at this frequency is roughly equal to that of $^{32}SF_6$ molecules at the frequency of 946-cm^{-1} 10P(18) laser line shifted approximately 1.8 cm^{-1} to the long-wave region from the Q-branch of the $\nu_3 = 1 \leftarrow \nu_3 = 0$ transition in $^{32}SF_6$ molecules.

In an attempt to obtain an amount of the ^{34}S-enriched SF_4 product sufficient for the measurements of its IR spectrum, we produced about 20 times more pulses than for the SF_6 irradiation by the 10P(18) laser line (with the ratio of $[^{32}S]/[^{34}S] \approx 22$ in the parent SF_6 gas). Figures 17b and 17c present the IR absorption spectra of $^{32}SF_4$ molecules, obtained by the SF_6 irradiation on the 10P(16) laser line, and of SF_4 molecules enriched in the ^{34}S isotope. Figure 17c exhibits a highly apparent absorption peak of $^{34}SF_4$ molecules. The enrichment factor $K_{34}^{\text{prod}} \approx 13 \pm 3$ obtained in these experiments is in good agreement with the expected value of this quantity, predicted from the spectral dependence of the SF_4 yield (Fig. 17a).

It is worth noting that the enrichment factor K_{34}^{prod} is somewhat smaller than the real one because in our experiments the dissociation of SF_6 molecules contained in the gasdynamic flow occurred concurrently with the dissociation of 'background' SF_6 molecules that accumulated in the chamber at $T \approx 300$ K in the course of flow irradiation. The selectivity of dissociation of the 'background' molecules was appreciably worse than that of the SF_6 molecules in the flow (probably $\alpha \leqslant 3$ [67, 201]). Estimates taking into account the average pressure of the 'background' SF_6 gas in the chamber ($\approx$ 3 mTorr) indicate (see, for instance, Ref. [185]) that the contribution of the 'background' SF_6 molecules to the SF_4 yield amounted to approximately 30%. Hence, the enrichment factor of SF_4 molecules comes to $K_{34}^{\text{prod}} \approx 17 \pm 5$ if recalculated per molecule undergoing dissociation in the molecular flow.

The analysis of spectral dependences of the SF_6 dissociation yield measured in a cell at low temperature and in a molecular beam indicates that in the majority of the above-cited works the expected selectivities at the same frequency did not exceed that in our experiments even though lower energy densities were used. An exception is the SF_6 dissociation in a cell at $T \approx 140$ K, when the expected selectivity at the above frequency [$\alpha(34/32) \approx 30$] was higher [201] than in our experiments. However, the dissociation of SF_6 molecules in work [201] occurred at a much smaller energy flux density $\Phi = 5$ J cm^{-2}.

Thus, studies on isotopically selective IRMPD of SF_6 molecules have demonstrated the possibility of producing and effectively collecting the isotopically enriched SF_4 product in a pulsed gasdynamic flow. They also suggest the spectral dependence of the SF_4 yield and provide the ^{34}S enrichment factor for the target product. In the case of molecular excitation at a frequency of 929-cm^{-1} 10P(36) laser line and a relatively high energy flux density $\Phi_{\text{av}} \geqslant 10$ J cm^{-2}, the enrichment factor $K_{34}^{\text{prod}} \approx 13 \pm 3$ and amounts to $K_{34}^{\text{prod}} \approx 17 \pm 5$ if recalculated per molecule dissociated in the flow. The measured enrichment factor is in good agreement with its value estimated from the spectral dependence of the $^{32}SF_4$ yield.

In the context of selectivity of SF_6 dissociation considered in this section, it is appropriate to mention the study by Dem'yanenko et al. [206] in which IR dissociation kinetics of SF_6 molecules was investigated by the IR – UV excitation technique. This research has demonstrated the production of S^+ and SF^+ ions on exposure to UV irradiation of SF_5 radicals yielded by the IR dissociation of SF_6 molecules. Kinetic curves for the yield of $^{34}S^+$ and $^{32}S^+$ ions in Ref. [206] were used to derive a selectivity value which proved to be very high [$\alpha(34/32) \approx 80$] and was regarded as the primary selectivity of the IR dissociation of gasdynamically cooled SF_6 molecules in a beam. However, only part of the possible ion production channels were found in this investigation. Therefore, it would be incorrect to associate the selectivity measured in those experiments with the process of SF_6 IR dissociation alone. The authors of later studies [207, 208] have demonstrated concurrent UV fragmentation of SF_5 radicals and highly vibrationally excited SF_6 molecules. This means that the observed selectivity in the resulting fragments $^{34}S^+$ and $^{32}S^+$ is due to the combined processes of IR – UV excitation of the molecules in addition to their IR dissociation. In paper [209], prepared by the same group, the UV photoionization technique was applied to detect CF_2 radicals produced by the IRMPD of CF_2HCl molecules in a cell at room temperature, as well as in a molecular flow. Based on the amount of CF^+ ion fragments, the authors of Ref. [209] measured the selectivity of molecular dissociation under experimental conditions as $\alpha(13/12) \approx 18$ in the case of molecular excitation at room temperature, and as $\alpha(13/12) \approx 45.5$, i.e., significantly higher, in the case of excitation in a gasdynamically cooled pulsed molecular beam.

6.3 Selective dissociation of UF_6

In what follows, we shall briefly discuss the results of investigations into isotopically selective dissociation of UF_6 molecules. We should recall that natural uranium consists mostly of the ^{235}U isotope (0.71%) and ^{238}U isotope (99.28%), while enriched uranium containing 3 – 4% of ^{235}U is needed for uranium reactors of nuclear power plants. UF_6 is the parent molecule for uranium isotope separation by the IRMPD technique. Of all known uranium compounds, UF_6 is the most convenient for enriching in ^{235}U isotope because it has the highest vapor pressure and there is only one stable isotope of fluorine (^{19}F).

It has been mentioned in Section 4.7.1 that the intense ν_3 vibration band of the UF_6 molecule lies in the 16-μm region (≈ 627.7 cm^{-1} for $^{238}UF_6$ [157]). The isotope shift for $^{235}UF_6$ and $^{238}UF_6$ molecules in this band is around 0.6 cm^{-1}, the absorption bandwidth at room temperature is ≈ 20 cm^{-1}, and the Q-branch is roughly 3.5 cm^{-1} wide. Due to this, the absorption spectra of $^{235}UF_6$ and $^{238}UF_6$ molecules almost completely overlap [24]. The population of the ground state at $T \approx 300$ K does not exceed $\approx 0.45\%$. Consequently, a relatively high selectivity of UF_6 dissociation is feasible only in a jet- or flow-cooled gas using a two- or three-frequency excitation scheme.

The sources of UF_6 excitation at the 16-μm band include para-H_2 rotational Raman lasers [158, 159] and CO_2-pumped molecular CF_4 lasers (see, for instance, Refs [210, 211]). It should be noted that many studies have been devoted to UF_6 dissociation by both single- and double (IR – IR, IR – UV)-frequency radiation (see, for instance, review article [212] and the literature cited therein). No isotopic selectivity has been observed in experiments on UF_6 dissociation in a cell at room temperature [213]. Paper [214] (see also Ref. [215] by the same team) was one of the first reported on isotopically selective dissociation of UF_6 molecules by IR radiation. In those experiments, the molecular beam was produced effusively as an equimolar mixture of UF_6 isotopomers outflowed through a 25 μm-diameter pinhole. The molecules in the beam were excited by radiation at two frequencies obtained by Raman scattering of a CO_2 laser emission in para-hydrogen (see Section 4.7.3). One of the frequencies used for the selective molecular dissociation was scanned over a range of 613.4 – 628.9 cm^{-1}, while the other (fixed at 596.8 cm^{-1}) caused the excited molecules to dissociate. The irradiation over, the molecules in the beam were analyzed for isotopic composition. The selectivity was determined as the ratio of depletion of the beam current of $^{235}UF_6$ molecules to that of $^{238}UF_6$ molecules. Evidently, the more this ratio departs from unity, the higher the selectivity. The largest deviations from unity (1.2 and 0.73) were recorded at excitation frequencies of 627.8 and 613.4 cm^{-1}, respectively.

Studies [216, 217] were designed to evaluate the effects of H_2, CH_4, and C_2H_6 molecules on the selectivity of dissociation of UF_6 molecules cooled down to $-35\,^{\circ}$C in a cell placed in the field of a para-H_2 Raman laser with a pulse energy of 0.1 – 0.16 J, uranium hexafluoride pressure of 0.2 – 0.4 Torr, and an additional gas pressure of 1 Torr. The maximum selectivity of 1.043 was achieved during the irradiation of UF_6 molecules free from admixture, and of a UF_6/CH_4 mixture. The selectivity in the UF_6/H_2 and UF_6/C_2H_6 mixtures amounted to 1.028 and 1.024, respectively.

Papers [218, 219] report experimental results on the double-frequency excitation of an overcooled mixture of UF_6, CH_4, Ar, or Kr at the outlet of a supersonic nozzle (for $T \leqslant 100$ K). A continuously tunable para-H_2-based Raman laser served as a source of exciting radiation. The resultant selectivity was estimated at ~ 4. In the most recent studies carried out at the Institute of Physical and Chemical Research (RIKEN, Japan), the maximum selectivity (product enrichment) of about 5 was achieved in similar conditions by three-frequency irradiation. Such selectivity is sufficient to enrich natural uranium in the ^{235}U isotope up to 3 – 3.5% and thus procure fuel for nuclear power plants. It should be noted, however, that the building of production units for the laser separation of uranium isotopes by IRMPD of UF_6 molecules is considered to lack cost-effectiveness at the modern level of laser technology [212]. What is needed to-day is the optimization of all stages of this rather complicated process at the available facilities, including those such as the selective excitation and multiple photon dissociation of UF_6 molecules, parameters of laser radiation sources, and gas flows.

6.4 Methods for improving the efficiency of the isotopically selective dissociation of molecules

It has been demonstrated in Section 6.1 that feeding a buffer or acceptor gas into the chamber where a molecular flow is formed and irradiated provides a method to enhance the product yield in isotopically selective dissociation of molecules in the flow (exemplified by CF_3I). This procedure has practically no effect on product enrichment. Our recent studies [220 – 227] have shown that a rather simple and convenient method to increase the efficiency of isotopically selective dissociation of molecules in gasdynamically cooled jets and flows consists of the formation of a compression shock in front of the solid surface on which the flow falls. The results of these studies are discussed in detail in Ref. [100]. Here is a brief description of the essence of the method [221 – 223].

The method is based on the formation of a compression shock in front of a solid surface. It has been shown in works [221 – 223] that the interaction of an intense gasdynamically cooled supersonic molecular flow (or jet) with a solid surface gives rise to a compression shock (shock wave) [228 – 230]. The nonequilibrium conditions in the compression shock are the reverse of the nonequilibrium conditions in the incident (undisturbed) flow, ($T_{tr} \leqslant T_{rot} \leqslant T_{vib}$ in the incident flow, and $T_{tr} \geqslant T_{rot} \geqslant T_{vib}$ in the compression shock). This makes it possible to study the isotopically selective IRMPD of molecules in the new nonequilibrium conditions and substantially improve the efficiency of selective dissociation (see Sections 6.4.1 and 6.4.2).

6.4.1 Molecular excitation in a flow incident on a surface. It was shown in Refs [220, 221] that for a flow of SF_6 molecules incident on a surface and being excited under conditions where the distance between the excitation zone and the surface $\Delta x \gtrsim 30$ mm, the HF^* luminescence pulse consists of two peaks separated in time, and the larger the distance Δx, the greater the separation. It should be recalled that HF^* luminescence accompanies the SF_6 dissociation in the presence of H_2 or CH_4 molecules (see Section 3.4). It has been found that the first peak is caused by the molecular dissociation in the excitation zone, and the second by the dissociation of molecules in the region where the flow interacts with the surface, i.e., in the compression shock. When $\Delta x \leqslant 20$ mm, these peaks could not be resolved in time because of the small transmission band (≈ 16 kHz) of the IR detector. However, HF^* luminescence intensity showed strong dependence on whether or not there was a surface in the path of the flow. If the flow encounted the surface, the luminescence intensity was five to eight times higher than in an undisturbed flow.

The increase in HF^* luminescence intensity in the case of molecular excitation in a flow incident on a surface is associated with the increase in the molecular dissociation yield due to the formation of a compression shock in front of the surface [228 – 230]. In the case of IR multiple photon excitation, an ensemble of highly excited molecules with a rather broad distribution over vibrational states is formed [12, 14]. As a result, some of the molecules dissociate

radiatively (i.e., experience no collisions), while others undergo dissociation by collisions involving highly excited molecules. In an undisturbed flow, there is only radiative dissociation, because the deficit of collisions precludes collisional dissociation of highly excited molecules, whose contribution to the total yield is normally very large (see, for instance, Refs [12, 67]). Both gas density and temperature are much higher in the compression shock formed in front of the surface where the excited molecules land than they are in the incident flow. Therefore, the conditions within the shock wave are conducive to collisions between highly excited molecules, leading to an enhanced dissociation yield. As shown in works [220 – 223], selectivity of the process is only slightly worse (by 10 – 12%) than that of molecular dissociation in an undisturbed flow.

6.4.2 Molecular excitation in the compression shock. When molecules were excited directly in the compression shock (at a distance $\Delta x = 1-5$ mm from the surface), the maximum intensity of HF^* luminescence was at least 10 times higher than during molecular excitation in the undisturbed flow [221 – 226]. As the distance Δx between the surface and the excitation zone decreased (increased), the HF^* luminescence intensity in the compression shock also rose (fell).

It was established in experiments [221 – 223] that luminescence intensity in the compression shock increased dramatically with a rise in the primary beam intensity (gas pressure above the nozzle) because the gas density in the shock also increased. Under a low stagnation pressure ($\leqslant 0.2$ atm), with the concentration of molecules in the flow being $N_{\rm fl} \leqslant 3\times 10^{14}$ cm^{-3}, the compression shock is of low intensity and only weakly manifests itself in the luminescence signal. Under a comparatively high pressure above the nozzle ($\geqslant 1$ atm), the intensity of luminescence in the shock wave is much higher (by a factor of 20 – 30) than in the undisturbed flow. Similar results were obtained for CF_3I molecules [227]. When CF_3I was excited in the flow incident on the surface, the yield of C_2F_6 molecules was 2 – 3 times that produced on excitation in an undisturbed flow. The CF_3I excitation within the compression shock resulted in a C_2F_6 yield that was higher than in the undisturbed flow by a factor of 15.

The works [221 – 223] cited in the preceding paragraph showed (see Table 2) that in the case of SF_6 excitation in an undisturbed flow at an energy density of ≈ 10 J cm^{-2}, the enrichment factor $K_{34}^{\rm prod} = 17 \pm 5$ and may be compared with $K_{34}^{\rm prod} = 14 \pm 3$ in the compression shock. When CF_3I molecules were excited in the undisturbed flow and in the compression shock, the enrichment factors at an energy density of ≈ 1.5 J cm^{-2} amounted to $K_{13}^{\rm prod} = 21 \pm 3$ and $K_{13}^{\rm prod} = 15 \pm 3$, respectively. This means that selectivity of molecular dissociation within the compression shock is only slightly (by approximately 25 – 30%) lower than that in the undisturbed flow, whereas the product yield in the shock wave was more than 10 times higher [223, 227].

Thus, the rise in the product yield upon excitation of molecules in the compression shock is caused by the following factors [221 – 223]: (1) increased gas density, and (2) increased molecular dissociation yield due, first, to the more efficient excitation of molecules in the compression shock and, second, to the collisional dissociation of molecules that are excited by an IR pulse below the dissociation threshold and fail to dissociate in an undisturbed flow owing to a deficit of collisions. Comparatively high selectivity in the compression shock is a consequence of rather low vibrational temperature of molecules in the shock wave [225].

To conclude, the studies reported in papers [220 – 227] have demonstrated that the formation of a compression shock in front of a solid surface significantly improves the efficiency of isotopically selective IRMPD of molecules in gasdynamically cooled pulsed molecular flows.

6.5 Summary

The above-considered investigations provided data on isotopically selective IRMPD of CF_3I and SF_6 molecules in gasdynamically cooled pulsed molecular flows. Parameters ($N_{\rm fl}$, $\Delta x_{\rm fl}$, η) of the CF_3I molecular flow were determined. The studies revealed the dependence of the yield of the target product C_2F_6 on the energy flux density of the exciting laser radiation, the number of pulses, and the CF_3I pressure above the nozzle. They also demonstrated the dependence of the ^{13}C content in the C_2F_6 product on the laser radiation frequency. Optimal conditions were found for the CF_3I dissociation in terms of the C_2F_6 yield and the enrichment coefficient.

The studies enabled the evaluation of the effects of a buffer (acceptor) gas on the C_2F_6 and COF_2 yields. One of the proposed methods helps to substantially diminish the loss of radicals on the chamber walls, namely, the radicals formed in the course of isotopically selective IRMPD of CF_3I molecules in pulsed gasdynamic flows. The method consists of feeding a rarefied buffer (acceptor) gas into the chamber where the molecular flow is formed; this procedure increases the yield of the target products.

It was shown that the yield of the target product C_2F_6 strikingly decreases with a decreasing concentration of CF_3I molecules in the flow (and the concentration of CF_3 radicals being formed). This means that highly ^{13}C-enriched products can be obtained provided a rather high concentration ($N \geqslant 10^{13}$ cm^{-3}) of $^{13}CF_3$ radicals is attained in the flow and/or an acceptor gas (for example, oxygen) is introduced into the chamber. The effect of radical acceptors (e.g., oxygen) on the product yield is especially well pronounced at low concentrations of the CF_3 radicals being formed.

Table 2. SF_4 and C_2F_6 product yields and their ^{34}S- and ^{13}C-enrichment factors for SF_6 and CF_3I molecules excited in an undisturbed flow, in a flow incident on a surface, and in a compression shock [223, 227].

Gas composition and stagnation pressure, atm		CO_2 laser line	Energy density, J cm^{-2}	Product yield (SF_4, C_2F_6), rel. units			Enrichment factors ($K_{34}^{\rm prod}$, $K_{13}^{\rm prod}$)		
				Undisturbed flow	Incident flow	Compression shock	Undisturbed flow	Incident flow	Compression shock
SF_6	1.25	10P(16)	12	1 ± 0.2	2.5 ± 0.5	12 ± 3			
	1.25	10P(36)	10				17 ± 5	15 ± 3	14 ± 3
CF_3I	1.5	9R(12)	1.3	1 ± 0.2	2.5 ± 0.5	14 ± 3			
	1.5	9P(20)	1.5				21 ± 3	19 ± 3	15 ± 3

Specific features of the IR absorption spectrum of CF_3I molecules (close coincidence of the frequencies of the $\nu_2 + \nu_3$ vibration in $^{12}CF_3I$ molecules and the excitable ν_1 vibration in $^{13}CF_3I$ molecules) make the production of highly ^{13}C-enriched compounds problematic even in gasdynamic jets and flows. It appears more realistic to enrich the residual gas in the ^{13}C isotope as realized in works [231, 232] (see Section 7).

Experiments with SF_6 molecules demonstrated the possibility of producing and effectively collecting SF_4 product enriched in the target isotope in a pulsed flow. The spectral dependence of the SF_4 yield was obtained, and the ^{34}S enrichment factor for the end product measured. When the molecules were excited at a frequency of 929-cm^{-1} 10P(36) laser line and relatively high energy flux density $\Phi_{av} \geqslant 10$ J cm^{-2}, the enrichment factor amounted to $K_{34}^{prod} \approx 13 \pm 3$; when recalculated per molecule dissociating in the flow, the enrichment factor $K_{34}^{prod} \approx 17 \pm 5$. These experimental values of the enrichment factor were consistent with the expected ones derived from the spectral dependence of the $^{32}SF_4$ yield.

Experiments with UF_6 molecules have revealed that relatively high selectivity of dissociation is attainable only under conditions of gasdynamic cooling and molecular excitation by multifrequency radiation.

7. Selective dissociation of molecules in a small-extent pulsed gasdynamic flow

This section is focused on the results of studies [231, 232] of the selective dissociation of molecules (CF_3I as an example) in a gasdynamically cooled small-extent pulsed flow ($\Delta x_{fl} \leqslant 1$ cm), when the entire flow is subjected to high-intensity IR laser radiation. These results illustrate a new approach to the realization of isotopically selective dissociation of molecules. The use of shortened flows ensures high dissociation yields of resonantly excited molecules in the entire flow volume and thereby permits us to obtain the highly enriched residual gas during one irradiation cycle.

7.1 Rationale of the method

It has been shown in Section 6.1 that selective dissociation of CF_3I molecules in jets and flows entails difficulties associated with the production of a desired compound. The products of the dissociation and subsequent chemical reactions are difficult to obtain and effectively collect, bearing in mind the high chemical activity of CF_3 radicals being formed upon molecular dissociation and their low concentrations in gasdynamic flows. Their interactions on the walls of the chamber may predominate and substantially modify the production channels and kinetics of the process. Moreover, the attainable degrees of selectivity are, as a rule, small ($\alpha \leqslant 2-5$) when the dissociation involves molecules whose IR absorption spectra are characterized by a small isotope shift. For this reason, it is impossible to obtain a highly enriched product during a single cycle of irradiation of the primary gas. Hence, it is recommended in many cases to 'burn out' a nontarget component in the starting mixture and enrich the residual gas in the target isotope.

However, it is impossible to obtain a high enrichment factor for the residual gas when employing gasdynamic jets and flows without multiple irradiation of the circulating gas. Due to a relatively small period-to-pulse duration ratio for laser radiation, only a small fraction η of the molecules in a flow can be irradiated during one cycle; this fraction is defined by the expression

$$\eta = \frac{\Delta x_L f}{v_x}, \tag{7.1}$$

where Δx_L is the laser beam dimension along the x-axis, f is the laser pulse repetition frequency, and v_x is the mean flow rate. In the case under consideration, the laser pulse is assumed to be orthogonal to the x-axis, and the flow to be limited in the direction of axes y and z; hence, it is fully irradiated by a laser beam.

The use of powerful pulse-periodic CO_2 lasers [233] allows parameters $\Delta x_L \approx 1$ cm and $f \approx 500$ Hz to be realized. Given the characteristic average rate $v_x \approx 5 \times 10^4$ cm s^{-1} of the molecular flow, the fraction of molecules undergoing irradiation amounts to $\eta \approx 10^{-2}$. (Here, it is assumed that the CO_2-laser pulse duration $\tau_p \leqslant 1$ μs and $\tau_p \ll \Delta x_L/v_x$; this implies that the spatial position of the molecular flow during the laser pulse action is virtually unaltered.) When the dissociation yield $\beta \approx 0.2$, the fraction of molecules that dissociate in the flow during the time of exposure equals approximately $\eta_\beta \approx \eta\beta \approx 2 \times 10^{-3}$. Consequently, residual gas enrichment in the course of one irradiation cycle is negligibly small.

The situation improves when pulsed molecular flows are utilized. If the characteristic nozzle-opening pulse duration $\tau_{noz} \approx 200$ μs, the extent of the molecular flow will reach $\Delta x_{fl} \approx v_x \tau_{noz} \approx 10$ cm. In this case, a single laser pulse may be sufficient to irradiate a fraction $\eta = \Delta x_L/\Delta x_{fl} \approx 0.1$ of molecules in the flow; at $\beta \approx 0.2$, one finds $\eta_\beta \approx 2 \times 10^{-2}$. However, this fraction is also rather small, as is the residual gas enrichment factor.

The situation is quite different when small-extent pulsed molecular flows ($\Delta x_{fl} \leqslant 1$ cm) are used. Such flows are produced using a nozzle with a small opening time, $\tau_{noz} \leqslant 20$ μs. This ensures high-intensity IR laser irradiation of the entire flow. The enrichment factor for the residual gas will be largely dependent on the dissociation yield of resonantly excited molecules. When the dissociation yield $\beta \approx 1$, even for moderate selectivity values $\alpha \geqslant 3$, the residual gas becomes highly enriched even if the mixture of isotopomers is irradiated by a single laser pulse.

This approach has been developed in works [231, 232], where its potential is illustrated by the example of isotopically selective dissociation of CF_3I molecules. The choice of CF_3I molecules for studying isotopically selective dissociation processes was substantiated in Section 6.1. In the above works, CF_3I molecules were used mainly for their relatively low dissociation energy (≈ 2.3 eV [193]) and efficient dissociation at a moderate excitation energy flux density ($\Phi \leqslant 4$ J cm^{-2}) [188–191]. With such a molecule, it is easy to realize conditions in which the dissociation yield is very close to unity.

7.2 Relationship between parameters of an elementary separation act in a concrete experiment

When the entire molecular flow is subjected to laser irradiation, the relationship between the parameters of an elementary separation act is described by expressions (6.1)–(6.6) in which $\eta = 1$.

Therefore, if the laser radiation is tuned in resonance with molecular vibrations, so that the dissociation predominantly involves molecules corresponding to the index 1, i.e., $\beta_1 > \beta_2$, and its selectivity is defined as usual, viz., $\alpha = \beta_1/\beta_2$, the

enrichment factor for the residual gas has the form [see relation (6.5)]

$$K_2^{\text{res}} = \frac{1-\beta_2}{1-\beta_1} = \frac{1-\beta_1/\alpha}{1-\beta_1}\,. \tag{7.2}$$

The enrichment factor for the dissociation products is given by relation (6.6) from which it follows that it is necessary to achieve a rather high degree of dissociation selectivity if a compound highly enriched in a desired isotope is to be obtained. This, however, is sometimes infeasible, especially if the molecules exhibit a small isotope shift.

At the same time, there emerges the possibility of producing (even at relatively low selectivity, $\alpha \geqslant 3$) a highly enriched residual gas by effecting molecular dissociation under conditions in which the intense laser radiation acts on the entire molecular flow and the dissociation yield of resonantly excited molecules comes close to unity.

It follows from relation (7.2) that the enrichment factor K_2^{res} of the residual gas shows only weak selectivity dependence (for $\alpha \geqslant 3$) but is strongly dependent on the dissociation yield in the $\beta \approx 1$ region. This is quite apparent in Fig. 18 showing the $K_2^{\text{res}}(\beta_1)$ dependences. For example, a change of α from 2 to 10^3 at $\beta_1 \approx 0.95$ leads to a rise in K_2^{res} from about 10 to 20, i.e., only two-fold. At the same time, the value of K_2^{res} grows significantly as $\beta_1 \to 1$ regardless of α (if $\alpha \geqslant 3$). By way of illustration, a change in β_1 from 0.9 to 0.99 at $\alpha = 5$ results in a rise in K_2^{res} from 10 to 100; as $\beta_1 \to 1$, we have $K_2^{\text{res}} \to \infty$. These data suggest that under conditions of the complete irradiation of a molecular flow by laser beam and the dissociation yield of resonantly excited molecules being close to unity ($\beta_1 \approx 1$), the highly enriched residual gas can be obtained during a single laser pulse. Just these conditions were realized in our works [231, 232].

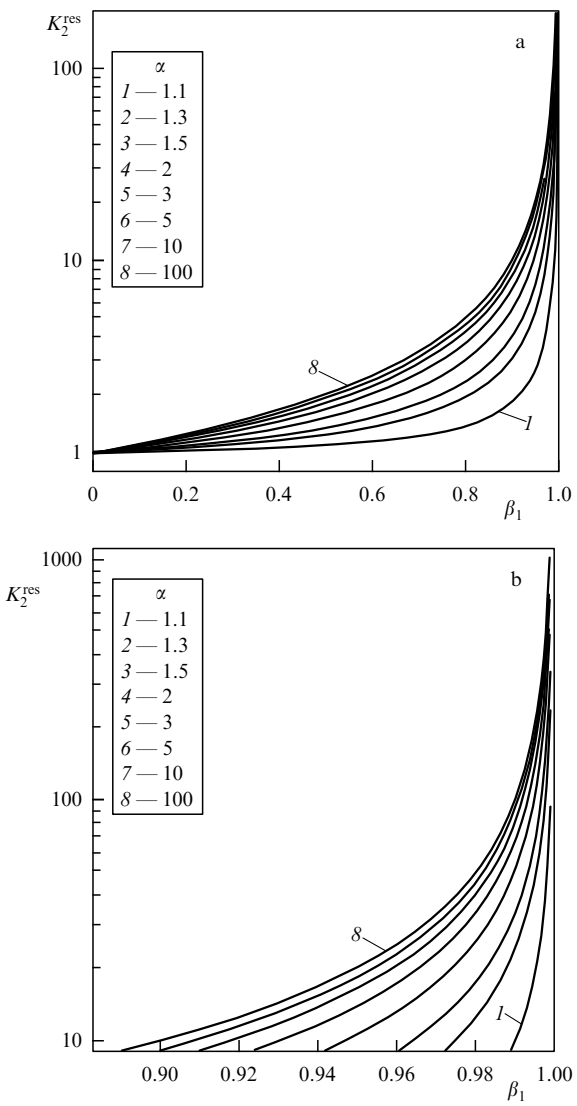

Figure 18. Plots of the enrichment factor K_2^{res} of the residual gas versus dissociation yield β_1 at different values (shown in the figure) of selectivity α during irradiation of a two-component isotopic mixture in the conditions where $\beta_1 > \beta_2$ and (a) $0 \leqslant \beta_1 < 1$, (b) $0.9 \leqslant \beta_1 < 1$. (Taken from Refs [231, 232].)

7.3 Experiment

The schematic of the experiment is illustrated in Fig. 19a. The molecular flow was produced using a pulsed 'current loop' nozzle [95, 97]. The opening time of the nozzle measured 18 μs (at half-height). The diameter of the nozzle opening was 0.75 mm. The pressure above the nozzle could be varied from ≈ 1 to 5 atm. The number N_{fl} of molecules flowing out from the nozzle in a single pulse depended on the pressure above the nozzle and was $N_{\text{fl}} \approx 10^{16}$ molecules per pulse when the CF_3I pressure above the nozzle measured ≈ 2 atm. The nozzle could operated either in a single-pulse mode or in a mode with a pulse repetition rate of up to 1 Hz.

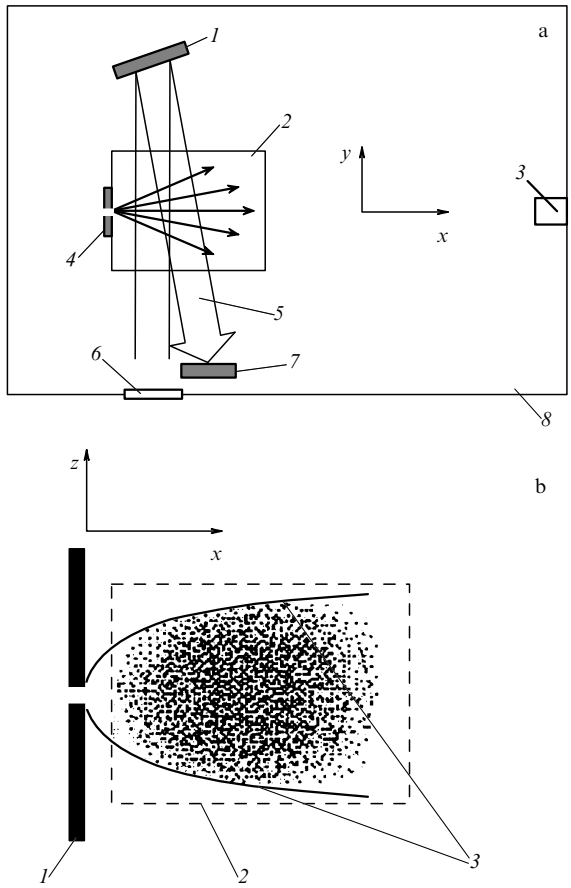

Figure 19. (a) Schematic of the experiment: *1* — mirror, *2* — flow-forming strips, *3* — pyroelectric detector, *4* — pulsed nozzle, *5* — laser beam, *6* — window, *7* — absorber, *8* — vacuum chamber. (b) Geometry of laser irradiation of a molecular flow: *1* — pulsed nozzle, *2* — laser beam cross section, *3* — flow-forming strips. (Taken from Ref. [232].)

The molecular flow was formed (see Fig. 19b) with two thin (100 μm) metallic strips sized 2.5×2.5 cm^2 and attached directly to the nozzle outlet in such a way that they formed a dihedral angle with the edge parallel to the y-axis. In the xz-plane, these two strips had a varying curvature radius. The maximum opening angle of the strips (at the back edge of the nozzle) ran to $\approx 60°$, with the minimum (at the nozzle opening) and maximum distances between them 1.5 and 8 mm, respectively. Since the 'bunch' of the molecules as they flowed out from the nozzle had a length $\Delta x_{\rm fl} = v_x \tau_{\rm noz} \leqslant 7.5$ mm (at half-height), it was totally enclosed in the area between the strips where the molecules underwent irradiation.

The molecules were excited by the radiation from a CO_2 laser that generated pulses with an energy of up to 3 J. The laser radiation was focused by a lens ($f_{\rm L} = 1$ m) and directed into the vacuum chamber to the area between the strips that bounded the molecular flow. The laser beam was perpendicular to the flow. The minimal distance between the back edge of the nozzle and the boundary of the excitation region was approximately 3 mm. The laser beam cross section in the area of its interaction with the molecular flow measured $\approx 6 \times 6$ mm^2. Vertically (along the z-axis), the laser beam spanned the entire region between the strips that bounded the molecular flow, whereas its size $\Delta x_{\rm L} \approx 6$ mm along the x-axis was smaller than the flow length $\Delta x_{\rm fl} \approx 7.5$ mm. In order to fully irradiate the molecular flow, the system included a mirror that reflected the laser beam at a small angle to opposite direction and thus ensured the size $\Delta x_{\rm L} \approx 12$ mm of the treated region along the x-axis. Due to this, the high-intensity laser radiation acted on the entire molecular flow. The laser energy flux density in the excitation area amounted to 8 J cm^{-2}, which was sufficient for the dissociation of CF_3I molecules with a close-to-unity yield [42, 189].

Procedures for the collection and analysis of the residual gas and dissociation products were described in detail in Section 6.1.3. Both the residual CF_3I gas and the resulting products (mainly C_2F_6) were collected into the trap. One irradiation cycle consisted of 50 to 500 pulses. The pressure in the vacuum chamber during the irradiation was maintained at below 10^{-2} Torr. Indeed, as many as $N_\Sigma \approx N_{\rm fl} \times n \approx 10^{16} \times 500 \approx 5 \times 10^{18}$ particles were ejected from the nozzle to the chamber in 500 pulses. The chamber volume being $V_{\rm ch} \approx 2 \times 10^4$ cm^3, the pressure increment was $\Delta p_{\rm ch} \approx \Delta NkT/V_{\rm ch} \approx 2.5 \times 10^{14} kT \approx 7 \times 10^{-3}$ Torr. The mean concentration of the molecules in the excitation region was approximately 10^{16} cm^{-3}.

A Specord 75 IR spectrophotometer was used to analyze the gas. The gas absorption was measured over a frequency range between 680 and 1400 cm^{-1}, which spans the most intense absorption bands of CF_3I and C_2F_6 molecules [195, 197]. The measurement of absorption in a few bands was necessary to more precisely determine the amount of the collected gas. The enrichment of the residual gas in the ^{13}C or ^{12}C isotope was estimated from the IR absorption spectrum of CF_3I molecules in the ν_4 vibration band (1187 cm^{-1} [195]) where the absorption spectra of the $^{12}CF_3I$ and $^{13}CF_3I$ isotopomers were fairly well resolved ($\Delta\nu_{\rm is} = 33$ cm^{-1}). The enrichment factor was even more accurately evaluated from the respective mass spectra (see Section 6.1.3).

7.4. Production of residual highly ^{13}C-enriched CF_3I gas

The CF_3I molecules were excited in the ν_1 vibration band (1075 cm^{-1} for $^{12}CF_3I$, and 1047.1 cm^{-1} for $^{13}CF_3I$ [195]) for which the isotope shift measures $\Delta\nu_{\rm is} = 27.9$ cm^{-1} [195]. $^{12}CF_3I$ molecules were excited at the frequencies of the 9R(10) (1071.9 cm^{-1}) or 9R(12) (1073.3 cm^{-1}) laser lines, and $^{13}CF_3I$ molecules at the frequency of the 9P(24) (1043.2 cm^{-1}) laser line. It was shown in Ref. [42] that the 9R(10) and 9R(12) laser lines are optimal for the dissociation of $^{12}CF_3I$ molecules cooled in a gasdynamic pulsed jet. The 9P(24) line is redshifted relative to the 9R(10) line approximately by the value of the isotope shift.

The results are presented in Fig. 20. Curve *1* corresponds to the absorption spectrum of CF_3I molecules fed into the chamber with the flow from the nozzle but unexcited by the laser radiation. As expected, the ratio of isotopomers in the mixture remained natural (with content of the isotope $^{13}C \approx 1.1\%$, and $[^{12}C]/[^{13}C] \approx 90$). The absorption spectrum (curve *2*) of CF_3I molecules in the flow exposed to the laser radiation at the frequency of the 9R(10) line and the excitation energy flux density $\Phi \approx 8$ J cm^{-2} was measured in an experiment where laser pulses crossed the molecular flow only in one direction, because the reflecting mirror was removed from the system. As a result, only part of the molecules in the flow underwent irradiation ($\Delta x_{\rm L} < \Delta x_{\rm fl}$, $\Delta x_{\rm L} \approx 6$ mm, and $\Delta x_{\rm fl} \approx 7.5$ mm at half-height). A seven-fold enrichment of the residual gas in the ^{13}C isotope was achieved ($K_{13}^{\rm res} \approx 6.8$). Curve *3* represents the absorption spectrum of the molecules irradiated in the flow at the frequency of the 9R(12) line and the laser fluence $\Phi \approx 3.5$ J cm^{-2}. This spectrum was obtained under conditions that provided for the complete irradiation of the flow with laser beams (using the reflecting mirror at $\Delta x_{\rm L} \approx 12$ mm). This allowed an almost five-fold ^{13}C-enrichment of the residual CF_3I gas to be obtained ($K_{13}^{\rm res} \approx 5.2$). At the energy density of the exciting radiation used in the present experiment, the CF_3I dissociation yield was close but not equal to unity [189, 194]. Finally, curve *4* depicts the

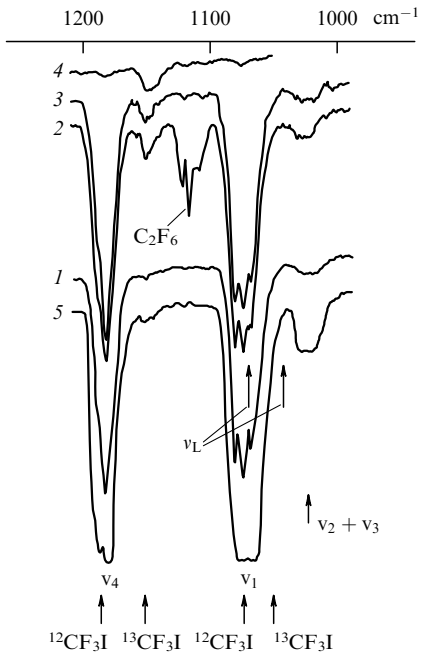

Figure 20. IR absorption spectra of CF_3I molecules having natural isotopic composition before (curve *1*) and after irradiation in a molecular flow under resonant excitation of $^{12}CF_3I$ (curves *2–4*) and $^{13}CF_3I$ (curve *5*) molecules. (Taken from Ref. [232]).

absorption spectrum of the molecules irradiated at the frequency of 9R(10) line under conditions in which the entire flow was exposed to high-intensity laser pulses ($\Phi \approx 7.5$ J cm^{-2}, $\Delta x_{\rm L} \approx 12$ mm). It can be seen that practically all $^{12}CF_3I$ molecules contained in the natural mixture ($\approx 99\%$) underwent dissociation. The residual CF_3I gas was largely composed of $^{13}CF_3I$ molecules ($\geqslant 82\,\%$). In this experiment, an almost 400-fold enrichment of the residual CF_3I gas in the ^{13}C isotope was achieved. The selectivity was evaluated based on the C_2F_6 yield and the IR absorption spectra of CF_3I molecules (including dissociated $^{12}CF_3I$ molecules); it amounted to $\alpha \geqslant 10$. A more accurate assessment of selectivity was impossible because the dynamic range of the available mass spectrometer was less than 10^3. The dissociation yield of $^{12}CF_3I$ molecules in this experiment was $\beta_{12} \approx 99.8\%$.

It should be borne in mind that selectivity, dissociation yield, and residual gas enrichment in the experiment under consideration were independent of the pulse number and characterized the separation process in individual pulses. A series of pulses were needed to obtain a larger amount of the enriched gas. In other words, the above enrichment coefficients for the residual gas were obtained by the irradiation of the CF_3I molecular flow with a single laser pulse.

Figure 20 also demonstrates (curve *5*) the absorption spectrum of CF_3I molecules irradiated in a flow at the frequency of the 9P(24) laser line resonant with the $^{13}CF_3I$ molecules at the laser energy flux density $\Phi \approx 8$ J cm^{-2}. In this experiment, as in the case with spectrum *2*, only part of the molecular flow was exposed to the laser radiation, with no reflecting mirror present in the chamber. Evidently, the residual gas contained much less $^{13}CF_3I$ molecules than the primary one. An almost two-fold enrichment of the residual gas in the ^{12}C isotope was achieved ($K_{12}^{\rm res} \approx 2.2$). The selectivity of dissociation deduced from the measured yield of a C_2F_6 product was $\alpha_{13} \approx 11$. This rather low selectivity accompanying $^{13}CF_3I$ dissociation is attributable to the fact that the excitable ν_1 vibration in $^{13}CF_3I$ molecules adjoins the $\nu_2 + \nu_3$ vibrational band of $^{12}CF_3I$ molecules (≈ 1028 cm^{-1} [195]). It is worth noting that the enrichment of the residual gas attainable during the excitation of $^{13}CF_3I$ molecules is 1.5–2 times smaller than during the excitation of $^{12}CF_3I$ molecules (the irradiation conditions being identical). In all likelihood, this observation can be accounted for by the exchange reaction between $^{13}CF_3$ radicals and parent $^{12}CF_3I$ molecules. Also, it is found that the amount of the final C_2F_6 product decreases dramatically when the concentration of CF_3I molecules in the flow falls. This is believed to be due to the peculiarities of C_2F_6 formation under conditions of pair collisions of CF_3 radicals.

The residual gas enrichment factor $K_{13}^{\rm res}$ derived from the relationship analogous to Eqn (6.5), namely

$$K_{13}^{\rm res} = \frac{1-\beta_{13}\eta}{1-\beta_{12}\eta} = \frac{1-\beta_{12}\eta/\alpha_{12}}{1-\beta_{12}\eta}\,, \qquad (7.3)$$

can be used to estimate the fraction η of molecules irradiated in the flow. By way of example, the experimentally obtained enrichment factor $K_{13}^{\rm res} \approx 6.8$ can be used for the purpose (see curve *2* in Fig. 20). When laser radiation affects only part of the molecular flow, β_{12} in relation Eqn (7.3) should be replaced by $\beta_{1,\rm eff}$ ($\beta_{1,\rm eff} = \beta_{12}\eta$). Further substitution of $\alpha_{12} = 10$ and $K_{13}^{\rm res} = 6.8$ into Eqn (7.3) gives $\beta_{12}\eta = 0.86$. Because the dissociation yield $\beta_{12} \approx 1$, one finds $\eta \approx 0.86$.

Also, relationship (7.3) may be applied to determining the dissociation yield of $^{12}CF_3I$ molecules in the case of their irradiation at $\Phi \approx 3.5$ J cm^{-2} (see curve *3* in Fig. 20). The substitution of $\alpha_{12} = 10$ and $K_{13}^{\rm res} = 5.2$ into Eqn (7.3) gives $\beta_{12} \approx 0.82$.

7.5 Summary

The approach developed in Refs [231, 232] makes it possible to use isotopically selective IRMPD of molecules for the production of a highly enriched residual gas during one irradiation cycle. This method is based on the treatment of a small-extent ($\Delta x_{\rm fl} \leqslant 1$ cm) pulsed molecular flow. The isotopically selective dissociation of CF_3I molecules has been investigated in such a flow. It was found that with high-intensity laser radiation affecting the entire flow, the dissociation yield of resonantly excited molecules was practically equal to unity. An almost 400-fold enrichment of the residual gas in the ^{13}C isotope was achieved by means of irradiation of the CF_3I molecular flow of natural isotopic composition by a single laser pulse.

Because the approach of interest makes high enrichment factors for residual gases an achievable goal at moderate selectivity ($\alpha \geqslant 2-3$), it can probably be applied to molecules with intrinsically small isotope shifts. In particular, it appears suitable for the high-quality purification of gaseous substances from impurities [234]. The unit performance and the utilization of laser radiation can be improved by using pulsed slotted nozzles.

8. Conclusions

The results of our studies have created the basis for developing spectroscopy of IRMPE of molecules in gasdynamically cooled beams, jets, and flows. Methods have been proposed by which to study molecular excitation and dissociation processes, namely, pyroelectric techniques for the detection of molecular beams and measurement of absorbed energy; diode spectroscopy of molecular excitation dynamics at different rotational sublevels; selective multifrequency excitations of upper vibrational states of molecules, and isotopically selective dissociation of molecules in small-extent pulsed beams and in flows interacting with solid surfaces. The data obtained provide a deeper insight into the physical nature of interactions between intense laser IR radiation and polyatomic molecules. Also, they have greatly promoted the understanding of mechanisms of molecular excitation in the region of lower vibrational levels and isotopically selective molecular dissociation by high-intensity IR radiation, as well as many related processes and phenomena. Analysis of spectral and energy characteristics of the MPA of molecules (exemplified by SF_6 and CF_3I molecules) revealed (practically at all excitation frequencies) the dependences of the absorbed energy on the exciting pulse energy density (intensity) in the form $E_{\rm ab} \sim \Phi^n$ ($E_{\rm ab} \sim I^n$), where $n > 1$, characteristic of multiphoton processes. In addition, an MPA cross section of molecules was shown to grow with increasing excitation energy density. These findings lead to the conclusion that multiphoton transitions in the system of lower vibrational levels play an important role in molecular excitation in the beam under collisionless conditions.

The results of investigations into the excitation of SF_6 and CF_3I in molecular beams and jets suggest the importance of the intensity (duration) of an exciting pulse for multiphoton absorption and dissociation of molecules under collisionless conditions. It is shown that a rise in intensity (over the range of $I \leqslant 50$ MW cm^{-2}) entails a substantial increase in both the

absorbed energy and the dissociation yield. In addition, it was found that the intensity dependence of these variables is especially pronounced on the wings of LAS — that is, in the frequency range where multiple photon resonances are predominantly located.

Some works reviewed in this paper dealt with the role of vibrational and rotational temperatures in the formation of MPA spectra. The results obtained contributed to the understanding of the main factors that influence the formation of MPA and MPD spectra of molecules. Specifically, it was shown that both the position of the maximum (the magnitude of the 'redshift') and the width of the MPA spectra are largely determined by vibrational temperature, i.e., by the initial distribution of molecules among vibrational states.

Examination of the MPA spectra of vibrationally excited molecules (exemplified by SF_6) differing in the initial distribution over lower vibrational levels demonstrated that the spectral structure is determined by one- and two-photon resonances between the anharmonic sublevels of the excitable ν_3 mode in the region of lower vibrational states (up to $\nu_3 \approx 4-5$). Also, it was established that resonant action of several simultaneous IR laser pulses can be used to effectively populate selected high-lying vibrational states of molecules. This method may be considered for the simultaneous enhancement of the efficiency and selectivity of IRMPE and IRMPD processes in molecules.

The double IR – IR resonance technique using diode lasers for probing vibrationally excited molecules was employed to study the dynamics of excitation of SF_6 and NH_3 molecules located on individual rotational sublevels of the ground vibrational state by intense IR radiation. It was shown that the fraction of excited molecules depends on the excitation energy density and the degree of frequency detuning. These dependences were found to be similar for spectroscopically different SF_6 and NH_3 molecules and determined by the mode structure of the CO_2 laser radiation. The fraction of molecules excited from individual rotational sublevels strongly depends on the spectral width and mode composition of the exciting pulse.

The use of diode spectroscopy for studying molecular excitation dynamics greatly promoted the understanding of interactions between intense IR radiation and polyatomic molecules. The results of these studies and their comparison with theoretical models underscore the importance of taking into consideration the real temporal form and the mode composition of the exciting laser pulse for the adequate description of experimental findings. In other words, it is essential to solve a rather complicated problem of interaction between a multilevel quantum system (molecule) and multifrequency IR radiation. The solution would facilitate the quantitative description of the MPE of molecules by intense IR laser radiation.

Studies of isotopically selective molecular dissociation in gasdynamically cooled jets and flows demonstrated the possibility of obtaining isotopically enriched products (C_2F_6, SF_4) in a pulsed flow. The studies documented the spectral dependences of SF_4 and C_2F_6 dissociation yields and permitted the evaluation of the enrichment factors of SF_4 and C_2F_6 products in the ^{34}S and ^{13}C isotopes, respectively. It was shown using SF_6 molecules that the measured enrichment coefficients are in good agreement with the expected values deduced from the spectral dependence of the $^{32}SF_4$ yield.

It was found that the dissociation of CF_3I molecules at low temperatures and concentrations of the gas is accompanied by a considerable loss of radicals on the chamber walls, resulting in the impaired selectivity and product yield. We proposed to introduce a rarefied buffer (acceptor) gas into the chamber, where a molecular flow is formed, to significantly reduce the loss of the radicals being formed and thereby to improve both the selectivity and the yield of the target products. It was shown that a relatively high concentration of $^{13}CF_3$ radicals in the flow ($N \geqslant 10^{13}$ cm^{-3}) and/or the presence of an acceptor gas in the chamber are needed if the end products are to be efficiently enriched in the ^{13}C isotope.

Studies on the interaction of intense pulsed molecular flows and jets with a solid surface demonstrated that a flow incident on such a surface gives rise to a compression shock in front of it. This effect can be used to substantially improve the efficiency of isotopically selective molecular dissociation in gasdynamically cooled jets and flows.

The reviewed works provided prerequisites for the development of a method that permits us to produce a highly enriched residual gas during one cycle of the isotopically selective IRMPD of molecules. The method is based on the use of a small-extent molecular flow ($\Delta x_{\text{fl}} \leqslant 1$ cm). This approach gives a tool for the production of a highly ^{13}C-enriched residual gas in a single cycle of laser irradiation using a CF_3I molecular flow of natural isotopic composition. The method appears to be suitable for the high-quality purification of gaseous substances from impurities.

To summarize, the results and the methods of investigations discussed in the present review constitute a basis for the further development of laser isotope separation processes in gasdynamically cooled jets and flows.

The bulk of the materials included in this review have been obtained in the studies on laser spectroscopy and selective interactions of laser radiation with matter conducted in the Department of Laser Spectroscopy, Institute of Spectroscopy (Troitsk), Russian Academy of Sciences. Results on diode spectroscopy of molecular excitation dynamics were obtained jointly with the Laboratory of High-Resolution Molecular Spectroscopy and Analytical Spectroscopy of the same Institute. The author is grateful to R V Ambartsumyan and V S Letokhov for their support of early studies on the IRMPE of molecules in gasdynamically cooled molecular beams and jets. Fruitful collaboration with V M Apatin, L M Dorozhkin, V V Krivtsun, Yu A Kuritsyn, V N Lokhman, D E Malinovskiĭ, V R Mironenko, D D Ogurok, I Pak, A N Petin, and M V Sotnikov during various stages of the work is gratefully acknowledged. Also, I wish to thank S S Alimpiev, V N Bagratashvili, V G Koloshnikov, A A Makarov, A A Puretskiĭ, E A Ryabov, and B G Sartakov for helpful discussions of a number of results. Studies of the MPA of SF_6 molecules in a large-scale gasdynamic flow were carried out jointly with E Ronander, V Gouws, S P van Heerden, and K van der Merwe (Atomic Energy Corporation, Pretoria, RSA). The work was supported in part by the Russian Foundation for Basic Research (grant No. 03-02-17067).

References

1. Ambartsumyan R V et al. *Pis'ma Zh. Eksp. Teor.Fiz.* **20** 597 (1974) [*JETP Lett.* **20** 273 (1974)]
2. Ambartsumyan R V et al. *Pis'ma Zh. Eksp.Teor. Fiz.* **21** 375 (1975) [*JETP Lett.* **21** 326 (1975)]
3. Ambartsumyan R V et al. *Zh. Eksp. Teor. Fiz.* **69** 1956 (1975) [*Sov. Phys. JETP* **42** 993 (1975)]

4. Letokhov V S, Moore C B *Kvantovaya Elektron.* **3** 248, 485 (1976) [*Sov. J. Quantum Electron.* **6** 129, 259 (1976)]
5. Karlov N V, Prokhorov A M *Usp. Fiz. Nauk* **118** 583 (1976) [*Sov. Phys. Usp.* **19** 285 (1976)]
6. Ambartzumian R V, Letokhov V S "Multiple photon infrared laser photochemistry", in *Chemical and Biochemical Applications of Lasers* Vol. 3 (Ed. C B Moore) (New York: Academic Press, 1977) p. 167
7. Bloembergen N, Yablonovitch E *Phys. Today* **31** (5) 23 (1978)
8. Schulz P A et al. *Annu. Rev. Phys. Chem.* **30** 379 (1979)
9. Alimpiev S S et al. *Lazernoe Razdelenie Izotopov* (Laser Isotope Separation) (Moscow: VINITI, 1981)
10. Letokhov V S *Nelineĭnye Selektivnye Fotoprotsessy v Atomakh i Molekulakh* (Non-Linear Selective Photoprocesses in Atoms and Molecules)(Moscow: Nauka, 1983)
11. Steinfeld J I (Ed.) *Laser-Induced Chemical Processes* (New York: Plenum Press, 1981) [Translated into Russian (Moscow: Mir, 1984)]
12. Bagratashvili V N et al. *Multiple Photon Infrared Laser Photophysics and Photochemistry* (Chur: Harwood Acad. Publ., 1985)
13. Molin Yu N, Panfilov V N, Petrov A K *Infrakrasnaya Fotokhimiya* (Infrared Photochemistry) (Novosibirsk: Nauka, 1985)
14. Cantrell C D (Ed.) *Multiple-Photon Excitation and Dissociation of Polyatomic Molecules* (Topics in Current Physics, Vol. 35) (Berlin: Springer-Verlag, 1986)
15. Lyman J L, in *Laser Spectroscopy and Its Applications* (Optical Engineering, Vol. 11, Eds L J Radziemski, R W Solarz, J A Paisner) (New York: M. Dekker, 1987) p. 417
16. Letokhov V S, Ryabov E A "Mnogofotonnaya izotopicheski-selektivnaya IK dissotsiatsiya molekul" ("Isotopically selective multiphoton dissociation of molecules"), in *Izotopy*: *Svoĭstva, Poluchenie, Primenenie* (Isotopes: Properties, Production, Applications) (Ed. V Yu Baranov) (Moscow: IzdAT, 2000) p. 329
17. Baranov V Yu et al. "Razdelenie izotopov ugleroda metodom IK MFD molekul" ("Carbon isotope separation by IR MPD of molecules"), in *Sbornik Dokladov 2-ĭ Vseross. Nauchnoĭ Konf. "Fiziko-Khimicheskie Protsessy pri Selektsii Atomov i Molekul", Zvenigorod, 1997* (Collected Reports of the *2nd All-Russia Scientific Conf. Physico-Chemical Processes in Selection of Atoms and Molecules, Zvenigorod, 1997*) (Eds V Yu Baranov, Yu A Kolesnikov) (Moscow: TsNIIatominform, 1997) p. 21
18. Baranov V Yu, Dyad'kin A P "Lazernoe razdelenie izotopov ugleroda" ("Laser separation of carbon isotopes"), in *Izotopy*: *Svoĭstva, Poluchenie, Primenenie* (Isotopes: Properties, Production, Applications) (Ed. V Yu Baranov) (Moscow: IzdAT, 2000) p. 343
19. Baranov V Yu et al. *Proc. SPIE* **4165** 314 (2000)
20. Dyad'kin A P et al. "Optimizatsiya tekhnologicheskogo protsessa lazernogo razdeleniya izotopov ugleroda" ("Optimization of technological process of laser carbon isotope separation"), in *Sbornik Dokladov VIII Vseross.* (*Mezhdunarodnoĭ*) *Nauchnoĭ Konf. "Fiziko-Khimicheskie Protsessy pri Selektsii Atomov i Molekul", Zvenigorod, 2003* (Collected Reports of the *VIIIth All-Russia* (*Intern.*) *Scientific Conf. Physico-Chemical Processes in Selection of Atoms and Molecules, Zvenigorod, 2003*) (Ed. Yu A Kolesnikov) (Moscow: TsNIIatominform, 2003) p. 121
21. Letokhov V S, Ryabov E A "Laser isotope separation", in *The Optics Encyclopedia*: *Basic Foundations and Practical Applications* Vol. 2 (G-L) (Eds Th G Brown et al.) (Weinheim: Wiley-VCH, 2004) p. 1015
22. Anderson J B "Molecular beams from nozzle sources", in *Molecular Beams and Low Density Gasdynamics* (Gasdynamics, Vol. 4, Ed. P P Wegener) (New York: M. Dekker, 1974)
23. Miller D R "Free jet sources", in *Atomic and Molecular Beam Methods* Vol. 1 (Ed. G Scoles) (New York: Oxford Univ. Press, 1988)
24. Jensen R J et al. *Laser Focus* **12** (5) 51 (1976)
25. Levy D H, Wharton L, Smalley R E, in *Chemical and Biochemical Applications of Lasers* Vol. 2 (Ed. C B Moore) (New York: Academic Press, 1977) p. 1
26. Apatin V M, Makarov G N *Appl. Phys. B* **28** 367 (1982)
27. Apatin V M, Makarov G N *Zh. Eksp. Teor. Fiz.* **84** 15 (1983) [*Sov. Phys. JETP* **57** 8 (1983)]
28. Radloff W, Stert V, Ritze H H *Appl. Phys. B* **38** 179 (1985)
29. Borsella E et al. *Chem. Phys. Lett.* **93** 523 (1982)
30. Alimpiev S S et al. *Kvantovaya Elektron.* **10** 562 (1983) [*Sov. J. Quantum Electron.* **13** 331 (1983)]
31. Bassi D et al. *Laser Chem.* **5** 143 (1985)
32. Apatin V M, Lokhman V N, Makarov G N *Opt. Spektrosk.* **63** 762 (1987) [*Opt. Spectrosc.* **63** 452 (1987)]
33. Makarov G N et al. *Appl. Phys. B* **65** 583 (1997)
34. Makarov G N, Lokhman V N, Ronander E *Opt. Spektrosk.* **83** 232 (1997) [*Opt. Spectrosc.* **83** 215 (1997)]
35. Scoles G (Ed.) *Atomic and Molecular Beam Methods* Vol. 1 (New York: Oxford Univ. Press, 1988)
36. Scoles G (Ed.) *Atomic and Molecular Beam Methods* Vol. 2 (New York: Oxford Univ. Press, 1992)
37. Kuritsyn Yu A et al. *Chem. Phys.* **122** 97 (1988)
38. Bagratashvili V N, Ionov S I, Makarov G N, in *Laser Spectroscopy of Highly Vibrationally Excited Molecules* (Ed. V S Letokhov) (Bristol: A. Hilger, 1989)
39. Grant E R et al. *Chem. Phys. Lett.* **52** 595 (1977)
40. Sudbø Aa S et al. *J. Chem. Phys.* **70** 912 (1979)
41. Sudbo Aa S et al. *J. Chem. Phys.* **68** 1306 (1978)
42. Apatin V M, Makarov G N *Kvantovaya Elektron.* **10** 1435 (1983) [*Sov. J. Quantum Electron.* **13** 932 (1983)]
43. Borsella E et al. *Nuovo Cimento D* **4** 548 (1984)
44. del Bello U et al. *Chem. Phys. Lett.* **114** 467 (1985)
45. Apatin V M, Makarov G N *Appl. Phys. B* **30** 207 (1983)
46. Apatin V M, Makarov G N *Kvantovaya Elektron.* **10** 1308 (1983) [*Sov. J. Quantum Electron.* **13** 847 (1983)]
47. Apatin V M, Makarov G N *Kvantovaya Elektron.* **9** 1668 (1982) [*Sov. J. Quantum. Electron.* **12** 1067 (1982)]
48. Apatin V M, Bezuglova T V, Makarov G N *Opt. Commun.* **42** 255 (1982)
49. Apatin V M, Lokhman V N, Makarov G N *Laser Chem.* **5** (4) 231 (1985)
50. Letokhov V S, in *Laser Spectroscopy of Highly Vibrationally Excited Molecules* (Ed. V S Letokhov) (Bristol: A. Hilger, 1989)
51. Kuritsyn Yu A et al. *Zh. Eksp. Teor. Fiz.* **94** (11) 65 (1988) [*Sov. Phys. JETP* **67** 1122 (1988)]
52. Makarov G N, Thesis for Doctorate of Physicomathematical Sciences (Troitsk: Inst. of Spectroscopy of the USSR Acad. of Sciences, 1989)
53. Puretskiĭ A A, Thesis for Doctorate of Physicomathematical Sciences (Moscow: Inst. of Physical Chemistry of the USSR Acad. of Sciences, 1987)
54. Letokhov V S, Makarov A A *Usp. Fiz. Nauk* **134** 45 (1981) [*Sov. Phys. Usp.* **24** 366 (1981)]
55. Lee I-R et al. *J. Phys. Chem. A* **104** 10595 (2000)
56. Windhorn L et al. *Chem. Phys. Lett.* **357** 85 (2002)
57. Windhorn L et al. *J. Chem. Phys.* **119** 641 (2003)
58. Robinson P J, Holbrook K A *Unimolecular Reactions* (London: Wiley-Intersci., 1972) [Translated into Russian (Moscow: Mir, 1975)]
59. Eyring H, Lin S H, Lin S M *Basic Chemical Kinetics* (New York: Wiley, 1980)
60. Ambartsumyan R V et al. *Pis'ma Zh. Eksp. Teor. Fiz.* **23** 26 (1976) [*JETP Lett.* **23** 22 (1976)]
61. Larsen D M, Bloembergen N *Opt. Commun.* **17** 254 (1976)
62. Larsen D M *Opt. Commun.* **19** 404 (1976)
63. Isenor N R et al. *Can. J. Phys.* **51** 1281 (1973)
64. Akulin V M et al. *Zh. Eksp. Teor. Fiz.* **69** 836 (1975) [*Sov. Phys. JETP* **42** 427 (1975)]
65. Bloembergen N *Opt. Commun.* **15** 416 (1975)
66. Letokhov V S, Makarov A A *Opt. Commun.* **17** 250 (1976)
67. Ambartsumyan R V et al. *Zh. Eksp. Teor. Fiz.* **71** 440 (1976) [*Sov. Phys. JETP* **44** 231 (1976)]
68. Ambartsumyan R V et al. *Pis'ma Zh. Eksp. Teor. Fiz.* **23** 217 (1976) [*JETP Lett.* **23** 194 (1976)]
69. Ambartzumian R V et al. *Opt. Commun.* **18** 517 (1976)
70. Akulin V M et al. *Pis'ma Zh. Eksp. Teor. Fiz.* **25** 428 (1977) [*JETP Lett.* **25** 400 (1977)]
71. Shuryak E V *Zh. Eksp. Teor. Fiz.* **71** 2039 (1976) [*Sov. Phys. JETP* **44** 1070 (1976)]
72. Grant E R et al. *Phys. Rev. Lett.* **40** 115 (1978)
73. Schulz P A et al. *J. Chem. Phys.* **72** 4985 (1980)
74. Fuss W, Kompa K L *Prog. Quantum Electron.* **7** 117 (1981)

75. Bagratashvili V N et al. *Pis'ma Zh. Eksp. Teor. Fiz.* **44** 450 (1986) [*JETP Lett.* **44** 580 (1986)]
76. Ionov S I et al. *Appl. Phys. B* **47** 229 (1988)
77. Bagratashvili V N et al. *Zh. Eksp. Teor. Fiz.* **93** 1188 (1987) [*Sov. Phys. JETP* **66** 670 (1987)]
78. Bagratashvili V N et al. *Chem. Phys. Lett.* **146** 599 (1988)
79. Nitzan A, Jortner J *Chem. Phys. Lett.* **60** 1 (1978)
80. Nitzan A, Jortner J *J. Chem. Phys.* **71** 3524 (1979)
81. Ambartsumyan R V, Makarov G N, Puretskiĭ A A *Pis'ma Zh. Eksp. Teor. Fiz.* **28** 696 (1978) [*JETP Lett.* **28** 647 (1978)]
82. Karny Z et al. *Chem. Phys.* **37** 15 (1979)
83. Hudgens J W et al. *J. Chem. Phys.* **70** 5906 (1979)
84. Makarov A A, in *Lazernaya Spektroskopiya Kolebatel'no-Vozbuzhdennykh Molekul* (Laser Spectroscopy of Vibrationally Excited Molecules) (Ed. V S Letokhov) (Moscow: Nauka, 1990)
85. Bagratashvili V N et al. *Chem. Phys.* **97** 13 (1985)
86. Makarov A A, Tyakht V V *Zh. Eksp. Teor. Fiz.* **83** 502 (1982) [*Sov. Phys. JETP* **56** 274 (1982)]
87. Kay K G *J. Chem. Phys.* **75** 1690 (1981)
88. Platonenko V T *Kvantovaya Elektron.* **5** 1783 (1978) [*Sov. J. Quantum Electron.* **8** 1010 (1978)]
89. Quack M *J. Mol. Struct.* **292** 171 (1993)
90. Nesbitt D J, Field R W *J. Phys. Chem.* **100** 12735 (1996)
91. Malinovsky A L et al. *J. Phys. Chem. A* **102** 9353 (1998)
92. Gruebele M *Adv. Chem. Phys.* **114** 193 (2000)
93. Bagratashvili V N et al. *Pis'ma Zh. Eksp.Teor. Fiz.* **30** 502 (1979) [*JETP Lett.* **30** 471 (1979)]
94. Knuth E L *J. Chem. Phys.* **107** 9125 (1997)
95. Gentry W R, Giese C F *Rev. Sci. Instrum.* **49** 595 (1978)
96. Gentry W R *Comments Atom. Mol. Phys.* **IX** 113 (1980)
97. Gentry W R "Low-energy pulsed beam sources", in *Atomic and Molecular Beam Methods* Vol. 1 (Ed. G Scoles) (New York: Oxford Univ. Press, 1988)
98. Bassi D, in *Atomic and Molecular Beam Methods* Vol. 1 (Ed. G Scoles) (New York: Oxford Univ. Press, 1988)
99. Zen M, in *Atomic and Molecular Beam Methods* Vol. 1 (Ed. G Scoles) (New York: Oxford Univ. Press, 1988)
100. Makarov G N *Usp. Fiz. Nauk* **173** 913 (2003) [*Phys. Usp.* **46** 889 (2003)]
101. Makarov G N *Usp. Fiz. Nauk* **174** 225 (2004) [*Phys. Usp.* **47** 217 (2004)]
102. Apatin V M et al. *Appl. Phys. B* **29** 273 (1982)
103. Ambartzumian R V et al. *Appl. Phys.* **22** 409 (1980)
104. Ambartzumian R V, Makarov G N, Puretzky A A *Opt. Commun.* **34** 81 (1980)
105. Gallagher R J, Fenn J B *J. Chem. Phys.* **60** 3487 (1974)
106. Makarov A A et al. *Appl. Phys.* **23** 391 (1980)
107. Kompa K L et al. *J. Chem. Phys.* **84** 2020 (1986)
108. Ambartzumian R V et al. *Opt. Commun.* **25** 69 (1978)
109. Ambartsumyan R V, Makarov G N, Puretskiĭ A A *Pis'ma Zh. Eksp. Teor. Fiz.* **28** 246 (1978) [*JETP Lett.* **28** 228 (1978)]
110. Purezky A A, Tyakht V V, in *Laser Spectroscopy of Highly Vibrationally Excited Molecules* (Ed. V S Letokhov) (Bristol: A. Hilger, 1989)
111. Evseev A V, Puretzky A A, Tyakht V V *Laser Chem.* **8** (2–4) 137 (1988)
112. Alimpiev S S et al. *Kvantovaya Elektron.* **12** 434 (1985) [*Sov. J. Quantum Electron.* **15** 289 (1985)]
113. Quick C R (Jr), Wittig C *Chem. Phys. Lett.* **48** 420 (1977)
114. Alimpiev S S *Izv. Akad. Nauk SSSR, Ser. Fiz.* **45** 1070 (1981)
115. Alimpiev S S et al. *Kvantovaya Elektron.* **10** 376 (1983) [*Sov. J. Quantum Electron.* **13** 208 (1983)]
116. Okada Y et al. *J. Nucl. Sci. Technol.* **31** 130 (1994)
117. Bagratashvili V N et al. *Opt. Commun.* **18** 525 (1976)
118. Ham D O, Rothschild M *Opt. Lett.* **1** 28 (1977)
119. Deutsch T F *Opt. Lett.* **1** 25 (1977)
120. Lyman J L et al. *Opt. Lett.* **3** 238 (1978)
121. Lyman J L et al. *Chem. Phys.* **45** 325 (1980)
122. Judd O P *J. Chem. Phys.* **71** 4515 (1979)
123. Lyman J L, Quigley G P, Judd O P, in *Multiple-Photon Excitation and Dissociation of Polyatomic Molecules* (Topics in Current Physics, Vol. 35, Ed. C D Cantrell) (Berlin: Springer-Verlag, 1986)
124. Alimpiev S S et al. *Opt. Commun.* **26** 45 (1978)
125. Alimpiev S S et al. *Pis'ma Zh. Eksp. Teor. Fiz.* **30** 279 (1979) [*JETP Lett.* **30** 246 (1979)]
126. Alimpiev S S et al. *Opt. Commun.* **31** 309 (1979)
127. Pine A S, Robiette A G *J. Mol. Spectrosc.* **80** 388 (1980)
128. Apatin V M, Makarov G N *Zh. Eksp. Teor. Fiz.* **91** 1219 (1986) [*Sov. Phys. JETP* **64** 721 (1986)]
129. Apatin V M, Makarov G N *Pis'ma Zh. Eksp. Teor. Fiz.* **38** 120 (1983) [*JETP Lett.* **38** 141 (1983)]
130. Bagratashvili V N et al. *Laser Chem.* **1** (3) 133 (1983)
131. Boriev I A et al. *Chem. Phys. Lett.* **105** 555 (1984)
132. Bagratashvili V N, Ionov S I, Makarov G N, in *Lazernaya Spektroskopiya Kolebatel'no-Vozbuzhdennykh Molekul* (Laser Spectroscopy of Vibrationally Excited Molecules) (Ed. V S Letokhov) (Moscow: Nauka, 1990)
133. Apatin V M et al. *Chem. Phys. Lett.* **127** 438 (1986)
134. Bagratashvili V N, Dolzhikov V S, Letokhov V S *Zh. Eksp. Teor. Fiz.* **76** 18 (1979) [*Sov. Phys. JETP* **49** 8 (1979)]
135. Bagratashvili V N et al. *Zh. Eksp. Teor. Fiz.* **80** 1008 (1981) [*Sov. Phys. JETP* **53** 512 (1981)]
136. McDowell R S et al. *Spectrochim. Acta A* **42** 351 (1986)
137. Akhmanov A S et al. *Opt. Commun.* **23** 357 (1977)
138. Black J G et al. *Phys. Rev. A* **19** 704 (1979)
139. Kolodner P, Winterfeld C, Yablonovitch E *Opt. Commun.* **20** 119 (1977)
140. Baranov V Yu et al. *Kvantovaya Elektron.* **6** 1062 (1979) [*Sov. J. Quantum Electron.* **9** 621 (1979)]
141. Alimpiev S S et al. *Kvantovaya Elektron.* **6** 2597 (1979) [*Sov. J. Quantum Electron.* **9** 1536 (1979)]
142. Borsella E et al. *Chem. Phys. Lett.* **101** 86 (1983)
143. Dilonardo M, Capitelli M, Cantrell C D *Chem. Phys.* **101** 337 (1986)
144. Alimpiev S S, Sartakov B G *Laser Chem.* **12** (3–4) 147 (1992)
145. Karlov N V, in *Primenenie Lazerov v Atomnoĭ, Molekulyarnoĭ i Yadernoĭ Fizike* (Lasers in Atomic, Molecular, and Nuclear Physics) (Moscow: Nauka, 1979)
146. Borsella E et al. *Chem. Phys. Lett.* **87** 284 (1982)
147. Jensen C C et al. *Opt. Commun.* **20** 275 (1977)
148. Patterson C W, Krohn B J, Pine A S *Opt. Lett.* **6** 39 (1981)
149. Patterson C W, Krohn B J, Pine A S *J. Mol. Spectrosc.* **88** 133 (1981)
150. Letokhov V S, Chebotaev V P *Printsipy Nelineĭnoĭ Lazernoĭ Spektroskopii* (Principles of Non-Linear Laser Spectroscopy) (Moscow: Nauka, 1975); see also *Nonlinear Laser Spectroscopy* (Berlin: Springer-Verlag, 1977)
151. Makarov G N *Kvantovaya Elektron.* **13** 1801 (1986) [*Sov. J. Quantum Electron.* **16** 1184 (1986)]
152. Thiart C J H et al. *NO J.* (South Africa) **9** 31 (1993)
153. Moulton P F et al. *Opt. Lett.* **1** 51 (1977)
154. Dubs M et al. *J. Chem. Phys.* **77** 3824 (1982)
155. Patterson C W, Pine A S *Opt. Commun.* **44** 170 (1983)
156. Okada Y et al. *Appl. Phys. B* **59** 475 (1994)
157. Harzer R, Schweizer G, Selter K *J. Mol. Spectrosc.* **132** 310 (1988)
158. Byer R L *IEEE J. Quantum Electron.* **QE-12** 732 (1976)
159. Midorikawa K et al. *Appl. Phys. Lett.* **47** 1033 (1985)
160. Alimpiev S S et al. *Pis'ma Zh. Eksp. Teor. Fiz.* **38** 349 (1983) [*JETP Lett.* **38** 421 (1983)]
161. Apatin V M et al. *Pis'ma Zh. Eksp. Teor. Fiz.* **37** 365 (1983) [*JETP Lett.* **37** 431 (1983)]
162. Apatin V M et al. *Opt. Commun.* **47** 251 (1983)
163. Kuritsyn Yu A et al. *Laser Chem.* **8** 151 (1988)
164. Kuritsyn Yu A et al. *Kvantovaya Elektron.* **16** 1664 (1989) [*Sov. J. Quantum Electron.* **19** 1072 (1989)]
165. Kuritsyn Yu A et al. *Opt. Spektrosk.* **69** 543 (1990) [*Opt. Spectrosc.* **69** 325 (1990)]
166. Kuritsyn Yu A et al. *Appl. Phys. B* **53** 58 (1991)
167. Ambartsumyan R V et al. *Pis'ma Zh. Eksp. Teor. Fiz.* **22** 96 (1975) [*JETP Lett.* **22** 43 (1975)]
168. Alimpiev S S et al. *Pis'ma Zh. Eksp. Teor. Fiz.* **25** 582 (1977) [*JETP Lett.* **25** 547 (1977)]
169. Knyazev I N, Letokhov V S, Lobko V V *Opt. Commun.* **25** 337 (1978)
170. Cantrell C D, Galbraith H W *Opt. Commun.* **18** 513 (1976)
171. Cantrell C D, Galbraith H W *Opt. Commun.* **21** 374 (1977)

172. Herzberg G *Molecular Spectra and Molecular Structure* Vol. 2 *Infrared and Raman Spectra of Polyatomic Molecules* (New York: Van Nostrand, 1945) [Translated into Russian (Moscow: IL, 1949)
173. Akulin V M et al. *Zh. Eksp. Teor. Fiz.* **74** 490 (1978) [*Sov. Phys. JETP* **47** 257 (1978)]
174. Hodgkinson D P et al. *Chem. Phys. Lett.* **90** 230 (1982)
175. Hodgkinson D P, Taylor A J *Opt. Commun.* **50** 214 (1984)
176. Tosa V et al. *Appl. Phys. B* **36** 55 (1985)
177. Rak I, Thesis for Candidate of Physicomathematical Sciences (Troitsk: Inst. of Spectroscopy of the USSR Acad. of Sciences, 1989)
178. Davarashvili O I et al. *Kvantovaya Elektron.* **17** 1077 (1990) [*Sov. J. Quantum Electron.* **20** 993 (1990)]
179. Kunets A V et al. *Opt. Commun.* **84** 37 (1991)
180. Steinfeld J I, Houston P, in *Laser and Coherence Spectroscopy* (Ed. J I Steinfeld) (New York: Plenum Press, 1978) [Translated into Russian (Moscow: Mir, 1982)]
181. Makarov A A, Tyakht V V *Opt. Commun.* **54** 270 (1985)
182. Bobin B et al. *J. Mol. Spectrosc.* **121** 91 (1987)
183. Patterson C W et al. *J. Mol. Spectrosc.* **108** 31 (1984)
184. Makarov G N et al. *Kvantovaya Elektron.* **25** 545 (1998) [*Quantum Electron.* **28** 530 (1998)]
185. Makarov G N et al. *Khim. Fiz.* **18** (3) 71 (1999)
186. Makarov G N *Pis'ma Zh. Tekh. Fiz.* **24** (12) 35 (1998) [*Tech. Phys. Lett.* **24** 921 (1998)]
187. Bittenson S, Houston P L *J. Chem. Phys.* **67** 4819 (1977)
188. Drouin M et al. *Chem. Phys. Lett.* **60** 16 (1978)
189. Bagratashvili V N et al. *Zh. Eksp. Teor. Fiz.* **77** 2238 (1979) [*Sov. Phys. JETP* **50** 1075 (1979)]
190. Gauthier M, Hackett P A, Willis C *Chem. Phys.* **45** 39 (1980)
191. Bagratashvili V N et al. *Appl. Phys.* **20** 231 (1979)
192. Weulersse J M, Genier R *Appl. Phys.* **24** 363 (1981)
193. Gurvich LV et al. *Energii Razryva Khimicheskikh Svyazeĭ. Potentsialy Ionizatsii i Srodstvo k Elektronu* (Energies of Chemical Bond Rupture. Ionization Potentials and Electron Affinity) (Ed. V N Kondrat'ev) (Moscow: Nauka, 1974)
194. Abdushelishvili G I et al. *Kvantovaya Elektron.* **9** 743 (1982) [*Sov. J. Quantum Electron.* **12** 459 (1982)]
195. Fuss W *Spectrochim. Acta A* **38** 829 (1982)
196. Makarov G N *Zh. Eksp. Teor. Fiz.* **108** 404 (1995) [*JETP* **81** 218 (1995)]
197. Weiblen D G, in *Studies upon Fluorine and Certain Fluorides* (Ed. J H Simons) (Easton, Pa., 1924) [Translated into Russian (Moscow: IL, 1956) Ch. 7, p. 431]
198. Takahachi M et al. *Appl. Phys. B* **41** 91 (1986)
199. Makarov G N, Petin A N *Khim. Vys. Energ.* **34** 440 (2000) [*High Energy Chem.* **34** 384 (2000)]
200. Gower M C, Billman K W *Opt. Commun.* **20** 123 (1977)
201. del Bello U et al. *Appl. Phys. B* **42** 147 (1987)
202. Brunner F, Proch D *J. Chem. Phys.* **68** 4936 (1978)
203. Levin I W, Berney C V *J. Chem. Phys.* **44** 2557 (1966)
204. Christe K O et al. *Spectrochim. Acta A* **32** 1141 (1976)
205. Baldacchini G, Marchetti S, Montelatici V *J. Mol. Spectrosc.* **91** 80 (1982)
206. Dem'yanenko A V et al. *Chem. Phys. Lett.* **320** 594 (2000)
207. Lokhman V N et al. *Z. Phys. Chem.* **215** 1469 (2001)
208. Lokhman V N et al. *Chem. Phys.* **286** 385 (2003)
209. Lokhman V N, Ogurok D D, Ryabov E A *Chem. Phys.* **271** 357 (2001)
210. Tiee J J, Wittig C *Appl. Phys. Lett.* **30** 420 (1977)
211. Baranov V Yu et al. *Kvantovaya Elektron.* **23** 782 (1996) [*Quantum Electron.* **26** 762 (1996)]
212. Baranov V Yu et al. "Lazerno-molekulyarnoe razdelenie izotopov urana" ("Laser-assisted molecular separation of uranium isotopes"), in *Izotopy: Svoĭstva, Poluchenie, Primenenie* (Isotopes: Properties, Production, Applications) (Ed. V Yu Baranov) (Moscow: IzdAT, 2000) p. 357
213. Alimpiev S S et al. *Kvantovaya Elektron.* **6** 2155 (1979) [*Sov. J. Quantum Electron.* **9** 1263 (1979)]
214. Rabinowitz P et al. *Opt. Lett.* **7** 212 (1982)
215. Rabinowitz P, Kaldor A, Gnauck A *Appl. Phys. B* **28** 187 (1982)
216. Takeuchi K et al. *J. Nucl. Sci. Technol.* **23** 282 (1986)
217. Kato S et al. *J. Nucl. Sci. Technol.* **26** 256 (1989)
218. Kato S et al., in *Intern. Symp. Advanced Nuclear Energy Research. Near-Future Chemistry in Nuclear Energy Field: Proceedings, February 15 – 16, 1989, Ibaraki, Japan* (Tokyo: The Institute, 1989) p. 53
219. Takeuchi K et al. *J. Nucl. Sci. Technol.* **26** 301 (1989)
220. Makarov G N, Petin A N *Kvantovaya Elektron.* **30** 738 (2000) [*Quantum Electron.* **30** 738 (2000)]
221. Makarov G N, Petin A N *Pis'ma Zh. Eksp. Teor. Fiz.* **71** 583 (2000) [*JETP Lett.* **71** 399 (2000)]
222. Makarov G N, Petin A N *Chem. Phys. Lett.* **323** 345 (2000)
223. Makarov G N, Petin A N *Zh. Eksp. Teor. Fiz.* **119** 5 (2001) [*JETP* **92** 1 (2001)]
224. Makarov G N, Petin A N *Chem. Phys.* **266** 125 (2001)
225. Apatin V M et al. *Opt. Spektrosk.* **91** 910 (2001) [*Opt. Spectrosc.* **91** 852 (2001)]
226. Makarov G N, Petin A N *Khim. Vys. Energ.* **36** 472 (2002) [*High Energy Chem.* **36** 431 (2002)]
227. Makarov G N, Mochalov S A, Petin A N *Kvantovaya Elektron.* **31** 263 (2001) [*Quantum Electron.* **31** 263 (2001)]
228. Landau L D, Lifshitz E M *Gidrodinamika* (Fluid Mechanics) (Moscow: Nauka, 1986) [Translated into English (Oxford: Pergamon Press, 1987)]
229. Zel'dovich Ya B, Raĭzer Yu P *Fizika Udarnykh Voln i Vysokotemperaturnykh Gidrodinamicheskikh Yavleniĭ* (Physics of Shock Waves and High-Temperature Hydrodynamic Phenomena) (Moscow: Nauka, 1966) [Translated into English (New York: Academic Press, 1967)]
230. Abramovich G N *Prikladnaya Gazovaya Dinamika* Pt. 1 (Applied Gasdynamics) (Moscow: Nauka, 1991)
231. Makarov G N, Malinovsky D E, Ogurok D D *Laser Chem.* **17** 205 (1998)
232. Makarov G N, Malinovskiĭ D E, Ogurok D D *Zh. Tekh. Fiz.* **69** (1) 35 (1999) [*Tech. Phys.* **44** 31 (1999)]
233. Velikhov E P et al. *Impul'snye CO_2-Lazery i Ikh Primenenie dlya Razdeleniya Izotopov* (Pulsed CO_2 Lasers and Their Application to Isotope Separation) (Moscow: Nauka, 1983)
234. Ambartsumyan R V et al. *Kvantovaya Elektron.* **4** 171 (1977) [*Sov. J. Quantum Electron.* **7** 96 (1977)]